4-2016

Magnesium regulates transcription of the mgtA (magnesium transporter) gene in Salmonella enterica serovar typhimurium via prolyl-bond formation during translation of the mgtL leader ORF

Aaron R. Gall
Purdue University

Graduate School Form
30 Updated 12/26/2015

PURDUE UNIVERSITY
GRADUATE SCHOOL
Thesis/Dissertation Acceptance

This is to certify that the thesis/dissertation prepared

By Aaron R. Gall

Entitled

Mg2+ regulates transcription of mgtA in Salmonella enterica serovar Typhimurium via prolyl-bond formation during translation of the mgtL leader ORF

For the degree of Doctor of Philosophy

Is approved by the final examining committee:

John N. Anderson
Chair

Laszlo N.Csonka

Bruce Applegate

Michael Gribskov

To the best of my knowledge and as understood by the student in the Thesis/Dissertation Agreement, Publication Delay, and Certification Disclaimer (Graduate School Form 32), this thesis/dissertation adheres to the provisions of Purdue University's "Policy of Integrity in Research" and the use of copyright material.

Approved by Major Professor(s): Laszlo N.Csonka

Approved by: Jeffrey Lucas 4/22/2016

Head of the Departmental Graduate Program Date

MAGNESIUM REGULATES TRANSCRIPTION OF THE *MGTA* (MAGNESIUM TRANSPORTER) GENE IN *SALMONELLA ENTERICA* SEROVAR TYPHIMURIUM VIA PROLYL-BOND FORMATION DURING TRANSLATION OF THE *MGTL* LEADER ORF

A Dissertation

Submitted to the Faculty

of

Purdue University

by

Aaron R Gall

In Partial Fulfillment of the

Requirements for the Degree

of

Doctor of Philosophy

May 2016

Purdue University

West Lafayette, Indiana

"But whatever things were gain to me, those things I have counted as loss for the sake of Christ. More than that, **I count all things to be loss in view of the surpassing value of knowing Christ Jesus my Lord**, for whom I have suffered the loss of all things, and count them but rubbish so that I may gain Christ."

Philippians 3:7-8

ACKNOWLEDGEMENTS

I want to extend my gratitude to Laszlo Csonka for accepting me into his lab as an M.S. student in 2010. It has been a wonderful experience. One of my favorite parts of the research is isolating spontaneous mutants on MacConkey agar, which is such a simple, yet profound technique. Thank you, Laszlo, for reminding me how beautiful is God's creation.

Kiryl Datsenka has been a blessing to me in more ways than he may know. Only the Lord can bring two scientists with very different beliefs together as friends, which reflects the grace (e.g. unmerited favor) that He pours out on people every day. Thank you, Kiryl, for listening and sharing your life with me.

I also want to recognize Shelli Taylor for her joy-filled assistance in the office and the undergraduate students who benefited our lab over the last several years: Erich Leazer, Daniel Bennett, Matt Sacco, Chelsea Hall, Brenda Gonzalez, Bridget Perkins and Katie Yohe.

As a TA in BIOL 221 for more than 4 years, I had so many opportunities to help students understand the Microbiology material and how to do experiments. I really enjoyed learning how to teach and better adapt to the influx of new (and some returning) students each semester. Looking back, I can see how I was placed in the program to influence so many lives and share hope with others, both academically beyond the exams and spiritually beyond the grave.

My brother Aubrey, Chris Biang and Wilkins Morency were three men, who independently asked me after I came to Purdue as an M.S. student with desires of continuing afterwards to be a doctor if medical school was right for me. They asked me if I asked God what He thought. I said, "No." When I stopped and asked the Lord, it was an overwhelming, "Stay here and grow in your faith." God called me to a greater mission, so instead of people being healed physically, I have an opportunity to lead people to Christ to be healed spiritually. In many ways, I am in the medical field, but one that is eternal.

Whom can I truly praise but the Lord? I am thankful to not only receive a Ph.D. degree, but also in the process, to see the right hand of God redeem, restore, renew and reconcile. I most assuredly acknowledge Jesus Christ and the salvation that is found in no other name. I was lost, wandering for most of my life, and yet the Good Shepherd pursued me, because He saw that I was worth pursuing. Thank You, my Lord and my God, for the privilege to be Your ambassador and light to this lost world.

TABLE OF CONTENTS

Page

Page

Page

LIST OF TABLES

LIST OF FIGURES

Figure Page

LIST OF ABBREVIATIONS

$CHCl_3$	chloroform
DNA	deoxyribonucleic acid
F	Faraday
kbp	kilobase-pair
$MgSO_4$	magnesium sulfate
Na_2CO_3	sodium carbonate
OD_{420}/OD_{600}	optical density at wavelength 420 nm/600 nm
ONPG	ortho-nitrophenyl-B-D-galactoside
RNA	ribonucleic acid
SDS	sodium dodecyl sulfate
T	time
Tn10	transposable element containing tetracycline resistance gene
Tn10d-Cm^R	transposable element containing chloramphenicol resistance gene
UV	ultraviolet light
V	volume

ABSTRACT

Gall, Aaron R. Ph.D., Purdue University, May 2016. Magnesium Regulates Transcription of the *mgtA* (Magnesium Transporter) Gene in *Salmonella enterica* Serovar Typhimurium via Prolyl-bond Formation during Translation of the *mgtL* Leader ORF. Major Professor: Laszlo N. Csonka.

In *Enterobacteriaceae*, the *mgtA* gene encodes a P-type ATPase that mediates Mg^{2+} uptake and is up-regulated by the PhoQP two-component system during invasion of host epithelial cells and macrophages. The regulation of *mgtA* has recently gained special interest given that it exists at several stages, including transcription, post-transcription and post-translation, in response to Mg^{2+} availability. The *mgtA* mRNA has a 264-nucleotide 5' leader that contains a 17 codon, proline-rich ORF, termed *mgtL*, whose translation has been proposed to affect the folding of the 5' leader mRNA, which in turn regulates whether transcription is terminated before the *mgtA* structural gene at high Mg^{2+} concentrations, or is allowed to read through at limiting Mg^{2+} concentrations. We hypothesize that Mg^{2+} directly regulates translation of *mgtL* by facilitating prolyl-bond formation. We find that rescue of ribosome stalling at proline codons of *mgtL* by translation factor EF-P and methylation of $tRNA^{Pro}$ with m^1G37 by TrmD both play roles in the regulation of *mgtL* translation. Of potential significance is that TrmD is dependent on Mg^{2+} for its tRNA methylation activity, implying an underlying role of Mg^{2+} in the regulation. We suggest a complex interaction between Mg^{2+}, proline, EF-P and TrmD in the regulation of *mgtL* translation and *mgtA* transcription. In addition, we provide preliminary results implicating an unknown transcription factor and other potential growth conditions in the regulation of *mgtA* expression.

CHAPTER 1. INTRODUCTION

1.1 Overview

A member of the Gram-negative, rod-shaped bacterial family, *Enterobacteriaceae,* the human host pathogen, *Salmonella enterica* serovar Typhi, is responsible for millions of cases of infection per year worldwide, resulting in Typhoid fever, systemic inflammation, and in many cases, death (Rahman et al., 2013). Sites of host infection, residence and proliferation range from non-phagocytic cells, such as gastrointestinal epithelial cells, to the cytosol of macrophages and intracellular compartments, termed *Salmonella*-containing vacuoles (SCV) (García-del Portillo et al., 2008). Development of these modified SCVs depends on factors that regulate expression of virulence genes, which antagonize acidification, reactive oxygen species, and nutrient depravation by host defenses (Eriksson et al., 2003). The food-borne pathogen, *Salmonella enterica* serovar Typhimurium (referred to, hereafter, as *Salmonella*), is a model organism for studying pathogenicity, bacterial physiology and gene expression (Garai et al., 2012).

Horizontally-acquired genomic regions, termed *Salmonella* Pathogenicity Islands (SPI), harbor virulence genes that are regulated during infection and proliferation, many of which encode proteins that modify the cell membrane, adapt to environmental stresses and exert negative effects directly or indirectly on the host (Hensel, 2007). Environmental signals that induce virulence gene expression vary from changes in pH, concentrations of nutrients and metabolites, to exposure to host-specific proteins (Heithoff et al., 1999). Sensory regulators and two-component systems (TCS) modulate gene expression in response to external stimuli, many of which are interconnected and overlapping in regulation (Rychlik and Barrow, 2005). In the classical TCS, a membrane-bound sensor protein transduces an environmental signal by activating a DNA-binding transcriptional regulator, which in turn activates or represses expression of target genes, many of which encode proteins that relate to the environmental signal, leading to transport, biosynthesis, degradation, adaptation, or other cellular processes (Mitrophanov and Groisman, 2008).

One of the most extensively studied TCS, PhoQP regulates ~5% of the *Salmonella* genome (Monsieurs et al., 2005). In response to low pH, host antimicrobial peptides (APs) and low Mg^{2+}, the sensor kinase, PhoQ, auto-phosphorylates, resulting in a conformational change, and in turn activates its cognate DNA-binding transcriptional regulator, PhoP, by phosphorelay (Bader et al., 2005; Prost et al., 2007; Soncini et al., 1996). In repressing conditions, the phosphatase activity of PhoQ deactivates both itself and the PhoP protein (Castelli et al., 2000; Chamnongpol et al., 2003; Montagne et al., 2001). The expression of PhoP and PhoQ is regulated by multiple small non-coding RNAs (sRNA) that bind to the *phoP* and *phoQ* promoters, either down-regulating or up-regulating the transcription of the structural genes (Coornaert et al., 2013; Coornaert et al., 2010). PhoP recognizes a consensus sequence, termed the PhoP Box (Lejona et al., 2003; Zwir et al., 2012), and either activates or represses transcription of genes and operons involved in acid stress, AP resistance, and Mg^{2+} homeostasis (Groisman, 2001). The PhoQP regulon consists of PhoP-activated genes (PAG) and PhoP-repressed genes (PRG) (Groisman, 2001; Kato et al., 1999), most of which are similarly regulated in *Escherichia coli*, although some are unique to *Salmonella* (Monsieurs et al., 2005; Park and Groisman, 2014).

The PhoQP TCS is interconnected with other TCSs and regulatory factors by overlapping functions and signals (Gunn and Richards, 2007; Rychlik and Barrow, 2005). For example, the PmrAB TCS, which responds to periplasmic Fe^{2+} and controls resistance to APs, can be activated in a PhoQP-dependent manner via the PmrD protein (Kox et al., 2000). In this case, low Mg^{2+} induces expression of PmrA-regulated genes via PhoP-dependent transcription activation of *pmrD*, and in turn, PmrD binds the transcriptional regulator PmrA, preserving its phosphorylated state (Kato and Groisman, 2004). In addition, various stresses and nutrient limitations induce the stationary phase response sigma factor, RpoS, which regulates genes and operons involved in nutrient transport, metabolism, relief of various stresses, and many other processes, for long-term survival (Schellhorn, 2014). Levels of RpoS are lowest during exponential phase and increase at the onset of stationary phase by a network of factors that regulate RpoS expression at multiple levels including transcription, post-transcription and post-translation (Battesti et al., 2012; Hengge-Aronis, 2002; Hengge, 2009). The PhoQP TCS is connected to RpoS by a multi-tier regulatory network. In response to inducing signals, such as Mg^{2+}-starvation, PhoP activates transcription of two

independent genes, *iraM* and *iraP*, that encode stabilizer proteins (Eguchi et al., 2011; Tu et al., 2006). Then, IraM or IraP binds to an anti-adaptor protein, RssB, which normally mediates proteolysis of RpoS via ClpXP during exponential phase (Eguchi et al., 2011; Tu et al., 2006). Consequentially, IraM or IraP inhibits RssB-mediated proteolysis of RpoS, increasing levels of RpoS during Mg^{2+}-starvation in a PhoP-dependent manner (Eguchi et al., 2011; Tu et al., 2006).

Magnesium is an essential divalent cation important in enzymatic reactions, stabilization of membranes, and many other cellular processes (Silver, 1996). *Salmonella* harbors three Mg^{2+} transporters: CorA is a constitutively-active, bidirectional channel, while MgtA and MgtB are P-type ATPase transporters that mediate influx of Mg^{2+} in response to limiting extra-cytoplasmic Mg^{2+} (Papp-Wallace and Maguire, 2008). Not only does CorA preferentially transport Mg^{2+} with a higher K_m value than MgtA and MgtB, but it also mediates both influx and efflux of Ni^{2+} and Co^{2+}, and is required for virulence (Papp-Wallace and Maguire, 2008; Papp-Wallace et al., 2008). Upon infection of epithelial cells and macrophages, PhoP activates transcription of the *mgtA* structural gene and the *mgtCBR* operon (Heithoff et al., 1999; Smith et al., 1998; Tao et al., 1998; Véscovi et al., 1996). Located on SPI-3, the *mgtCBR* operon encodes a virulence protein, MgtC, the Mg^{2+} transporter, MgtB, and a regulatory protein, MgtR (Alix and Blanc-Potard, 2008).

MgtA shares ~50% amino acid sequence identity with MgtB (Maguire) and is wide-spread across bacterial genera (Perez et al., 2009); however, the *mgtCBR* operon is present in only a subset of *Enterobacteriaceae* (Blanc-Potard and Groisman, 1997). Speculation whether MgtA and MgtB have other functions other than Mg^{2+} transport arose when deletion of either gene had no effect on virulence of *Salmonella* in mice (Blanc-Potard and Groisman, 1997). On the other hand, deletion of both the *mgtA* and *mgtB* genes resulted in attenuation of *Salmonella* virulence in mice, despite a functional CorA (Papp-Wallace et al., 2008). Deletion of the *mgtC* gene alone resulted in attenuation, indicating that MgtC is required for replication inside macrophages (Rang et al., 2007). In addition, MgtC is shared with extracellular pathogens, such as *Pseudomonas aeruginosa*, and functions in preventing phagosome acidification in a similar manner, by inhibiting the F_1F_0-ATP synthase and preventing influx of H^+ (Belon et al., 2015).

Expression of the *mgtCBR* operon is regulated by interplay of multiple factors, including PhoP-dependent transcription activation (Véscovi et al., 1996), independent translation of two tandem leader open reading frames (ORFs), termed *mgtM* and *mgtP* (Lee et al., 2014; Lee and Groisman, 2012a, b), antisense *amgR*-mediated regulation of the *mgtC* structural gene (Lee and Groisman, 2010), and MgtR-mediated MgtC degradation via FtsH proteolysis (Alix and Blanc-Potard, 2008). Not only does expression of the *mgtC* virulence gene exhibit strict regulation, but expression of the *mgtA* structural gene does so also.

A second transcriptional regulator, Rob, a member of the MarA/SoxS family, mediates resistance to antimicrobials, superoxide, organic solvents, and heavy metals (Duval and Lister, 2013). Bile salts and fatty acids increase expression of the *acrAB* genes, which encode the AcrAB multidrug efflux pump, via Rob interaction (Rosenberg et al., 2003). Rob can activate *mgtA* when over-expressed by binding to a DNA region that overlaps the PhoP-dependent transcription start site (TSS), termed the Rob Box, in the absence of the PhoQP TCS (Barchiesi et al., 2008). MgtA and MgtB may not function in Mg^{2+} scavenging (Kehres and Maguire, 2002), since both mediate influx of Mg^{2+} with similar K_m values (approximately 10 μM) (Papp-Wallace and Maguire, 2008). The differences in amino acid sequence and protein folding between MgtA and MgtB, however, may allow either transporter to function in a novel regulatory role and/or under other physiological growth conditions. Overproduction of MgtA, due to a mutation conferring constitutive expression of the *mgtA* structural gene, increases resistance to killing by high temperature (O'Connor et al., 2009). In addition, osmotic stress induced by high NaCl increases *mgtA* expression, indicating a regulatory role of Mg^{2+} or MgtA as an osmoprotectant (Park et al., 2010).

Regulation of *mgtA* has gained particular attention because an unexpectedly high number of protein factors contribute to regulation of its expression at nearly every stage of synthesis, including transcription, post-transcription and post-translation, and regulation of transporter activity (Choi et al., 2012; Cromie et al., 2006; Hollands et al., 2012; Hollands et al., 2014; Park et al., 2010; Park and Groisman, 2014; Spinelli et al., 2008; Subramani et al., 2016; Zhao et al., 2011). The *mgtA* transcript contains a 264-nucleotide 5' leader region (5' LR) mRNA that encodes a proline-rich, 17-amino acid leader peptide, termed MgtL (Park et al., 2010; Zhao et al., 2011). A *R*ho-*ut*ilization (*rut*) site located downstream of *mgtL* and a pause region for RNA polymerase have been determined to facilitate Rho-dependent transcription termination and RNA

polymerase pausing, respectively (Hollands et al., 2012; Hollands et al., 2014). In addition, RNase E-mediated mRNA degradation (Spinelli et al., 2008), and MgtR-mediated MgtA proteolysis (Choi et al., 2012) occur, further regulating the *mgtA* structural gene and MgtA transporter, respectively.

Numerous genes encoding proteins involved in metabolite biosynthesis, degradation, secretion, and transport systems encode leader peptides, and rely on ribosome-mediated mechanisms to regulate transcription into their respective structural genes. These systems include HisL-regulated histidine biosynthesis, TnaC-regulated tryptophan degradation, SecM-regulated protein export, and MgtM- and MgtP-regulated Mg^{2+} transport (Chan and Landick, 1989; Landick et al., 1990; Lee and Groisman, 2012b; Nakatogawa and Ito, 2002). Typically, translation of a leader peptide facilitates transcription termination upstream of the structural gene by favoring a terminator stem loop in the upstream 5' LR mRNA; on the other hand, lack of translation, or ribosome stalling, facilitates transcription into the structural gene by favoring formation of an anti-terminator stem loop, which is usually mutually-exclusive with the terminator. Transcription termination in bacteria occurs by one of two mechanisms: 1) intrinsic or 2) Rho-dependent transcription termination. Most genes that harbor 5' LRs are regulated by an intrinsic transcription terminator, in which a GC-rich stem loop followed by a stretch of contiguous uracil nucleotides destabilizes the RNA-DNA transcription complex, resulting in termination (Peters et al., 2009). On the other hand, an ATP-dependent helicase Rho recognizes cytosine-rich, single-stranded regions of untranslated mRNA, binds and uncouples the RNA-DNA transcription complex, resulting in termination (Richardson, 2002).

1.2 Statement of the problem

In harboring numerous regulatory mechanisms, *mgtA* is an archetype of transcription-translation coupling and the interplay of multiple factors that contribute to control of its overall expression. Several models have been proposed for the regulation of *mgtA* expression, specifically for the roles of Mg^{2+}, proline (Pro), and translation of *mgtL* coupled to transcription of the *mgtA* structural gene (Cromie et al., 2006; Park et al., 2010; Zhao et al., 2011). The *mgtA* 5' LR mRNA may adopt mutually-exclusive conformations in which stem loops A and B expose, and stem loop C sequesters, the *rut* site, leading to termination or read through

of transcription into the *mgtA* structural gene, respectively (see Chapter 3) (Cromie et al., 2006; Hollands et al., 2012). Opposing hypotheses for the role of Pro in translation of *mgtL* have been made. One group proposed that it has no role (Zhao et al., 2011), while a second group proposed that Pro regulates translation of *mgtL* via Pro-charged $tRNA^{Pro}$ (Park et al., 2010).

Transcription of *mgtA* is dependent on the PhoQP TCS (Véscovi et al., 1996). Mg^{2+} regulates overall *mgtA* expression with a negative correlation in which low Mg^{2+} induces transcription, while high Mg^{2+} leads to transcription termination (Snavely et al., 1991; Tao et al., 1995). The ability to induce expression in limiting Mg^{2+} and repress expression in abundant Mg^{2+}, is termed differential Mg^{2+}-sensing control. Questions have arisen whether Mg^{2+} directly regulates transcription, and what roles translation of *mgtL* and the PhoQP TCS play in *mgtA* regulation when mutations resulting in constitutively high *mgtA-lacZ* expression were characterized. Constitutive expression is characterized by relatively invariable levels, either high or low expression, which signals would otherwise differentially regulate.

Based on our experimental findings, we propose a comprehensive model that supports a novel role for Mg^{2+} in the direct regulation of translation of *mgtL*, and speculate on the order and importance of the regulatory events involved in transcription-translation coupling of *mgtA* expression. In addition, we provide evidence for the involvement of novel factors in translation of *mgtL* and potential transcription activation of *mgtA* expression by regulators other than the PhoQP TCS and Rob and by growth conditions other than Mg^{2+} limitation.

CHAPTER 2. MATERIALS AND METHODS

2.1 Media and growth conditions

Luria-Bertani or Lysogeny Broth (LB), minimal medium M63 (M63), "Mg^{2+}-free" M63, MacConkey agar (1/2 salts) and Green plates were used, supplemented with carbon source, antibiotic, amino acid, and/or other nutrient requirements. Strains were grown aerobically with shaking at 37°C, unless otherwise noted.

2.1.1 Growth in defined media

Strains were grown aerobically with shaking at 37°C in LB until stationary phase ($0D_{600}$ ~ 4.0). Then, cultures were diluted 1:100 into defined M63 containing high (1.6 mM) or low (0.016 mM) concentration of $MgSO_4$, supplemented with 10 mM glucose as the carbon source. After overnight growth, cultures were diluted 1:25 into fresh defined M63, supplemented with 10 mM glucose. Aliquots of 1.5 mL were taken at mid-exponential phase ($0D_{600}$ ~ 0.3-0.6). Then, β-galactosidase activity was measured.

2.1.2 Growth in "Mg^{2+}-free" media

Strains were grown in LB broth until stationary phase ($0D_{600}$ ~ 4.0), diluted 1:100 into minimal medium M63 supplemented with 10 mM glucose as the carbon source and grown overnight aerobically with shaking at 37°C. Cells were washed three times in "Mg^{2+}-free" M63, diluted 1:25 into fresh "Mg^{2+}-free" M63 and grown aerobically with shaking at 37°C. Aliquots of cells were harvested at 3 hours and 6 hours for further analysis of β-galactosidase activity.

2.1.3 Growth on succinate as sole carbon source

Strains were grown aerobically with shaking at 37°C in LB until stationary phase ($0D_{600}$ ~ 4.0). Then, cells were washed twice in M63, diluted 1:100 into fresh M63 supplemented with succinate (20 mM), and grown

aerobically with shaking at 37°C. Aliquots of 1 mL were taken at the indicated time points, and OD_{600} was measured using a UV-1700 PharmaSpec Spectrophotometer (Shimadzu).

2.2 Strain construction

2.2.1 Bacterial strains, plasmids, and oligodeoxynucleotides

Bacterial strains and plasmids used in this work are listed in Tables 2.1 and 2.2, respectively. All *Salmonella enterica* serovar Typhimurium strains were derived from the non-pathogenic strain LT2 and constructed by P22 phage transduction, as described by Davis et al. (1980). All oligodeoxynucleotides and primers used in this work are listed in Table 2.3.

2.2.2 Isolation of spontaneous mutations linked to *mgtA*

Strain TL 4295 (*mgtA::MudJ*) and isogenic derivatives, both exhibiting the Lac^{--} (white) phenotype, were streaked onto MacConkey agar and incubated at 37°C. On the third day, spontaneous Lac^{+} (red) mutants arose in the centers of isolated Lac^{--} colonies. A number of the Lac^{+}/Lac^{--} mixed colonies were streaked onto LB agar to isolate purified Lac^{+} colonies, and several colonies from each random set were re-streaked onto new LB agar plates. After tooth-picking single colonies onto MacConkey agar, independent mutants that exhibited the Lac^{+} phenotype were selected. P22 phage lysates of individual Lac^{+} colonies were used to transduce the *mgtA::MudJ* fusion into strain TL 1 (wild-type *Salmonella* LT2), and kanamycin resistance (Kn^{R}) was selected along with the co-transduced Lac^{+} phenotype. After making colonies P22 sensitive by growth on Green plates and purifying select colonies onto new LB agar plates, the spontaneous mutants were whole-colony PCR-amplified using primers, AG1 and AG2, which anneal to the upstream promoter and *mgtA* coding regions, respectively. Purified DNA fragments of ~1500 bp in length were sent to the Low Throughput Laboratory (Purdue University) for Sanger Sequencing to characterize the spontaneous mutations linked to the *mgtA-lacZ* fusion.

2.2.3 Isolation of a strain with a chromosomal mutation in the *rpmA* gene

In the above selection of Lac^+ derivatives, we also isolated a strain with a mutation that was unlinked in P22 transductions (0% frequency) to Km^R. Because Rho-dependent termination requires accessory Nus proteins (Bubunenko et al., 2013; Sen et al., 2008), we tested whether the mutation in this strain might be in *nusA*, a gene encoding one of the Nus proteins. With the *argG* gene 1.1 kbp away from *nusA*, we used a donor *argG1895::*Tn*10* strain in P22 transductions for tetracycline resistance (Tc^R) and observed that ~20-30% of transductants of the Lac^+ mutant became Lac^-, indicating that the mutation was near *argG*. However, we did not find any mutation in *nusA* based on DNA sequencing of fragments amplified with PCR using primers specific for the structural gene. A subsequent 3-factor cross using *nlp*::Cm as the unselected donor and *argG1895::*Tn*10* in the Lac^+ mutant as the recipient, selecting Arg^+, suggested that the Lac^+ mutation was ~80-90% linked to *nlp*. The genomic interval between *argG1895::*Tn*10* and *nlp::Cm* contains a ribosomal operon containing the *rpmA* and *rplU* genes. Because it was plausible that mutations in ribosomal components could affect the efficiency of translation of *mgtL*, we amplified the *rpmA* gene with PCR using primers, AG105 and AG106, and determined the DNA sequence. Analysis revealed that the *rpmA* structural gene had a single point mutation (G23A). The isolate carrying this spontaneous mutation was named strain TL 5151.

2.2.4 Construction of a strain with a chromosomal deletion of the *efp* gene

A *Salmonella* strain deleted for the *efp* gene was generated by the one-step gene inactivation method (Datsenko and Wanner, 2000). A chloramphenicol resistance (Cm^R) cassette was PCR amplified from the pKD3 plasmid using primers, AG45 and AG46, and the resulting PCR fragment was transformed into the LT2 chromosome using strain TL 155 to generate TL 5282 (TL 155 Δ*efp::*Cm^R). We verified correct insertion of the Cm^R cassette by using upstream and downstream primers, AG71 and AG72, respectively. P22 phage grown on strain TL 5282 was used to transduce TL 4295 (*mgtA9226::MudJ*), selecting for Cm^R to generate TL 5332 (Δ*efp::*Cm^R *mgtA9226::MudJ*).

2.2.5 P22 phage transduction and sensitivity test

Cells were grown in P22 phage buffer overnight at 37°C, unless otherwise noted. The following day, 1 mL of culture was lysed by addition of 100 μL $CHCl_3$, and after centrifugation, the supernatant containing the P22 phage lysate was removed and stored at 6°C. Transductions were performed at ratios of 1:10 or 1:1 of P22 phage lysate to bacterial recipient strain. After incubation for 1 hr ± 15 min at 37°C, 100 μL of the transduction mixture was plated onto agar plates, selecting for the desired antibiotic resistance or phenotype. A number of transductants were streaked onto Green plates, incubated at 37°C, unless otherwise noted, and P22 phage-free (white or pale blue) colonies were selected from the P22 phage-infected (dark blue) colonies for purification on new LB agar plates and further analysis (Lawrence).

2.2.6 Site-directed mutagenesis

2.2.6.1 PCR amplification

Whole-colony PCR was performed using the RoboCycler® Gradient 96 (Strategene), as described previously (Kofoid, 1996). The QIAquick® PCR Purification Kit (QIAGEN) was used to isolate PCR-amplified fragments, which were stored at -20°C.

2.2.6.2 Linear DNA transformation

Linear DNA oligonucleotides were purchased from Integrated DNA Technologies (Table 2.3). Linear DNA transformation was performed, as described by (Datsenko and Wanner, 2000), with the following modifications: strain TL 4287 (Table 2.1) was whole-colony PCR amplified using primer, AG3, which anneals to a chloramphenicol resistance (Cm^R) cassette that is located upstream of the *mgtLA* promoter, and reverse complementary primers, AG7 and AG42, which contain mutation(s) in *mgtL*, to construct TL 5125 and TL 5139, respectively (Tables 2.1 and 2.3). Strain TL 1 was whole-colony PCR amplified using primer pairs, AG49 and AG42, AG47 and AG48, and AG64 and AG65 (Table 2.3), to construct TL 5141, TL 5135 and TL 4697, respectively (Table 2.1). After purification of the linear DNA product, 100 ng of purified linear DNA was electroporated into 50 μL of recombination-proficient cells at 2.5 volts (time constant, <4.5) and 25 μF capacitance using Gene Pulser™ (BIORAD). The recombination-proficient

strain, TL 5123, harbors a selectable marker in *mgtL* (see K. Datsenko for construction; Table 2.1), an *mgtA-lacZ* transcriptional fusion at the chromosomal locus of *mgtA*, and the L-arabinose-inducible recombinase plasmid, pKD46. Cells were recovered from electric shock in LB at 37°C for 4 hrs, and left overnight on the bench-top at room temperature (25°C). The following day, the culture was spun out, supernatant was removed, and cells were re-suspended in 100 µL fresh LB, and plated onto LB-Cm agar plates, selecting Cm^R. Transformants were re-streaked onto new LB agar plates, colonies purified, and whole-colony PCR amplification was performed using primers, AG1 and AG2, and DNA sequencing verified the desired mutation(s).

2.3 Genomic DNA purification and SMARTer 5' RACE protocol

We used the SMARTer® RACE 5'/3' Kit (Clontech Laboratories, Inc) to identify the transcription start site of the *mgtA* gene in strains TL 4295, TL 5055 and TL 5493 (Table 2.1). Sanger Sequencing at the Low Throughput Laboratory (Purdue University) was performed using primer, AG2, to reveal the 5' ends of complementary DNA (cDNA) templates that were generated for strains TL 4295, TL 5055 and TL 5493.

2.4 β-Galactosidase assay

β-Galactosidase assays were carried out at mid-exponential phase in defined M63, or at indicated time points in "Mg^{2+}-free" M63, in three independent experiments, performed in duplicate or triplicate, as described by Miller (1991). Values for OD_{420} and OD_{600} were measured using a UV-1700 PharmaSpec Spectrophotometer (Shimadzu). The following modifications were used: two or three micro-centrifuge tubes were brought to a volume of 1.0 mL with Z-buffer each with 0.05 ml, 0.10 ml, and/or 0.20 ml of cells that had been re-suspended in Z-buffer. Cells were lysed with 50 or 100 µl of 0.1% SDS and 50 or 100 µl of $CHCl_3$. The reaction was started by the addition of 0.170 ml ONPG and stopped by the addition of 0.430 ml 1 M Na_2CO_3. β-Galactosidase activity is expressed as Miller units, and calculated by the following formula:

$$\text{β-Galactosidase activity (Miller units)} = 1000 \times [(OD_{420})/(T \times V \times OD_{600})].$$

2.5 Bacterial strains

Table 2.1. List of bacterial strains

Name	Genotype	Source or construction
***Salmonella enterica* serovar Typhimurium**		
TH 4583	trpE91 tufA499 (Gln125Arg) tufB441::MudJ rne-2 zcg-9076::Tn10dTet	From D. Hughes
TL 1	wild type LT2	From J. L. Ingraham
TL 155	*hsdL6 hsdSA29 metA22 metE55 ilv?rpsL120 xyl-404 H1-b nml H2-enx* (Fels2)	From J. L. Ingraham
TL 126	Δ*proBA-47 F'128 proBA-74 lacZ*$^+$	L. Csonka (1988)
TL 1483	*hisD9953::MudJ* (*lacZ::*Tn*10*)	D. Overdier (1988)
TL 3259	Δ*proBA-47* Δ*putPA-557 proP1654*	L. Csonka (1982)
TL 3331	*rpoS::Ap*^{R}	Smith et al. (1998)
TL 3360	*5' LR* (chr-2) *mgtB*$^+$	O'Connor et al. (2009)
TL 4295	*mgtA9226::MudJ* (wild-type transcriptional fusion)	Smith et al. (1998)
TL 4299	*phoP1028::Tn10d-Cm*^{R}	
TL 4385	*5' LR* (UTR$^{re\text{-}100}$) *mgtA9226::MudJ*	Cromie et al. (2006)
TL 4514	*5' LR* (UTR$^{re\text{-}100}$) *mgtA9226::MudJ phoP7953::Tn10*	This study
TL 4523	*mgtL* (C98T) *mgtA*$^+$	O'Connor et al. (2009)
TL 4575	*mgtL* (C98T) *mgtA9226::MudJ*	This study
TL 4576	*mgtL* (A86C) *mgtA9226::MudJ*	This study
TL 4646	*mgtB12::MudJ*	Blanc-Potard and Groisman (1997)
TL 4674	*mgtA9226::MudJ* Δ*proBA-47* Δ*putPA-557 proP1654*	This study
TL 4697	*5' LR* (Δ9-244) *mgtA9226::MudJ*	This study
TL 4701	*mgtL* (C85-ACCCTGA-A86) *mgtA9226::MudA*	This study
TL 4704	*mgtA9226::MudA* rob::Kn^R	This study
TL 4705	*mgtA9226::MudJ phoQ5996::Tn10*	This study
TL 4854	*mgtA9226::MudJ* Δ*proBA-47*	This study
TL 4892	*mgtA9226::MudA*	Smith et al. (1998)
TL 4960	*hisD9953::MudJ*	From T. Elliot
TL 5055	*5' LR* (G138A) *mgtA9226::MudJ*	This study
TL 5132	*5' LR* (G138A) *mgtA9226::MudA rob::*Kn^R	This study
TL 5123	*mgtL* (selective marker) *mgtA9226::MudA*	From K. Datsenko
TL 5125	*mgtL* (C-deficient) *mgtA9226::MudA*	This study
TL 5131	*mgtL* (A86C) *mgtA9226::MudJ rob::*Kn^R	This study
TL 5133	*5' LR* (G138A) *mgtA9226::MudA phoP1028::Tn10d-Cm*^{R}	This study
TL 5135	Δ*mgtL* (Δ71-124) *mgtA9226::MudA*	This study
TL 5139	*mgtL* (G120C) *mgtA9226::MudA*	This study
TL 5143	*mgtL* (A86C, G120C) *mgtA9226::MudA*	This study
TL 5151	*rpmA* (G23A) *mgtA9226::MudJ*	This work
TL 5176	up-9251::Cm^R *plac*$_{1\text{-}6}$ *mgtA9226::MudA*	Cromie et al. (2006)
TL 5198	*mgtA9226::MudJ phoP1028::Tn10d-Cm*^{R}	This study
TL 5200	*mgtL* (A86C) *mgtA9226::MudJ phoP1028::Tn10d-Cm*^{R}	This study
TL 5216	*mgtL* (G138A) *mgtA9226::MudJ phoQ5996::Tn10*	This study
TL 5282	TL 155 Δ*efp::Cm*^{R}	This work
TL 5332	*mgtA9226::MudJ* Δ*efp::Cm*^{R}	This work
TL 5409	*5' LR* (Δ64-147) *mgtA9226::MudA phoP1028::Tn10d-Cm*^{R}	This study
TL 5453	*5' LR* (Δ64-147) *mgtA9226::MudA*	This study
TL 5493	*5' LR* (G138A) *mgtA9226::MudJ phoP1028::Tn10d-Cm*^{R}	This study

Table 2.1, continued

Name	Genotype	Source or construction
***Salmonella enterica* serovar Typhimurium**		
TL 5508	*mgtL-lacZ (MudJ) mgtA*$^{--}$	This study
TL 5527	*mgtA774::MudK* (wild-type translational fusion)	N. Figueroa-Bossi (2006)
TL 5528	*5' LR* (CC60-61AA) *mgtA774::MudK*	From N. Figueroa-Bossi
TL 5529	*5' LR* (GG62-63AA) *mgtA774::MudK*	From N. Figueroa-Bossi
TL 5530	*mgtL* (C98T) *mgtA9226::MudJ phoP1028::Tn10d-Cm*^{R}	This study
TL 5531	*5' LR* (Δ9-244) *mgtA9226::MudJ phoP1028::Tn10d-Cm*^{R}	This study
TL 5562	*mgtL* (A71C) *mgtA774::MudK*	From N. Figueroa-Bossi
TL 5563	*5' LR* [GGCA(203-206)TTAT] *mgtA774::MudK*	From N. Figueroa-Bossi
TL 5565	*5' LR* [GCCTG(219-223)CGGAC] *mgtA774::MudK*	From N. Figueroa-Bossi
TL 5566	*5' LR* (GG62-63AA) *mgtA774::MudK* IG$^{[rhlB\text{-}trxA]}$::Tpop Y80C-*rho*	From N. Figueroa-Bossi
TL 5567	*5' LR* [GG62-63AA, GGCA(203-206)TTAT] *mgtA774::MudK*	From N. Figueroa-Bossi
TL 5569	*5' LR* (GG62-63AA) *mgtL* (A71C) *mgtA774::MudK*	From N. Figueroa-Bossi
TL 5571	*mgtL* (CC118-119AA) *mgtA774::MudK*	From N. Figueroa-Bossi
TL 5573	*mgtA9226::MudJ* IG$^{[rhlB\text{-}trxA]}$::Tpop Y80C-*rho*	This study
TL 5606	*mgtL* (G120C) *mgtA9226::MudA* IG$^{[rhlB\text{-}trxA]}$::Tpop Y80C-*rho*	This study
TL 5607	*5' LR* (CC60-61AA) *mgtA774::MudK* IG$^{[rhlB\text{-}trxA]}$::Tpop Y80C-*rho*	This study
TL 5609	*mgtL* (CC118-119AA) *mgtA774::MudK* IG$^{[rhlB\text{-}trxA]}$::Tpop Y80C-*rho*	This study
TL 5622	*mgtA774::MudK* IG$^{[rhlB\text{-}trxA]}$::Tpop Y80C-*rho*	From N. Figueroa-Bossi
TL 5634	*mgtL* (ΔT111) *mgtA9226::MudA*	From N. Figueroa-Bossi
TL 5638	Δ*efp::Cm*^{R}	This study
TL 5666	*mgtL* (C77T, C84T, C89T) *mgtA9226::MudA*	This work
TL 5667	*mgtL* (C77T, G80T, C84T, C89T) *mgtA9226::MudA*	This work
TL 5692	*rpmE::Cm*^{R} *mgtA9226::MudA*	This work
TL 5716	*mgtL* (C77T, C84T, C89T) *5' LR* (G138A) *mgtA774::MudK*	This study
TL 5734	*5' LR* [GGCA(203-206)TTAT] *mgtA774::MudK* IG$^{[rhlB\text{-}trxA]}$::Tpop Y80C-*rho*	From N. Figueroa-Bossi
TL 5815	*trmA::Cm*^{R} *mgtA9226::MudJ*	From S. Porwollik
TL 5817	*trmB::Cm*^{R} *mgtA9226::MudJ*	From S. Porwollik
TL 5819	*trmE::Cm*^{R} *mgtA9226::MudJ*	From S. Porwollik
TL 5821	*mgtA9226::MudJ phoB::Cm*^{R}	From S. Porwollick
TL 5829	*mgtL-lacZ (MudJ) mgtA*$^{--}$ Δ*efp::Cm*^{R}	This study
TL 5833	*mgtA9226::MudA lepA::Kn*^{R}	From S. Porwollick
TL 5836	*rpmF::Kn*^{R} *mgtA9226::MudA*	From S. Porwollik
TL 5839	*mgtA9226::MudJ* S93N-*phoP phoQ5996::Tn10*	Cromie et al. (2006)
TL 5847	S88L-*trmD* (ts) *Cm*^{R} *mgtL-lacZ (MudK) mgtA*$^{-}$	This work
TL 5848	S88L-*trmD* (ts) *Cm*^{R} *mgtL* (C77T, C84T, C89T) *mgtA9226::MudA*	This work
TL 5850	*mgtA9226::MudJ* Δ*proBA-47* Δ*putPA-557 zcc-5::Tn10*	This study
TL 5855	*mgtA9226::MudJ* Δ*proBA-47 proP1654 zcc-5::Tn10*	This study
TL 5856	S88L-*trmD* (ts) *Cm*^{R} *mgtA9226::MudJ*	This work
TL 5860	S88L-*trmD* (ts) *Cm*^{R} *mgtB12::MudJ*	This work
TL 5861	S88L-*trmD* (ts) *Cm*^{R} *hisD9953::MudJ*	This work
TL 5862	*mgtL-lacZ (MudJ) mgtA*$^{--}$ *rpmE::Cm*^{R}	This study
TL 5863	*mgtL-lacZ (MudJ) mgtA*$^{--}$ G23A-*rpmA*	This study
TL 5873	*mgtA9226::MudJ sdiA::Cm*^{R}	From S. Porwollick
TL 5874	*5' LR* (G138A) *mgtA9226::MudJ sdiA::Cm*^{R}	This study

Table 2.1, continued

Name	Genotype	Source or construction
***S. enterica* serovar Typhimurium**		
TL 5876	*tufB441::MudJ (lacZ::Tn10)*	From D. Hughes
TL 5877	*mgtA9226::MudA phoP1028::Tc^R phoR::*Kn^R	This study
TL 5879	*5' LR* (G138A) *mgtA9226::MudJ phoB:: Cm^R*	This study
TL 5880	*mgtL-lacZ (MudA) mgtA*$^-$	This study
TL 5917	*mgtA9226::MudA tufB::MudJ (lacZ::Tn10)*	This study
TL 5918	*mgtA9226::MudJ* Δ*proBA-47 proP1688::Mud1-8*	This study
TL 5926	*mgtL-lacZ (MudA) mgtA*$^-$ *tufB::MudJ (lacZ::Tn10)*	This study
TL 5927	*mgtL-lacZ (MudA) mgtA*$^-$ *lepA::Kn^R*	This study
TL 5928	*mgtL-lacZ (MudA) mgtA*$^-$ *rpmF::Kn^R*	This study
TL 5932	*mgtL* (C-def) *mgtA9226::MudA* IG$^{[rhlB\text{-}trxA]}$::Tpop Y80C-*rho*	This study
TL 5933	*5' LR* (G138A) *mgtA9226::MudA phoP1028::Tc^R phoR::*Kn^R	This study
TL 5980	ATCC 14028 *mgtA9226::MudJ*	This study
TL 5981	ATCC 14028 *mgtL* (C98T) *mgtA9226::MudJ*	This study
TL 5982	ATCC 14028 *5' LR* (Δ9-244) *mgtA9226::MudJ*	This study
TT 1232	LT2 *argG1895::Tn10*	From J. R. Roth

2.6 Plasmids list

Table 2.2. List of plasmids

Plasmid	Genotype	Genotype
pKD3	*repR_{R6K} Cm^R*	Datsenko and Wanner (2000)
pKD13	*repR_{R6K} Kn^R*	Datsenko and Wanner (2000)
pKD46	*rep$_{pSC101}{}^{ts}$ Ap^R p$_{araBAD}$ γ β exo*	Datsenko and Wanner (2000)

2.7 Primers list

Table 2.3. List of primers used in this work

Name	Sequence contained (5' to 3')	Comments
AG1 and AG2	TATCGCTTTGTCCCCGCAT and AGTACTACCGGCGCCATGAC	Used for amplifying nucleotides 4,699,118 to 4,700,610 to determine the location of *mgtA*-linked mutations.
AG3 and AG7	TGATTTCCCTACGCCGCTCAGGCGGGCGATGTCTTTGATA and CTTACACACCGGTAAGACAGCAGAGGCA GGCTTACCTAAACAAAAAAATTCTCCATCT CGGTAAAGGTGTTGGTTCAGGATCCATGT CGCCTCCGGTAAGTAAATAATTTGCGCCG; underlined sequences denote *mgtL* containing mutation(s)	Used for constructing the C-deficient mutation by amplifying nucleotides 4,699,248 to 4,699,578 containing the up-Cm^R cassette and *mgtL*.
AG3 and AG42	TGATTTCCCTACGCCGCTCAGGCGGGCGATGTCTTTGATA and ACTGTCTTACACACCGGTAAGACAGCAGA GGCAGGCTTACGGGAAAAGGAAAATTC; underlined sequences denote *mgtL* containing mutation(s)	Used for constructing the G120C mutation by amplifying nucleotides 4,699,248 to 4,699,583 containing the up-Cm^R cassette and *mgtL*.
AG8 and AG9	CTGGATGAGGTGAAAAGCCC and CTGTTCCTTCCTGCTACAGT	Used for amplifying nucleotides 3,456,290 to 3,457,838 to determine the location of unlinked mutation in *nusA* gene.

Table 2.3, continued

Name	Sequence contained (5' to 3')	Comments
AG45 and AG46	ATGGCGACTTACTATAGCAACGATTTTC GTTCCGGTGTGTAGGCTGGAGCTGCTTC and TTATTTTACGCGGGATACGTATTCGCCG GAACGGGTATTCCGGGGATCCGTCGACC; underlined sequences match the universal primers P1 and P4 flanking the Cm^R in plasmid pKD3	Used for constructing the Δ*efp*::Cm^R insertion by linear recombination by replacing sequences from 4,579,646 to 4,580,140 with Cm^R.
AG47 and AG48	ATCCGCGGCGCAAATTATTTACTTACCGG AGGCGACGCCTGCCTCTGCTGTCTTAC and ACTGTCTTACACACCGGTAAGACAGCA GAGGCAGGCGTCGCCTCCGGTAAGTAAAT; underlined sequences denote complementary base-pairing	Used for constructing the Δ*mgtL (Δ71-124)* mutation by complementary base-pairing with each other and excising nucleotides 4,699,458 to 4,699,583.
AG49 and AG42	ATCCGCGGCGCAAATTATTTACTTACC GGAGGCGACATGGACCCTGAACCCCCCCC and ACTGTCTTACACACCGGTAAGACAGCAGA GGCAGGCTTACGGGAAAAGGAAAATTC; underlined sequences denote *mgtL* containing mutation(s)	Used for constructing the A86C, G120C mutation by amplifying nucleotides 4,699,458 to 4,699,583 containing the *mgtL* mutations.
AG64 and AG65	TTAATTACGTAACGGTATGATACCGCCAT AATTGCCTCGGCGCGGAGGGATTACCT and TAATGATTTTTAGCATAGGTAATCCCTC CGCGCCGAGGCAATTATGGCGGTATCAT; underlined sequences denote complementary base-pairing	Used for constructing the Δ*5' LR (Δ9-244)* mutation by complementary base-pairing with each other and excising nucleotides 4,699,396 to 4,699,703.
AG71 and AG72	TAACAATTTCAGAGGGCCTT and ATTTTTCCCGATAACGTAAA	Used for amplifying nucleotides 4,579,590 to 4,580,196 to verify correct replacement of *efp* gene with Cm^R.
AG105 and AG106	TCTTCATGTATTGATGGTAG and ATGCCAATGCCTGCCTGCTG	Used for amplifying nucleotides 3,472,346 to 3,473,212 to determine the location of *rpmA* (G23A) mutation.

2.8 Supplements list

Table 2.4. List of supplements used in this work

Antibiotic	Amount used
Ampicillin	100 μg/mL
Chloramphenicol	12.5 μg/mL
Kanamycin	25 μg/mL
Tetracycline	20 μg/mL
Carbon source	**Amount used**
Glucose	10 mM
Succinate	20 mM
Amino acid	**Amount used**
Proline	0.4 or 2 mM
Histidine	0.2 mM
Reagent	**Amount used**
ONPG	4 mg/mL

CHAPTER 3. MAGNESIUM REGULATES TRANSCRIPTION OF *MGTA* IN *SALMONELLA ENTERICA* SEROVAR TYPHIMURIUM VIA PROLYL-BOND FORMATION DURING TRANSLATION OF THE LEADER PEPTIDE MGTL

3.1 Introduction

Magnesium is important for many cellular processes, including enzyme activity, nucleoside triphosphate-dependent phosphorylation reactions, and nucleic acid, protein and lipid stability (Silver, 1996). Furthermore, Mg^{2+} homeostasis is associated with thermotolerance in the food-borne pathogen *Salmonella enterica* (referred to, hereafter, as *Salmonella*), since survival of this organism at high termperature can be dramatically increased by the overproduction of Mg^{2+} transport proteins (O'Connor et al., 2009). *Salmonella* has three uptake systems for Mg^{2+}: CorA, which is a bi-directional channel, and MgtA and MgtB, which are P-type ATPase transporters. CorA is constitutively expressed, whereas Mg^{2+}-limitation induces MgtA and MgtB over a 100-fold at the level of transcription (Papp-Wallace and Maguire, 2008).

Transcription of the *mgtA* and *mgtB* genes (the latter gene resides in the middle of a virulence operon containing *mgtC* and *mgtR*) is dependent on the PhoQP two-component system, in which the inner membrane protein, PhoQ, phosphorylates and dephosphorylates the DNA-binding transcriptional regulator, PhoP, in response to periplasmic stimuli (Soncini et al., 1996). The PhoQP system directly or indirectly regulates the transcription of ~5% of the genes of *Salmonella* and *Escherichia coli* (Monsieurs et al., 2005; Park and Groisman, 2014), including the *phoQP* operon itself, and genes involved in virulence, cell membrane composition, antimicrobial peptide resistance, acid stress resistance (Groisman, 2001). The kinase activity of PhoQ is stimulated by a diverse set of signals, including low concentrations of Mg^{2+} (Groisman, 1998), acidic pH (Alpuche Aranda et al., 1992), and a number of antimicrobial peptides (Bader et al., 2005). Because the cytoplasms of macrophages and phagosomes are acidic and limiting for Mg^{2+}, it

has been proposed that *Salmonella* uses the PhoQP system to induce virulence genes that are needed for growth inside host cells (Groisman, 1998; Heithoff et al., 1999; Prost and Miller, 2008).

Superimposed on PhoQP-dependent regulation is a second layer of control of *mgtA* transcription. The *mgtA* mRNA has a 264 nucleotide-long 5' leader region (LR) that contains self-complementary sequences predicted to form mutually-exclusive secondary structures (stem loops "A" and "B" vs. stem loop "C"; Fig. 3.1) (Cromie et al., 2006). Originally, it was proposed that the 5' LR mRNA functions as a riboswitch that can adopt alternative secondary structures depending on intracellular concentrations of Mg^{2+}, and can regulate whether transcription is terminated upstream or allowed to continue into the *mgtA* structural gene (Cromie et al., 2006). According to this model, high Mg^{2+} concentrations favor the formation of stem loops A and B, which expose a *R*ho-*ut*ilization (*rut*) site at which the Rho helicase terminates transcription, while low Mg^{2+} concentrations promote formation of stem loop C, which sequesters the *rut* site and blocks Rho-dependent transcription termination (Cromie et al., 2006; Hollands et al., 2012). Subsequently, two groups discovered a short open reading frame (ORF), called *mgtL*, within the *mgtA* 5' LR, which encodes a proline-rich leader peptide that is highly conserved in *Enterobacteriaceae* (Fig. 3.1) (Park et al., 2010; Zhao et al., 2011). This feature is reminiscent of the *trp*, *his*, and some other amino acid biosynthetic operons (Yanofsky, 1981), in which the efficiency of translation of the leader peptide regulates termination or read-through of transcription into the first structural gene of the operon. However, the two groups that identified *mgtL* arrived at opposing conclusions for the role of intracellular proline (Pro) in the regulation of *mgtA* expression. Park et al. (2010) suggested that low levels of Pro-charged $tRNA^{Pro}$ during amino acid starvation increases expression of *mgtA*, whereas Zhao et al. (2011) concluded that intracellular Pro has no role in *mgtA* regulation.

Several questions about the model of transcriptional control of *mgtA*, nevertheless, have been unresolved. 1) It is unclear how the proposed Mg^{2+}-sensing riboswitch could form alternative secondary structures in order to govern termination or read-through of transcription, while translation of *mgtL* simultaneously affects the folding of the 5' LR mRNA. In addition, 2) it is unclear whether Mg^{2+}-sensing is carried out entirely by the riboswitch or whether translation of *mgtL* plays a role in this process. Finally, 3) it is not obvious why the abundance of Pro should be physiologically connected to the regulation of an

Mg^{2+} transporter gene. Providing answers to these questions will improve our understanding of the transport and homeostasis of Mg^{2+} in *Salmonella* and its role in host infection.

We addressed these issue by constructing a number *Salmonella* serovar Typhimurium strains that carry novel, *cis*- and *trans*-acting mutations resulting in altered expression of *mgtA*. Based on our results, we propose that translation of the Pro codons of *mgtL* is sensitive to the intracellular concentrations of Mg^{2+}, and provides the regulatory stimulus via ribosome-mediated transcriptional control of *mgtA*. We further show that both EF-P and TrmD are involved in the regulation of *mgtL* translation. These are significant findings given that EF-P is required to relieve ribosomes stalled at poly-Pro codons (Katz et al., 2013), and TrmD is required to methylate the guanine at position 37 (m^1G37) of Pro-charged $tRNA^{Pro}$ to ensure efficient translation of Pro codons (Christian et al., 2004), and is dependent on Mg^{2+} for methylation of $tRNA^{Pro}$ (Sakaguchi et al., 2014). The finding that both EF-P and TrmD regulate *mgtL* emphasizes the importance of translation of the Pro codons in *mgtL* and its role in Mg^{2+}-sensing in the regulation of *mgtA*.

3.2 Results

3.2.1 Poly-Pro and premature translation termination mutations in *mgtL* induce *mgtA* expression

To study the transcriptional regulation of *mgtA*, we use strains carrying *mgtA-lacZ* transcriptional fusions that enable the measurement of β-galactosidase activity as the readout for transcription of *mgtA*. Expression of *mgtA-lacZ* is repressed on MacConkey agar, giving rise to a Lac^{-} (white) phenotype. By selecting Lac^{+} (red) mutants on MacConkey agar, we isolated derivatives carrying spontaneous mutations linked to the *mgtA-lacZ* fusion that conferred increased expression of this fusion. Of 14 independent mutants, 13 acquired the identical A86C point mutation (Fig. 3.1), which results in a threonine-to-proline substitution at codon 6 in *mgtL*, generating a stretch of three contiguous Pro codons (Fig. 3.3A). This stretch of three Pro residues may constitutive a ribosome-stalling motif sequence that has been previously studied (Doerfel et al., 2013; Pavlov et al., 2009; Tanner et al., 2009; Ude et al., 2013). While *mgtA-lacZ* expression in the wild type was de-repressed by 7-fold upon lowering Mg^{2+} from 1.6 mM (high) to 0.016 mM (low), the *mgtL* (A86C) mutant exhibited a 13-fold increased expression of the *mgtA-lacZ* fusion at high Mg^{2+}, compared to the wild type (Fig. 3.2). The constitutively "ON" phenotype of the *mgtL* (A86C) mutant

Figure 3.1

Alternative RNA structures of the 5' leader region and regulation of the *Salmonella mgtA* gene in response to Mg^{2+}-sensing via prolyl-bond formation during translation of *mgtL*. Dashed boxes denote regulatory events in response to low Mg^{2+} (e.g. PhoP-dependent transcription activation, ribosome stalling and transcription elongation into the *mgtA* coding region) and high Mg^{2+} (e.g. TrmD-mediated methylation of $tRNA^{Pro}$, complete translation of *mgtL*, and Rho-dependent transcription termination). The *R*ho-*ut*ilization (*rut*) site is exposed in high Mg^{2+} for Rho helicase to bind (denoted by arrowhead). Proline codons are denoted with yellow boxes. Nucleotide substitutions labeled in green and red denote mutations that result in the constitutively "ON" and "OFF" phenotypes, respectively.

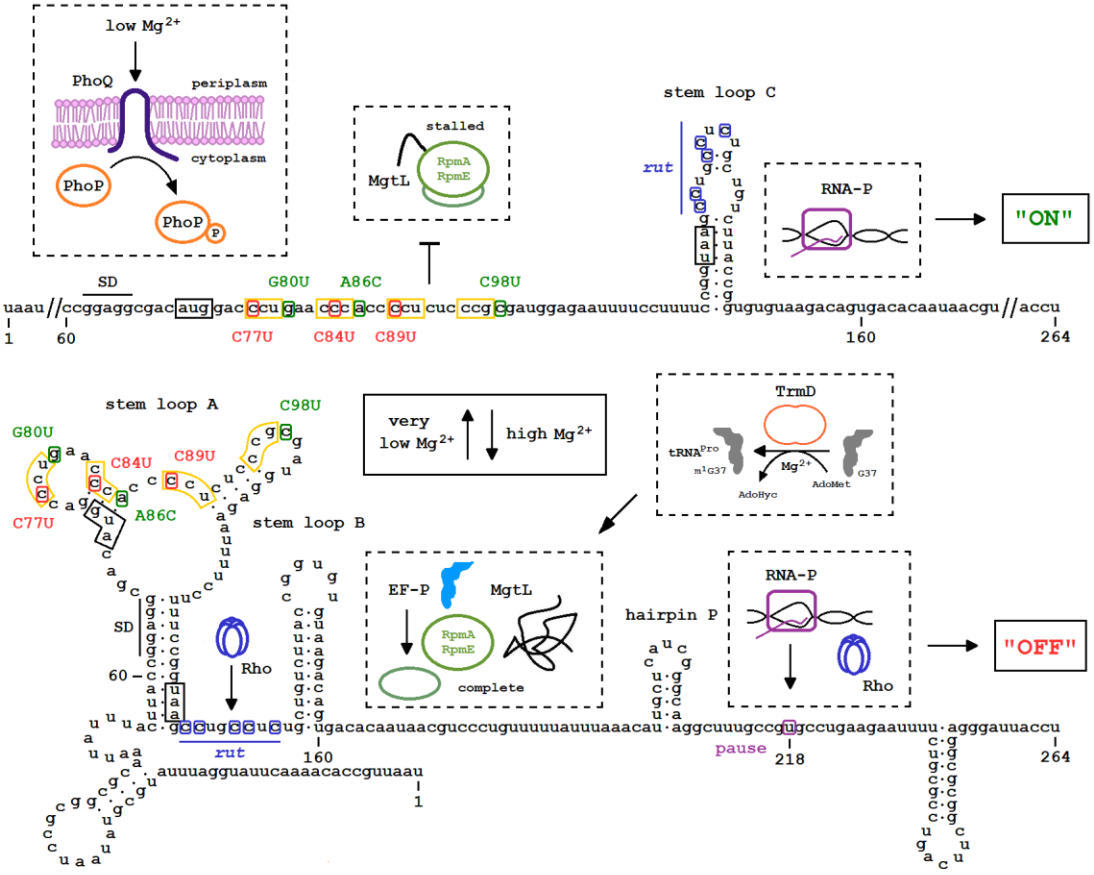
low Mg2+
PhoQ
periplasm
cytoplasm
PhoP
PhoP
P
stalled
MgtL
RpmA
RpmE
stem loop C
rut
RNA-P
"ON"
SD
G80U
A86C
C98U
uaau//ccggaggcgacaugacccuggaaccccaccuccuccgggauggagaauuuuccuuuuc·gugugaagacagugacacaauaacgu//accu
1
60
C77U
C84U
C89U
160
264
stem loop A
C98U
G80U
C84U
C89U
C77U
A86C
stem loop B
very
low Mg2+
high Mg2+
TrmD
tRNAPro
m1G37
Mg2+
G37
AdoHyc
AdoMet
SD
60
Rho
rut
160
1
EF-P
MgtL
RpmA
RpmE
complete
hairpin p
RNA-P
Rho
"OFF"
pause
218
264

Figure 3.1

generated by the poly-Pro mutation underscores that ribosome stalling may be involved in the Mg^{2+}-sensing regulation of *mgtA* transcription at the level of *mgtL* translation.

The remaining mutant carries a C98T transition (Fig. 3.1) that results in an arginine to nonsense substitution at codon 10 in *mgtL* (Fig. 3.3B), and exhibits a 27-fold increased expression of the *mgtA-lacZ* fusion at high Mg^{2+} (Fig. 3.2). The same allele was previously obtained in an *mgtA*$^{+}$ background during the selection of mutations that confer enhanced thermotolerance (O'Connor et al., 2009). The fact that this and other premature nonsense mutations in *mgtL* (Park et al., 2010) elevate the transcription of *mgtA* supports the notion that impairment of the translation of *mgtL* enables transcription to continue into the *mgtA* structural gene. The *mgtL* (C98T) mutation is not predicted to significantly affect folding of the *mgtA* 5' LR mRNA but only the amino acid sequence of *mgtL*. Our results and those by Park et al. (2010) support the notion that translation of *mgtL* influences folding of the 5' LR mRNA to adopt either the stem loop B (*rut* available) or stem loop C (*rut* blocked) conformation, leading to termination by Rho or read-through transcription into the *mgtA* structural gene, respectively.

3.2.2 Mutations in the ribosomal proteins L27 and L31 genes induce *mgtA* expression

As described in Materials and Methods (Section 3.4), we obtained a mutation in the *rpmA* gene that resulted in a 23-fold increased expression of the *mgtA-lacZ* fusion at high Mg^{2+} (Fig. 3.2). The *rpmA* mutation is a G23A transition that changes glycine at position 8 to glutamic acid in the N-terminus of the RpmA protein. After finding that mutation of a ribosmal protein can overcome the down-regulation of *mgtA* by high Mg^{2+}, we tested the effect of another ribosomal mutation on the expression of *mgtA*. Deletion of the *rpmE* gene, which encodes ribosomal protein L31 (Eistetter et al., 1999) and does not affect cell viability, resulted in a 11-fold increased expression of the *mgtA-lacZ* fusion at high Mg^{2+} (Fig. 3.2). Both the *rpmA* (G23A) and *rpmE::Cm*^{R} mutations are likely to impair the formation of peptide bonds, and therefore, our results support the notion that the efficiency of translation of *mgtL* may be important for the control of *mgtA* expression.

3.2.3 Deletion of the translation elongation factor P gene induces *mgtA* expression

Elongation factor P (EF-P) is a universal ribosome-binding protein that releases ribosomes stalled at poly-Pro stretches (Katz et al., 2013). We made a Δ*efp::Cm*^{R} mutant by the protocol of Datsenko and Wanner (2000). This mutation confers a 10-fold increased expression of the *mgtA-lacZ* fusion at high Mg^{2+} (Fig. 3.2). However, mutations in the *tufA*, *tufB*, and *lepA* genes, which encode other elongation factors (Dijl et al.; Hammarlöf and Hughes, 2008; Hughes, 1990; Pech et al., 2011), did not have significant effects on the expression of *mgtA* (Fig. 3.7), suggesting that loss of EF-P specifically hinders the translation of *mgtL*, despite harboring evenly-spaced Pro codons.

3.2.4 Replacement of Pro codons in *mgtL* impairs *mgtA* expression

In order to probe the role of the Pro codons in *mgtA* regulation, we constructed an *mgtL* (C77T, C84T, C89T or 3Pro-) mutant, in which the first three Pro codons were replaced with serine, leucine and serine codons, respectively (Fig. 3.3C). Notably, these site-directed mutations are not predicted to alter the ability of the 5' LR mRNA to adopt the stem loop B or stem loop C conformation (Fig. 3.1). A similar Pro codon-deficient construct was made previously, and yet a different conclusion was proposed, one in which *mgtA* responded to Mg^{2+} despite their Pro codon-deficient construct (Park et al., 2010). We observe very low *mgtA-lacZ* expression both at high and low Mg^{2+} (Fig. 3.2). We ruled out the possibility that the *mgtL* (3Pro-) mutation "locked" the 5' LR mRNA secondary structure into a constitutively "OFF" conformation by introducing a nonsense mutation (G80T) into the Pro codon-deficient *mgtL* mutant (Fig. 3.3D), which de-repressed *mgtA-lacZ* expression similar to C98T, the other premature translation termination mutation (Fig. 3.7). These results support the notion that efficient translation of the Pro codons in *mgtL* would favor the formation of stem loop B, which enables Rho to terminate transcription.

3.2.5 The availability of Mg^{2+} positively regulates *mgtL* translation without mRNA folding

We hypothesize that Mg^{2+} facilitates translation of *mgtL* specifically during prolyl-bond formation, allowing the presence of ribosomes to subsequently dictate folding of the 5' LR mRNA. In this case, high Mg^{2+} facilitates efficient translation and favors stem loop B, by causing terminating transcription upstream

of *mgtA*. Low Mg^{2+} hinders translation of *mgtL* and favors stem loop C, promoting transcription into *mgtA* (Fig. 3.1). To test this hypothesis, we investigated the effect of Mg^{2+} on translation of an *mgtL-lacZ* translational fusion at its chromosomal locus. The 5' LR mRNA of the *mgtL-lacZ* construct does not retain the ability to adopt the alternative stem loop B and C conformations (Fig. 3.4), allowing us to directly examine the effect of Mg^{2+} on *mgtL* translation. Compared to the wild type, which was up-regulated by low Mg^{2+}, reduction in the extra-cytoplasmic Mg^{2+} concentration from 1.6 mM to 0.016 mM decreased expression of the *mgtL-lacZ* translational fusion in exponential phase cells (Fig. 3.5). In addition, introduction of each of the single *rpmA* (G23A), *rpmE::Cm*^{R} and Δ*efp::Cm*^{R} mutations into the *mgtL-lacZ* background abolished the Lac^+ phenotype of the *mgtL-lacZ* construct on MacConkey plates (Table 3.1).

We also determined the effect of Mg^{2+}-starvation on the expressions of the *mgtA-lacZ* and *mgtL-lacZ* fusions over time in cells sub-cultured in nominally "Mg^{2+}-free" M63, which may contain trace Mg^{2+}. At 3 hours, the cells were able to grow in reduced levels of Mg^{2+}, whereas by 6 hours, cells reached stationary phase due to depletion of Mg^{2+}. Addition of exogenous Mg^{2+} into a separate culture increased cell density, ruling out glucose depletion as the cause for stationary phase growth (not shown). As expected, expression of the *mgtA-lacZ* fusion was up-regulated by Mg^{2+}-starvation, exhibiting the opposite response of the *mgtL-lacZ* fusion (Fig. 3.5). Expression of *mgtL-lacZ* construct was positively correlated with the external levels of Mg^{2+}, reaching an ultimate low in translation at 6 hours (Fig. 3.5). Intriguingly, the *mgtL-lacZ* construct was expressed at higher levels at high Mg^{2+} than at low Mg^{2+}, even though the translational fusion is transcribed from the native *mgtLA* promoter in a PhoP-dependent manner. This result calls into question whether or not PhoP-dependent activation of *mgtA* is completely inhibited at high Mg^{2+} concentrations (see Discussion in Section 3.3).

3.2.6 Mutation in the Mg^{2+}-dependent and $tRNA^{Pro}$-specific methyltransferase *trmD* gene induces *mgtA* expression

TrmD is an Mg^{2+}-dependent enzyme that catalyzes methyl transfer from *S*-adenosylmethionine (SAM) to the N^1 position of G37 in all three species of Pro-charged $tRNA^{Pro}$ (Fig. 3.1) (Christian et al., 2004). TrmD methylates the G37 position of $tRNA^{Leu}$ species that recognize the CUU and CUC codons, $tRNA^{Arg}$ species

Figure 3.2

Spontaneous and site-directed mutations in *mgtL*, the ribosomal protein L27 and L31 genes, and translation elongation factor P gene induce *mgtA-lacZ* expression by a ribosome-mediated transcription attenuation-like mechanism. Strains TL 4295 (*mgtL*$^+$ *mgtA-lacZ*), TL 4576 [*mgtL* (A86C) *mgtA-lacZ*], TL 4575 [*mgtL* (C98T) *mgtA-lacZ*], TL 5151 [*rpmA* (G23A) *mgtL*$^+$ *mgtA-lacZ*], TL 5692 (Δ*rpmE mgtL*$^+$ *mgtA-lacZ*), TL 5332 (Δ*efp mgtL*$^+$ *mgtA-lacZ*) and TL 5666 [*mgtL* (3Pro-) *mgtA-lacZ*] were grown to mid-exponential phase in minimal medium M63 containing high (1.6 mM) or low (0.016 mM) Mg^{2+} at 37°C. Shown are the mean and SD from at least three independent experiments. For panel 6, the activity was lower than the resolution of the figure following growth in high and low Mg^{2+}.

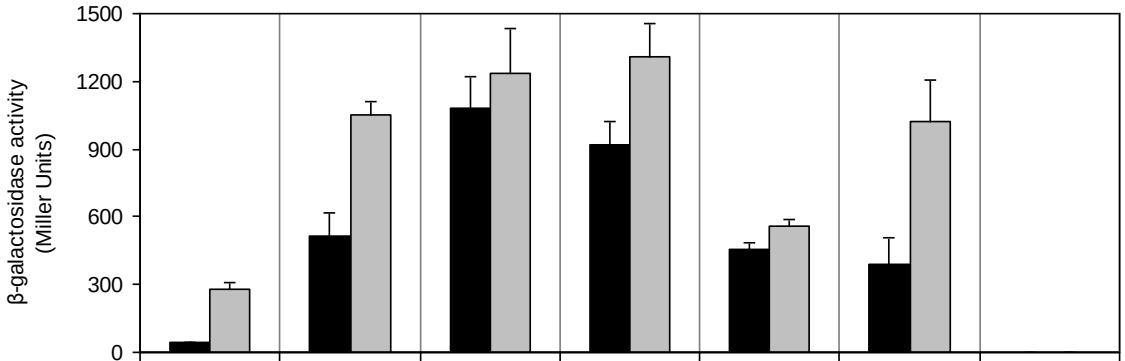

	WT	mgtL (A86C)	mgtL (C98T)	rpmA (G23A)	ΔrpmE	Δefp	mgtL (3Pro-)
■ 1.6 mM	40.6	513.2	1081.8	915.9	455.7	391.2	0.2
□ 0.016 mM	280.3	1049.6	1232.3	1312.0	557.5	1023.3	0.2

Figure 3.2

Figure 3.3

Schematics and regulation of the *mgtA* 5’ LR mRNA harboring **(A)** spontaneous poly-Pro (A86C) and **(B)** nonsense (C98T) mutations, **(C)** replacement of 3 out of the 4 Pro codons in *mgtL* (3Pro-), and **(D)** a nonsense mutation (G80T) introduced into the *mgtL* (3Pro-) background.

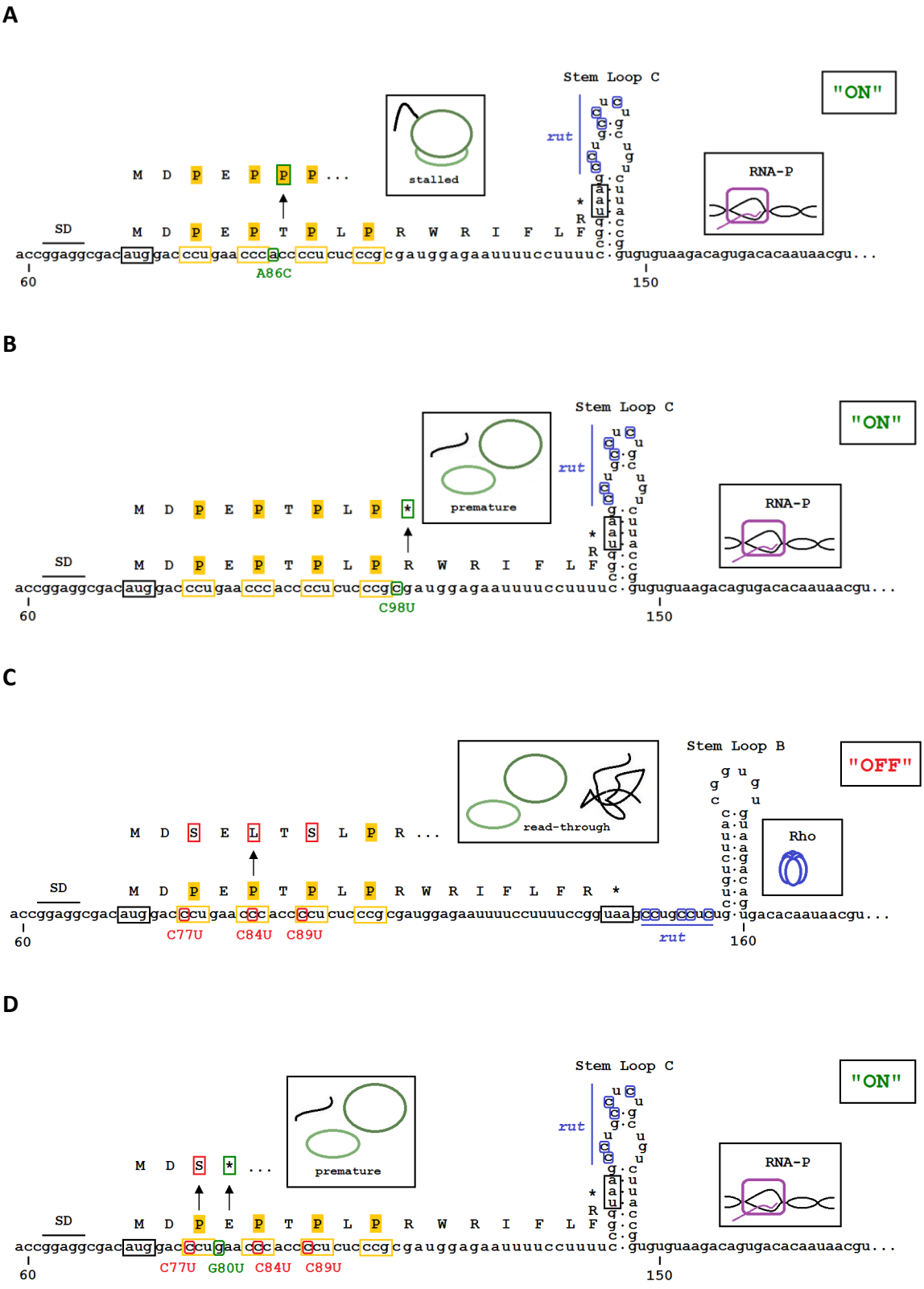
A
Stem Loop C
"ON"
stalled
rut
RNA-P
M D P E P P P ...
SD
M D P E P T P L P R W R I F L F
accggaggcgacaugGACccuGAAcccACCccuCUCccgCGAUGGAGAAUUUUCCUUUUC·GUGUGUAAGACAGUGACACAAUAACGU...
60
A86C
150
B
Stem Loop C
"ON"
premature
rut
RNA-P
M D P E P T P L P *
SD
M D P E P T P L P R W R I F L F
accggaggcgacaugGACccuGAAcccACCccuCUCccgCgAUGGAGAAUUUUCCUUUUC·GUGUGUAAGACAGUGACACAAUAACGU...
60
C98U
150
C
Stem Loop B
"OFF"
read-through
Rho
M D S E L T S L P R ...
SD
M D P E P T P L P R W R I F L F R *
accggaggcgacaugGACCcuGAACCCACCCcuCUCccgCGAUGGAGAAUUUUCCUUUUCCGGuaaGCCUGCCUCUG·UGACACAAUAACGU...
60
C77U C84U C89U
rut
160
D
Stem Loop C
"ON"
premature
rut
RNA-P
M D S * ...
SD
M D P E P T P L P R W R I F L F
accggaggcgacaugGACCcuGAACCCACCCcuCUCccgCGAUGGAGAAUUUUCCUUUUC·GUGUGUAAGACAGUGACACAAUAACGU...
60
C77U G80U C84U C89U
150

Figure 3.3

Figure 3.4

Reporter fusions of *lacZ* to *mgtA* and to *mgtL*. **(A)** Schematics for the transcriptional fusion of *mgtA* to *lacZ* from the MudJ cassette at the chromosomal locus of *mgtA* and the in-frame translational fusion of *mgtL* to *lacZ* from the MudK cassette at the chromosomal locus of *mgtL*. **(B)** Nucleotide and amino acid sequence of the in-frame translational fusion of *mgtL* to *lacZ* from the MudK cassette.

A

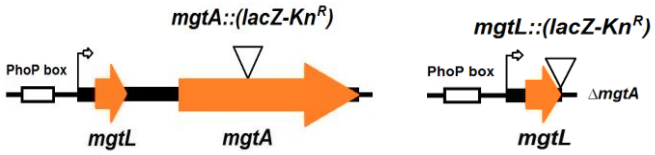

mgtA-*lacZ*
transcriptional fusion

mgtL-*lacZ*
translational fusion

B

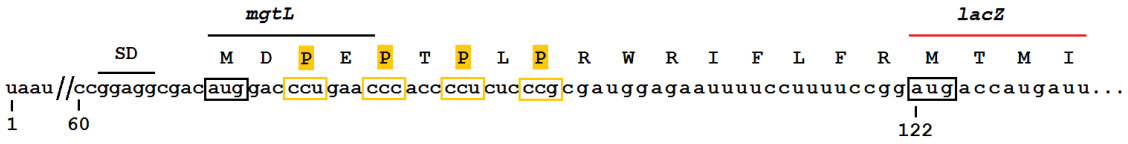

Figure 3.4

Figure 3.5

Translation of *mgtL* responds to the extra-cytoplasmic Mg^{2+} concentration in the opposite correlation to transcription of *mgtA*. Strains TL 4295 (*mgtL*$^{+}$ *mgtA-lacZ*) and TL 5508 (*mgtL-lacZ*) were grown as described in Fig. 3.2. Bacteria from overnight growth in LB broth were washed, sub-cultured and grown in "Mg^{2+}-free" M63 until growing phase or 3 hours (Grow; 3 hours), and stationary phase or 6 hours (Stat; 6 hours), at 37°C. Shown are the mean and SD from at least three independent experiments.

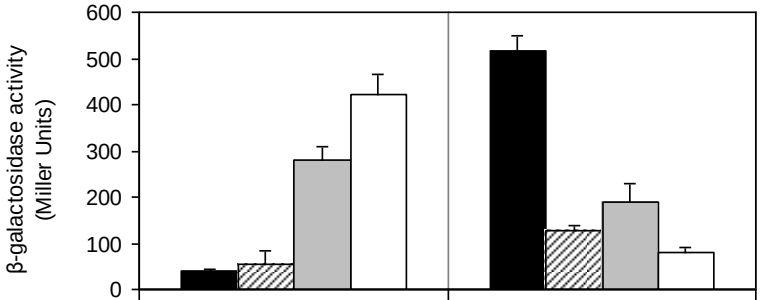

	mgtA-lacZ	mgtL-lacZ
1.6 mM	40.6	514.7
Grow (3 hrs)	55.3	126.3
0.016 mM	280.3	189.3
Stat (6 hrs)	420.1	79.4

Figure 3.5

that recognize the CGG codon and all three $tRNA^{Pro}$ species that recognize the four Pro codons (CCC, CCU, CCG and CCA) (Christian et al., 2004). Out of 17 codons, *mgtL* contains one CCC, one CCG, and two CCU Pro codons, one CUC and one CUU Leu codon, and one CGG Arg codon. Although TrmD is essential, a temperature-sensitve allele (S88L-TrmD) (Masuda et al., 2013) allowed us to test whether inhibition of G37-$tRNA^{Pro}$ methylation would decrease the efficiency of translation of the four Pro codons of *mgtL*. The S88L-*trmD* mutation interferes with the binding of *S*-adenosylmethionine (AdoMet), which TrmD uses as a substrate to methylate $tRNA^{Pro}$ at the G37 position (Masuda et al., 2013). We found that the S88L-*trmD* mutation resulted in a 19-fold increase in *mgtA-lacZ* expression at 30°C (Fig. 3.6), indicating that TrmD was partially active at the permissive temperature, as previously shown (Masuda et al., 2013). Expression of *mgtA-lacZ* at the less-permissive temperature (37°C) resulted in overall decreased levels (Fig. 3.8), most likely by affecting protein synthesis on a global scale.

Mutations in the *trmA*, *trmB*, and *trmE* genes, which encode other non-essential methyltransferases (Björk and Isaksson, 1970; Elseviers et al., 1984; Purta et al., 2005; Ranaei-Siadat et al., 2013), however, did not have significant effects on *mgtA-lacZ* expression (Fig. 3.7). Therefore, we investigated the specificity of TrmD in regulating the translation of *mgtL* by measuring the expressions of the *mgtL* (3Pro-), *mgtA-lacZ* transcriptional fusion and *mgtL-lacZ* translational fusion in the absence and presence of the S88L-*trmD* mutation. No increase in *mgtA-lacZ* expression was observed in the *mgtL* (3Pro-) mutant background by the S88L-*trmD* mutation at 30°C or 37°C, compared to the $trmD^{+}$ *mgtL* (3Pro-) mutant (Figs. 3.6 and 3.8). However, the S88L-*trmD* mutation decreased the expression of the *mgtL-lacZ* translational construct at both 30°C and 37°C (Figs. 3.6 and 3.8), supporting the role of methyltransferase activity in the translation of *mgtL*. These results indicate that the methyltransferase activity of TrmD is specific for Pro-charged $tRNA^{Pro}$, and that in the absence of Pro codons, TrmD cannot elicit its effect on translation of *mgtL*.

We used a strain harboring a *hisD-lacZ* transcriptional fusion to examine the specificity of TrmD methylation for other leader peptides. The histidine biosynthesis operon contains a leader ORF, termed *hisL*, that harbors seven contiguous histidine codons, which regulate transcription into the downstream structural genes by responding to intracellular $tRNA^{His}$ levels during translation (Chan and Landick, 1989).

The *hisD-lacZ* transcriptional fusion served as a control for the effect of TrmD on translation of leader peptides, since TrmD does not methylate $tRNA^{His}$ (Chan and Landick, 1989). Introduction of the S88L-*trmD* mutation into this background, however, did not have a significant effect on *hisD-lacZ* expression at 30°C or 37°C (Figs. 3.6 and 3.8). This result supports the fact that TrmD does not indirectly regulate translation of *hisL*, reinforcing the specificity of TrmD activity for *mgtL*.

3.3 Discussion

Multi-tiered regulation of the *Salmonella* Mg^{2+} transport gene *mgtA* has been documented over the last decade. The PhoQP two-component system was shown to activate transcription of *mgtA* (Véscovi et al., 1996), and the *mgtA* 5' LR mRNA has been proposed to function as an Mg^{2+}-sensing riboswitch that regulates Rho-dependent transcription termination or read-through at a site upstream of the *mgtA* structural gene, in response to intracellular Mg^{2+} (Cromie et al., 2006; Hollands et al., 2012). Subsequently, it was noted that translation of the Pro codon-rich *mgtL* ORF encoded in the *mgtA* 5' LR mRNA is also involved in the regulation (Park et al., 2010; Zhao et al., 2011). However, the questions of whether Mg^{2+}-sensing is mediated by direct recognition of this cation by a riboswitch or during translation of *mgtL* have not been addressed adequately. We propose that the intracellular concentration of Mg^{2+} positively regulates the efficiency of translation of *mgtL*, which in turn regulates the folding of the *mgtA* 5' LR mRNA such that Rho-dependent transcription termination occurs in high Mg^{2+} and read-through transcription into the *mgtA* structural gene occurs in low Mg^{2+}.

3.3.1 Novel mutations that clarify the role of *mgtL* translation in *mgtA* regulation

The spontaneous A86C mutation in *mgtL*, which inserts an extra Pro codon and generats three adjacent Pro codons, gave us the first insight into *mgtL* translational control of *mgtA*. Incorporation of Pro or other *N*-alkyl amino acids present an impediment to rapid translation (Pavlov et al., 2009), and studies with puromycin indicate the poor nature of Pro-charged $tRNA^{Pro}$ as a nucleophile (Muto and Ito, 2008). Nascent peptides containing stretches of Pro codons can induce ribosome stalling (Tanner et al., 2009; Ude et al., 2013). Our results for the poly-Pro mutant, which exhibited constitutively high *mgtA-lacZ* expression (Fig. 3.2), support the notion that stalling of ribosomes in *mgtL* allows the formation of stem loop C, which

Figure 3.6

Inhibition of the Mg^{2+}-dependent and $tRNA^{Pro}$-specific methyltransferase TrmD uncovers tight regulation of *mgtA* expression at 30°C. β-Galactosidase activity (Miller units) produced by *Salmonella* strains with an *mgtA-lacZ* transcriptional fusion at its chromosomal locus (TL 4295) and isogenic derivatives harboring the Pro codon-deficient mutation (TL 5666) and an *mgtL-lacZ* translational fusion (TL 5508), and *Salmonella* strain with a *hisD-lacZ* transcriptional fusion at its chromosomal locus (TL 4960), each harboring the S88L-*trmD* mutation (TL 5856, TL 5848, TL 5847 and TL 5861). Bacteria were grown as described in Fig. 3.2, except at 30°C, and TL 4960 and TL 5861 were supplemented with 0.2 mM histidine. Shown are the mean and SD from at least three independent experiments.

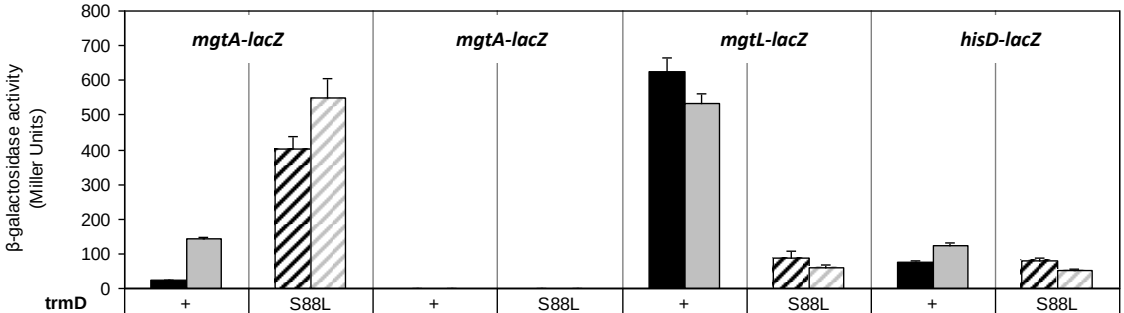

trmD	+	S88L	+	S88L	+	S88L	+	S88L
■ 1.6 mM	23.0	401.4	0.1	0.2	625.0	87.9	74.3	80.9
□ 0.016 mM	144.2	549.9	0.3	0.2	534.8	58.2	122.8	51.4
	mgtL⁺		*mgtL* (3Pro-)		*mgtL*⁺		*hisL*⁺	

Figure 3.6

sequesters the *rut* site within the mRNA secondary structure and precludes transcription termination by Rho. In addition, we isolated the C98T mutation in *mgtL*, which was characterized previously (Cromie et al., 2006; O'Connor et al., 2009), and shown to result in premature translation termination (Park et al., 2010). Despite its ability to adopt the stem loop B conformation for Rho-dependent transcription termination, the C98T mutation in *mgtL* confers the constitutively "ON" phenotype (Fig. 3.2), suggesting a different mode of regulation than the previously proposed Mg^{2+}-sensing riboswitch, since it is not predicted to significantly alter the 5' LR mRNA secondary structure.

We also characterized mutations, unlinked to *mgtA*, which could potentially be in novel, *trans*-acting genes involved in *mgtA* expression and provide insight into the mechanism of transcriptional regulation. We obtained the missense mutation (G23A) in the *rpmA* gene, which encodes the 50S ribosomal protein L27. This mutation, which generats a glycine to glutamic acid substitution at position 8 in the protein product, results in constitutively high *mgtA-lacZ* expression (Fig. 3.2). An essential component of the 50S ribosomal subunit, L27 is located near the peptidyltransferase center (PTC) of the ribosome (Wower et al., 1998). Its N-terminal end is important for stabilizing A-site tRNAs during peptidyltransfer (Trobro and Åqvist, 2008; Wang and Xiao, 2012). In addition, deletion of the *rpmE* gene, which encodes the 50S ribosomal protein L31, likewise conferred constitutively high *mgtA-lacZ* expression (Fig. 3.2). Ribosomal protein L31, which can be cross-linked to P-site tRNAs (Graifer et al., 1989), is also located near the PTC (Eistetter et al., 1999). Finally, we showed that loss of EF-P, which assists the incorporation of Pro residues into nascent peptides, also led to a 10-fold increased expression of *mgtA* at high Mg^{2+} (Fig. 3.2). Elimination of EF-P compromises *Salmonella* virulence during infection (Doerfel and Rodnina, 2013). These mutations provide evidence that the efficiency of translation of the Pro codons in *mgtL* is an important determinant of *mgtA* expression.

3.3.2 Pro codons within *mgtL* are critical for Mg^{2+}-sensing

We constructed an *mgtL* (3Pro-) mutant in which the first, second, and third Pro codons of *mgtL* were replaced by serine, leucine, and serine codons, respectively (Fig. 3.3C). In agreement with our proposed hypothesis, the *mgtL* (3Pro-) mutant exhibited the constitutively "OFF" phenotype, even in low Mg^{2+} (Fig.

3.2). In addition, upon introduction of the single *rpmA* (G23A), *rpmE::Cm*^{R} and Δ*efp::Cm*^{R} mutations into the *mgtL* (3Pro-) mutant background, we found no effect on *mgtA-lacZ* expression (Table 3.1). In the absence of Pro codons, the *mgtL* (3Pro-) mutant does not require ribosomal rescue by EF-P, and ribosomes are presumably able to complete translation of *mgtL* rapidly, which would facilitate the formation of stem loop B and thereby expose the *rut* site to Rho and terminate transcription. Both Park et al. (2010) and Zhao et al. (2011) constructed mutants in which various combinations of Pro codons in *mgtL* were substituted by codons specifying other amino acids. Because these mutants were present on plasmids, whereas our *mgtL* (3Pro-) mutation was present in single copy at its chromosomal locus, the data obtained by these authors are difficult to compare directly with ours. In addition, Park et al. (2010) reported only the ratio of the levels of mRNA specifying the *mgtA* coding region at low/high Mg^{2+} but not the effect of their Pro codon substitutions on absolute levels of *mgtA*. Nevertheless, we noted that substitutions of Pro codons diminished the sensitivity of their constructs to Mg^{2+} (Park et al., 2010; Zhao et al., 2011).

3.3.3 Translation of *mgtL* is regulated by Mg^{2+}

The data in Fig. 3.5 show that the concentration of Mg^{2+} is positively correlated with translation of *mgtL* and negatively correlated with transcription of *mgtA*. Because the *mgtA* 5' LR mRNA of the *mgtL-lacZ* construct is unable to form alternative stem loops B and C, our results support the claim that differential Mg^{2+}-sensing control of *mgtA* expression occurs at the level of *mgtL* translation and not the previously proposed Mg^{2+}-sensing riboswitch (Cromie et al., 2006; Park et al., 2010; Zhao et al., 2011).

3.3.4 PhoP-dependent activation of *mgtA* is not completely inhibited at high Mg^{2+} concentrations

One facet of the current model of *Salmonella* pathogenesis is that the PhoQP system, an important regulator of a number of virulence genes, is not active at high Mg^{2+} concentrations, that are likely found in environments where bacteria are free-living, and becomes activated when bacteria infect animal hosts where the concentration of Mg^{2+} is low (Groisman, 1998). The significance of regulation of pathogenesis-related genes by physiological concentrations of Mg^{2+} is controversial (Papp-Wallace and Maguire, 2008). In several of our mutants—e.g., the *mgtL* (A86C), *mgtL* (C98T), *rpmA* (G23A), *rpmE::Cm*^{R} and Δ*efp::Cm*^{R}

mutants (Fig. 3.2), derivatives isolated by O'Connor et al. (2009), and the *mgtL-lacZ* construct (Fig. 3.5)—the *mgtA-lacZ* transcriptional and *mgtL-lacZ* translational fusions in their respective backgrounds were expressed at high levels in minimal medium M63 containing high Mg^{2+}. In fact, some of the spontaneous, constitutively "ON" mutants were isolated as strains that formed Lac^+ colonies on MacConkey agar with a repressing Mg^{2+} concentration. Therefore, despite the decreased transcription of the *phoQP* operon and reduced phosphorylation of the PhoP protein in the presence of high Mg^{2+} (Soncini et al., 1996), transcription was initiated at high levels from the *mgtLA* promoter in these constitutively "ON" mutants. Expression of *mgtA* in these mutants still required transcriptional activator PhoP (O'Connor et al., 2009).

Because we used the non-pathogenic *S. enterica* serovar Typhimurium LT2 for our work, whereas much of the characterization of the PhoQP regulon has been carried out in the pathogenic strain ATCC 14028 (Groisman, 1998; Heithoff et al., 1999), the possibility exists that lack of repression of the *mgtLA* promoter at high Mg^{2+} might be a feature of LT2 derivatives. However, we ruled out this possibility by demonstrating that the *mgtL* (C98T) mutant, and a strain harboring deletion of the *mgtA* 5' LR (Δ9-244), were expressed at similarly high levels in both the LT2 and ATCC 14028 backgrounds even in the presence of 10 mM Mg^{2+} (Fig. 3.9). This result indicates that there is no substantial difference in Mg^{2+}-sensing by the PhoQP systems of the two strains. It has been shown by Lejona at al. (2004) that overexpression of PhoP can activate transcription of some of its target genes even in the absence of the sensor kinase PhoQ and thus Mg^{2+}-sensing. In our strains, PhoP is produced at wild-type levels; therefore, it is apparently able to function as a transcriptional activator of the *mgtLA* promoter in the constitutively "ON" mutants, activating transcription even at high Mg^{2+}concentrations.

3.3.5 Concluding remarks

The main new feature of our regulatory model for the expression of *mgtA* is that the function of the Pro codons in *mgtL* is to present a "speed bump" to translation that can be overcome by high Mg^{2+} concentrations. The efficiency of translation of *mgtL* affects the folding of the 5' LR mRNA, in which high Mg^{2+} concentrations facilitate rapid, complete translation of *mgtL*, favoring a secondary structure that exposes the *rut* site to the terminator protein Rho, thereby terminating transcription upstream of *mgtA*. On

the other hand, low Mg^{2+} concentrations result in ribosome stalling during translation of *mgtL*, favoring an alternative structure that blocks Rho, and allows read-through transcription into the *mgtA* structural gene. Our model proposes that the ribosomal proteins RpmA and RpmE, translation factor EF-P and methyltransferase TrmD contribute to the regulation of *mgtA* via translation of the Pro codons of *mgtL*, highlighting an interesting relationship among Mg^{2+} homeostasis, maintenance of protein-synthesis reading frame and $tRNA^{Pro}$ methylation. The discovery and biochemical details of which component of the translational apparatus might be the specific Mg^{2+}-sensor—e.g., RpmA, RpmE, EF-P, TrmD or some other ribosomal protein—presents an exciting area of study in understanding the regulation of *mgtA* transcription.

3.4 Supporting Information

3.4.1 SI Results

3.4.1.1 Deletion of the ribosomal protein L32 gene does not induce mgtA expression

To further investigate the influence of the 50S ribosomal subunit in *mgtA* regulation, we obtained a viable knockout of the *rpmF* gene from a *Salmonella* gene collection (Porwollik et al., 2014). Specifying ribosomal protein L32, RpmF is located near the PTC of the ribosome. Compared to the wild type, the *rpmF::Kn*^{R} mutation did not affect *mgtA-lacZ* expression (Fig. 3.7), indicating that RpmA and RpmE are specific ribosomal proteins involved in translation of *mgtL* and transcription of *mgtA*.

3.4.1.2 Mutations in the elongation factors EF-Tu or LepA genes do not induce mgtA expression

Translation efficiency is influenced by factors that contribute to accurate codon-anticodon recognition and to efficient translocation of the ribosome (Keiler, 2015). Elongation factor Tu (EF-Tu), encoded by two nearly identical genes, *tufA* and *tufB*, brings aminoacylated-tRNAs to the A-site and performs GTP hydrolysis upon accurate codon-anticodon reading (Kavaliauskas et al., 2012). The accommodated aa-tRNA in the A-site serves as the acceptor for peptidyl transfer from the P-site tRNA. After peptide-bond formation, the essential translocation factor EF-G catalyzes GTP-dependent translocation to move the A-site tRNA to the P-site and P-site tRNA to the E-site (Yamamoto et al., 2014). Elongation factor 4 (EF-4, or LepA), ubiquitous to all cells, competes with EF-G and induces back-translocation, allowing EF-G a

chance to correct errors of post-translocation of the ribosome (March and Inouye, 1985; Pech et al., 2011). We investigated the contribution of each of these translation factors in *mgtA* regulation by obtaining *tufB*$^{--}$ (Hammarlöf and Hughes, 2008) and *lepA::Kn*^{R} knockouts (Porwollik et al., 2014). Analysis showed that both the *tufB*$^{--}$ and *lepA::Kn*^{R} mutants had no major effect on *mgtA-lacZ* expression (Fig. 3.7). Introduction of the *mgtA-lacZ* transcriptional fusion into a strain harboring both the *tufA* (Q125R) and *tufB*$^{--}$ mutations retained the Lac^{--} phenotype on MacConkey agar (not shown), ruling out the possibility that TufA can functionally substitute the absence of TufB in the *tufA*$^{+}$ *tufB*$^{--}$ mutant.

3.4.1.3 Insertion of a nonsense mutation confirms that replacement of Pro codons affects mgtA expression via mgtL translation

We investigated whether the *mgtL* (3Pro-) mutant exhibited the constitutively "OFF" phenotype due to rapid, complete translation of *mgtL* or to an altered *mgtA* 5' LR mRNA secondary structure that constitutively favored the stem loop B conformation and thus transcription termination by Rho. Insertion of a nonsense mutation (G80T) within the *mgtL* (3Pro-) mutant (Fig. 3.7) resulted in a dramatic increase in *mgtA-lacZ* expression compared to the *mgtL* (3Pro-) single mutant (Fig. 3.2), supporting the claim that the ribosome indeed rapidly translates the Pro codon-deficient *mgtL* ORF.

3.4.1.4 Mutations in the methyltransferases TrmA, TrmB and TrmE genes do not induce mgtA expression

Modification of tRNAs is an important process for accurate identification and incorporation of amino acids into nascent peptides during translation (Björk et al., 1987). Multiple enzymes modify tRNAs by methylation at different positions (Hou and Perona, 2010). We investigated the contribution of three other methyltransferases: TrmA, TrmB and TrmE, which modify all tRNAs at the U54, G46 and U34 positions, respectively (Björk and Isaksson, 1970; Elseviers et al., 1984; Purta et al., 2005; Ranaei-Siadat et al., 2013). We obtained three knockouts (*trmA::Cm*^{R}, *trmB::Cm*^{R} and *trmE::Cm*^{R}) from a *Salmonella* gene collection (Porwollik et al., 2014). Absence of the TrmA, TrmB and TrmE methyltransferases may affect protein synthesis on a global scale but is not predicted to specifically affect translation of *mgtL*. Compared to the wild type, the *trmA::Cm*^{R}, *trmB::Cm*^{R} and *trmE::Cm*^{R} mutations only slightly affected *mgtA-lacZ*

expression (Fig. 3.7), supporting the role of TrmD as a novel, *trans*-acting factor that is specific for translation of *mgtL*.

3.4.2 Pro limitation and transcription of *mgtA*

Mutations in *mgtL* indicate an underlying role of translation in differential Mg^{2+}-sensing control via a ribosome-mediated mechanism. How translation of Pro codons may contribute to transcription of *mgtA* involves one of at least three aspects: 1) the chemical nature of the amino (rather "imino") acid Pro makes it unfavorable or slow to incorporate into a nascent peptide (Pavlov et al., 2009), 2) the structural nature of Pro makes it difficult to translate due to steric hindrances (Doerfel et al., 2015), and 3) the frequency of Pro codons influences translation efficiency (Chevance et al., 2014). Translation of the Pro codons in *mgtL* provides a potential regulatory site for Mg^{2+} to exert its effect on transcription of *mgtA*.

The two groups that independently discovered the proline-rich leader peptide MgtL encoded within the *mgtA* 5' LR published their models in which Pro 1) regulated the levels of intracellular Pro-charged $tRNA^{Pro}$, and in turn, translation of *mgtL* (Park et al., 2010) and 2) had no relevant role in the regulation of *mgtA* expression (Zhao et al., 2011). In the former model, Pro was proposed to regulate *mgtA* expression after observing an 8-fold increase in *mgtA* coding region by measuring mRNA levels in a single Δ*proB* mutant grown in the absence and presence of extra-cytoplasmic Pro (Park et al., 2010). In the latter model, Pro was ruled out as a regulator of *mgtA* expression after measuring β-galactosidase activity of a plasmid-borne *mgtA-lacZ* transcriptional fusion in strains harboring independent single deletions of *proB* and *proC* (Zhao et al., 2011).

We investigated the role of Pro in the regulation of *mgtA* expression by constructing several single, double and triple mutants harboring deletions of the Pro biosynthesis (Δ*proBA*) and/or Na^+-Pro transport (Δ*putP*) genes and/or decrease-of-function mutation in the H^+-Pro transport gene (*proP1654*) or deletion of the *proP* gene (Fig. 3.10). We did not take into account Pro degradation, which is catalyzed by the bifunctional transcriptional regulator and Pro dehydrogenase enzyme PutA (Fig. 3.11). We measured *mgtA-lacZ* expression of the wild type, single, double and triple mutants after growth in minimal media M63

Figure 3.7

How spontaneous and site-directed mutations in *mgtL* and the genes encoding ribosomal protein L32, translation elongation factors EF-Tu and LepA and methyltransferases TrmA, TrmB and TrmE affect *mgtA-lacZ* expression. β-Galactosidase activity (Miller units) produced by *Salmonella* strains with an *mgtA-lacZ* transcriptional fusion at its chromosomal locus (TL 4295) and isogenic derivatives with nonsense mutation (G80T) introduced into the *mgtL* (3Pro-) mutant (TL 5667), deletion of the *rpmF* structural gene (TL 5836), insertion knockout of the *tufB* structural gene (TL 5917), and deletions of the *lepA* (TL 5833), *trmA* (TL 5815), *trmB* (TL 5817) and *trmE* (TL 5819) structural genes. Bacteria were grown as described in Fig. 3.2. Shown are the mean and SD from at least three independent experiments.

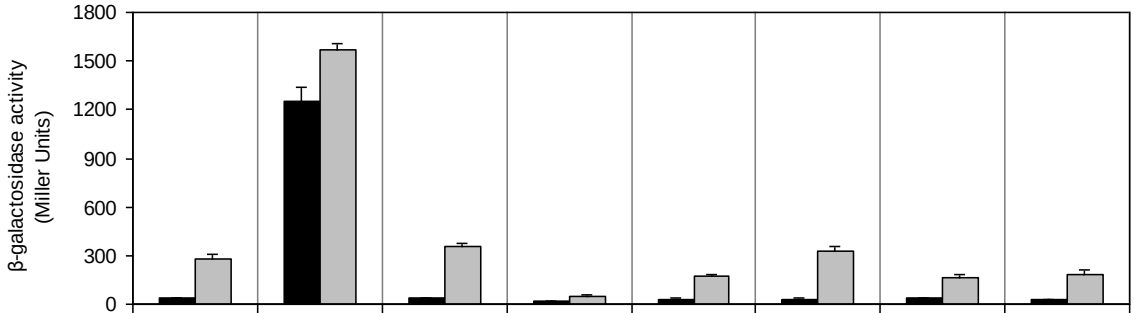

	WT	mgtL (G80T 3Pro-)	ΔrpmF	ΔtufB	ΔlepA	ΔtrmA	ΔtrmB	ΔtrmE
■ 1.6 mM	40.6	1252	35.3	21.1	31.0	32.0	38.5	26.2
□ 0.016 mM	280.3	1566.5	353.8	50.7	173.8	326.5	162.2	180.8

Figure 3.7

Figure 3.8

Mg^{2+}-dependent and $tRNA^{Pro}$-specific methyltransferase TrmD is specific for expression of *mgtA* but not *hisD* at 37°C. β-Galactosidase activity (Miller units) produced by the same *Salmonella* strains indicated in Fig. 4. Bacteria were grown as described in Fig. 3.6, except at 37°C. Shown are the mean and SD from at least three independent experiments.

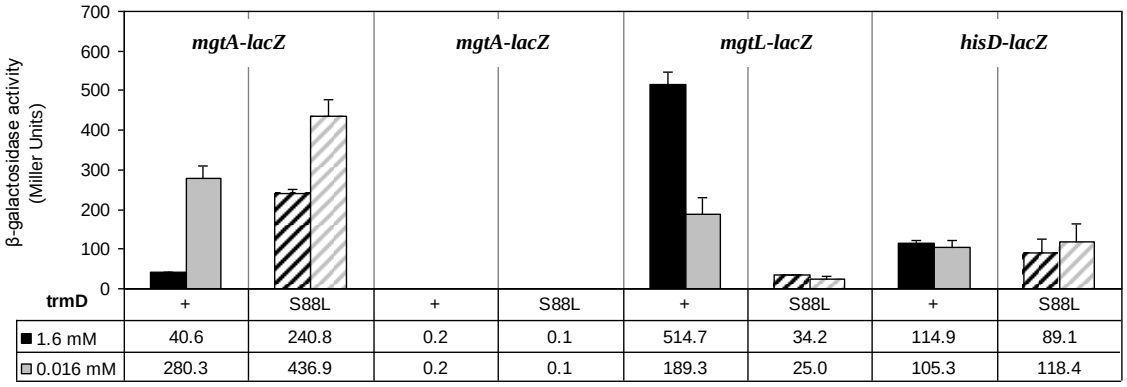

trmD	+	S88L	+	S88L	+	S88L	+	S88L
■ 1.6 mM	40.6	240.8	0.2	0.1	514.7	34.2	114.9	89.1
□ 0.016 mM	280.3	436.9	0.2	0.1	189.3	25.0	105.3	118.4
	***mgtL*$^+$**		***mgtL* (3Pro-)**		***mgtL*$^+$**		***hisL*$^+$**	

Figure 3.8

Figure 3.9

Mutants of strains LT2 and ATCC 14028 retain constitutively high *mgtA-lacZ* expression in high Mg^{2+}. β-Galactosidase activity (Miller units) produced by *S. enterica* serovar Typhimurium LT2 and ATCC 14028 strains with an *mgtA-lacZ* transcriptional fusion at its chromosomal locus (TL 4295 and TL 5980) and isogenic derivatives with a nonsense mutation (C98T) in *mgtL* (TL 4575 and TL 5981) and deletion of the 5' LR (TL 4697 and TL 5982). Bacteria were grown to mid-exponential phase in minimal medium M63 containing high (10 mM) or low (0.01 mM) Mg^{2+} at 37°C. Shown are the mean and SD from at least three independent experiments.

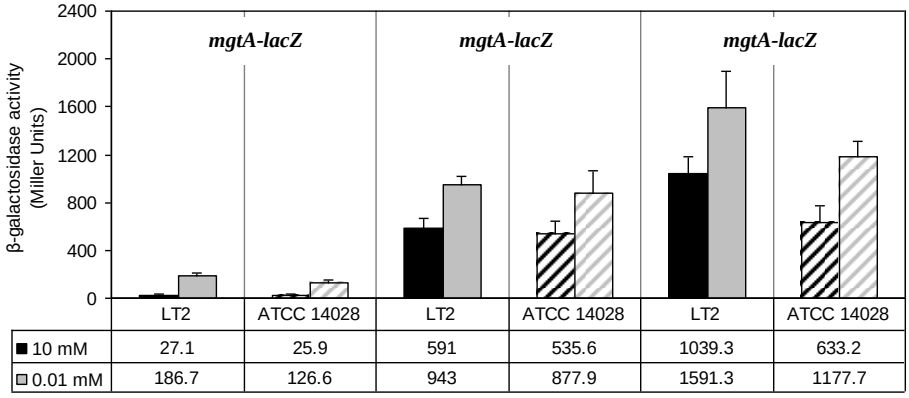
β-galactosidase activity (Miller Units)
2400
2000
1600
1200
800
400
0
mgtA-lacZ
mgtA-lacZ
mgtA-lacZ
LT2
ATCC 14028
LT2
ATCC 14028
LT2
ATCC 14028
10 mM
27.1
25.9
591
535.6
1039.3
633.2
0.01 mM
186.7
126.6
943
877.9
1591.3
1177.7
mgtL+
mgtL (C98T)
Δ5' LR (Δ9-244)

Figure 3.9

containing high (2 mM) or low (0.4 mM) Pro to complement Pro auxotrophy. We observed no effect on *mgtA-lacZ* expression in the Δ*proBA putP*$^{+}$ *proP*$^{+}$ mutant, compared to the wild type, which also exhibited no effect by the 5-fold difference in exogenous Pro added (Fig. 3.10). In addition, the double Δ*proBA putP*$^{+}$ *proP*$^{--}$ mutant exhibited only a slight effect on *mgtA-lacZ* expression under the conditions tested (Fig. 3.10). On the other hand, the triple Δ*proBA* Δ*putPA proP1654* mutant, which experienced a growth defect, exhibited a significant increase in *mgtA-lacZ* expression, compared to the wild type, but no significant difference in *mgtA-lacZ* expression between the concentrations of exogenous Pro added (Fig. 3.10).

These results indicate that both 1) the ion-Pro symporters (PutP and ProP) function efficiently to transport Pro in the wild type, single and double mutants**,** and 2) starvation of intracellular Pro must occur to reach regulatory levels. When intracellular Pro levels become low enough, then levels of Pro-charged $tRNA^{Pro}$ should decrease, leading to ribosome stalling and increased *mgtA-lacZ* expression. However, we propose that Pro may regulate *mgtL* translation and *mgtA* transcription via $tRNA^{Pro}$-charging with a second-order effect compared to Mg^{2+} limitation.

3.4.3 Native translation efficiency of *mgtL*

We hypothesized that intracellular Mg^{2+} facilitates prolyl-bond formation during translation of *mgtL*, and therefore, ribosome-mediated regulation of *mgtA* expression. To investigate the effect of Mg^{2+} on *mgtL* translation more directly, we constructed the chromosomal *mgtL-lacZ* translational fusion, which does not have ability to adopt the alternating stem loop B and C conformations (Fig. 3.1). Compared to the *mgtA-lacZ* transcriptional fusion, which was induced 7-fold by low Mg^{2+}, the *mgtL-lacZ* translational fusion exhibited the opposite effect, resulting in a dramatic decrease in expression by low Mg^{2+} (Fig. 3.5). In addition, Mg^{2+}-starvation corroborated these findings with induction of the *mgtA-lacZ* transcriptional fusion and repression of the *mgtL-lacZ* translational fusion (Fig. 3.5).

Previously, we showed that the 50S ribosomal proteins L27 (encoded by *rpmA*) and L31 (encoded by *rpmE*) that function in the PTC of the ribosome and the ribosome stalling-rescue factor EF-P are involved in the regulation of *mgtA* expression (see Chapter 3). Mutation in the *rpmA* gene or deletions of the *rpmE* and *efp* genes result in constitutively high *mgtA-lacZ* expression compared to the wild type (Figs. 3.2 and 3.5B). However, the *rpmF::Kn*^{R} (encoding 50S ribosomal protein L32), *tufB*$^{--}$ (encoding EF-Tu) or

Figure 3.10

Effect of Pro biosynthesis and transport mutations on *mgtA-lacZ* expression. Strains TL 4295 (*mgtL*$^+$ *mgtA-lacZ*), TL 4854 [Δ*proBA-47 putP*$^+$ *proP*$^+$ *mgtA-lacZ*], TL 5855 [Δ*proBA-47 putP*$^+$ *proP1654 mgtA-lacZ*], TL 5850 [Δ*proBA-47* Δ*putPA-557 proP*$^+$ *mgtA-lacZ*], and TL 4674 (Δ*proBA-47* Δ*putP-557 proP1654 mgtA-lacZ*) were grown to mid-exponential phase in minimal medium M63 containing high (2.0 mM) or low (0.4 mM) proline at 37°C. Shown are the mean and SD from at least two independent experiments.

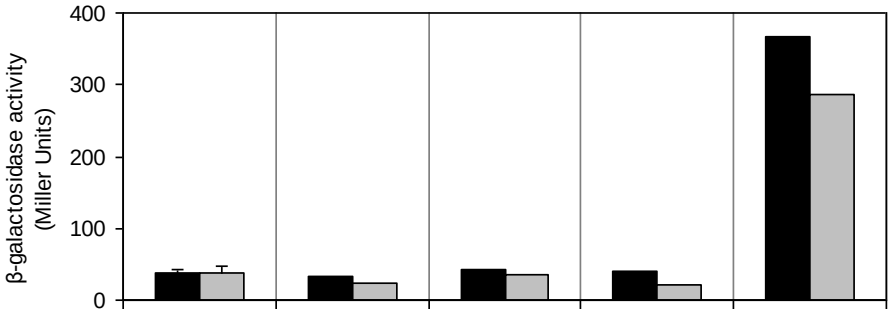

	WT	ΔproBA	ΔproBA proP1654	ΔproBA ΔputP	ΔproBA ΔputP proP1654
■ 2.0 mM	38.9	33.1	43.2	41.0	367.7
□ 0.4 mM	37.0	22.7	36.6	20.3	287.0

Figure 3.10

lepA::Kn^R (encoding EF-4) mutations had little or no effect on *mgtA-lacZ* expression (Figs. 3.5B and 3.5C). In addition, we showed that the Δ*efp::Cm*^{R} mutation is specific for the Pro codons of *mgtL* since introduction of the Δ*efp::Cm*^{R} mutation into the Pro codon-deficient *mgtL* (3Pro-) mutant background could not re-activate *mgtA-lacZ* expression, which was constitutively low in the single *mgtL* (3Pro-) *efp*$^+$ mutant (Fig. 3.5).

Here, we investigated the contributions of the 50S ribosomal proteins (RpmA, RpmE and RpmF) and elongation factors (EF-Tu, EF-4 and EF-P) in *mgtL* translation more directly by introducing the respective mutations into the *mgtL-lacZ* translational fusion background and observing the Lac phenotype of the independent double mutants on MacConkey agar. We noted that only the *rpmA* (G23A) and *rpmE::Cm*^{R} mutations eliminated the Lac$^+$ phenotype, exhibiting the Lac^{--} phenotype on MacConkey agar (Table 3.1). The *rpmF::Kn*^{R} mutation was unable to de-activate *mgtL-lacZ* expression (Table 3.1). These findings further support the specific roles RpmA and RpmE but not RpmF in *mgtL* translation, most likely in prolyl-bond formation. In addition, we introduced the *tufB*$^{--}$, *lepA::Kn*^{R} and Δ*efp::Cm*^{R} mutations into the *mgtL-lacZ* translational fusion background and observed that only the Δ*efp::Cm*^{R} mutation eliminated the Lac$^+$ phenotype (Table 3.1). Both the *tufB*$^{--}$ and *lepA::Kn*^{R} mutations had no apparent effect on *mgtL-lacZ* expression (Table 3.1). These findings further support the novel, specific role of EF-P, but not EF-Tu or EF-4, in *mgtL* translation.

Table 3.1

Effect of *trans*-acting factors on *mgtL-lacZ* expression and on *mgtA-lacZ* expressions in the *mgtL*$^{+}$ and *mgtL* (3Pro-) backgrounds. Plus (+) and minus (--) denote red (Lac^{+}) and white (Lac^{--}) colonies on MacConkey agar, respectively.

Table 3.1

Strain	**Genotype**	**Lac Phenotype**						
		WT	*rpmA**	*rpmE*$^{--}$	*rpmF*$^{--}$	*efp*$^{--}$	*tufB*$^{--}$	*lepA*$^{--}$
TL 4295	*mgtA9226::MudJ* (wild-type)	--	+	+	--	+	--	--
TL 5508	*mgtL-lacZ (MudJ) mgtA*$^{--}$	+	--	--	+	--	+	+
TL 5540	*mgtL* (3Pro-) *mgtA774::MudK*	--	--	--	--	--	--	--

Figure 3.11

Proline biosynthesis, degradation and transport in *Salmonella enterica*. The ProA, ProB and ProC enzymes synthesize L-proline from L-glutamate in a 3-step process, the PutA enzyme converts L-proline into L-glutamate in a 2-step process, and the ProU, ProP and PutP transporters mediate influx of proline.

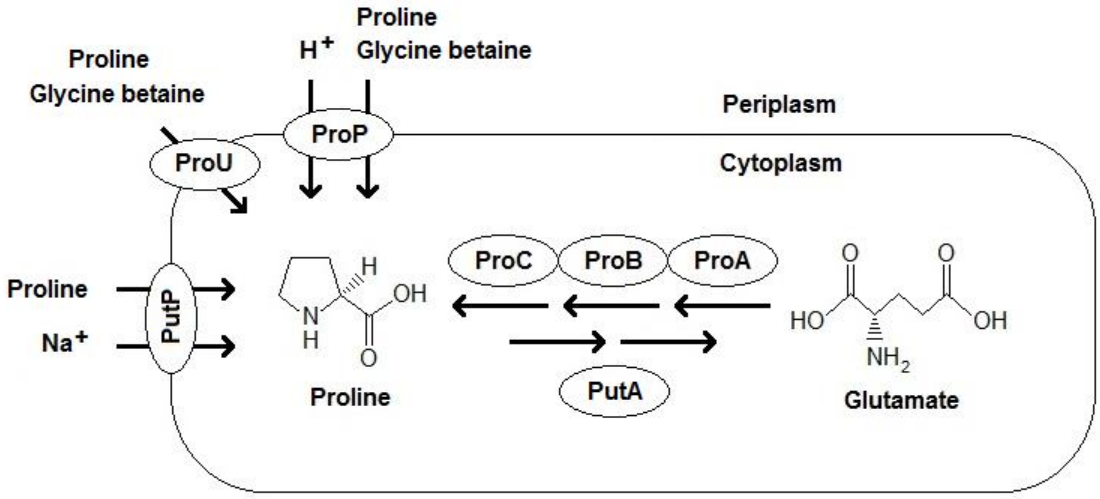
Proline
Glycine betaine
H+
Proline
Glycine betaine
Periplasm
ProP
ProU
Cytoplasm
Proline
Na+
PutP
H
N
H
OH
O
Proline
ProC
ProB
ProA
PutA
O
O
HO
OH
NH2
Glutamate

Figure 3.11

CHAPTER 4. EVIDENCE FOR THE ORDER OF *MGTA* REGULATORY EVENTS

4.1 Introduction

In *Salmonella*, multiple factors and events contribute to the regulation of *mgtA* expression, including PhoP-dependent transcription activation (Véscovi et al., 1996), translation of *mgtL* (Park et al., 2010; Zhao et al., 2011), folding of the *mgtA* 5' LR mRNA (Cromie et al., 2006), and Rho-dependent transcription termination (Hollands et al., 2012). We showed that Mg^{2+} directly regulates translation of *mgtL* and indirectly transcription of *mgtA* (see Chapter 3). We investigated compensatory mutations—combinations of mutations that result in opposite effects on *mgtA-lacZ* expression—at each regulatory level of transcription and translation to better understand the sequence of events and to infer which mechanism takes precedence over the other (Fig. 4.2). Based on our experimental findings by measuring β-galactosidase activity of compensatory mutants harboring an *mgtA-lacZ* transcriptional or translational fusion at its chromosomal locus, we speculated the order and importance of events involved in transcription-translation coupling and proposed an overall, comprehensive model for the regulation of *mgtA* expression (Fig. 4.1). In this model, key events for differential Mg^{2+}-sensing control of *mgtA* expression include: 1) PhoP-dependent transcription activation of the *mgtA* 5' LR, 2) RNA polymerase pausing upstream of the *mgtA* structural gene, 3) translation of *mgtL*, which regulates 4) folding of the *mgtA* 5' LR mRNA to adopt alternative stem loop structures, either favoring or blocking 5) Rho-dependent transcription termination (Fig. 4.1).

Figure 4.1

Speculation of the order of the regulatory events in *mgtA* expression. The interplay of five areas govern *mgtA* expression: 1) PhoP-dependent transcription termination, 2) RNA polymerase pausing, 3) translation of *mgtL* in response to the intracellular [Mg^{2+}], 4) folding of the *mgtA* 5' LR mRNA, and 5) Rho-dependent transcription termination, all of which lead to either transcription or termination upstream of the *mgtA* gene.

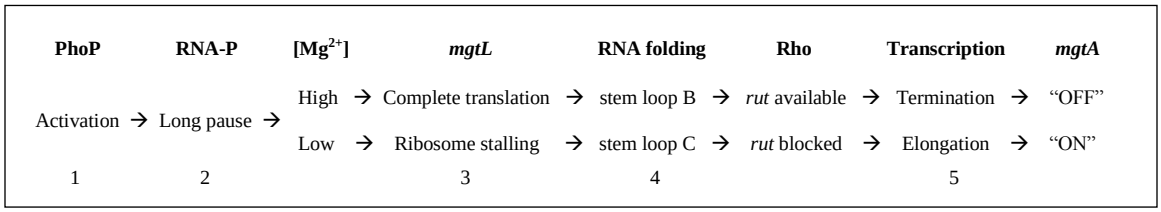

(**Note:** [Mg^{2+}] regulates *mgtL* translation directly, and EF-P and TrmD are excluded for simplicity—see Chapter 3)

Figure 4.1

Figure 4.2

Updated schematic for the alternative RNA structures of the 5’ leader region and regulation of the *Salmonella mgtA* gene in response to Mg^{2+}-sensing via prolyl-bond formation during translation of *mgtL*. Arrowheads denote response to the intracellular [Mg2+], RNA polymerase pausing at nucleotide +218, or effects on translation of *mgtL* by various mutations. Proline codons are denoted with yellow boxes. Nucleotide substitutions labeled in black, green and red denote mutations that result in the wild-type, constitutively “ON” and “OFF” phenotypes, respectively.

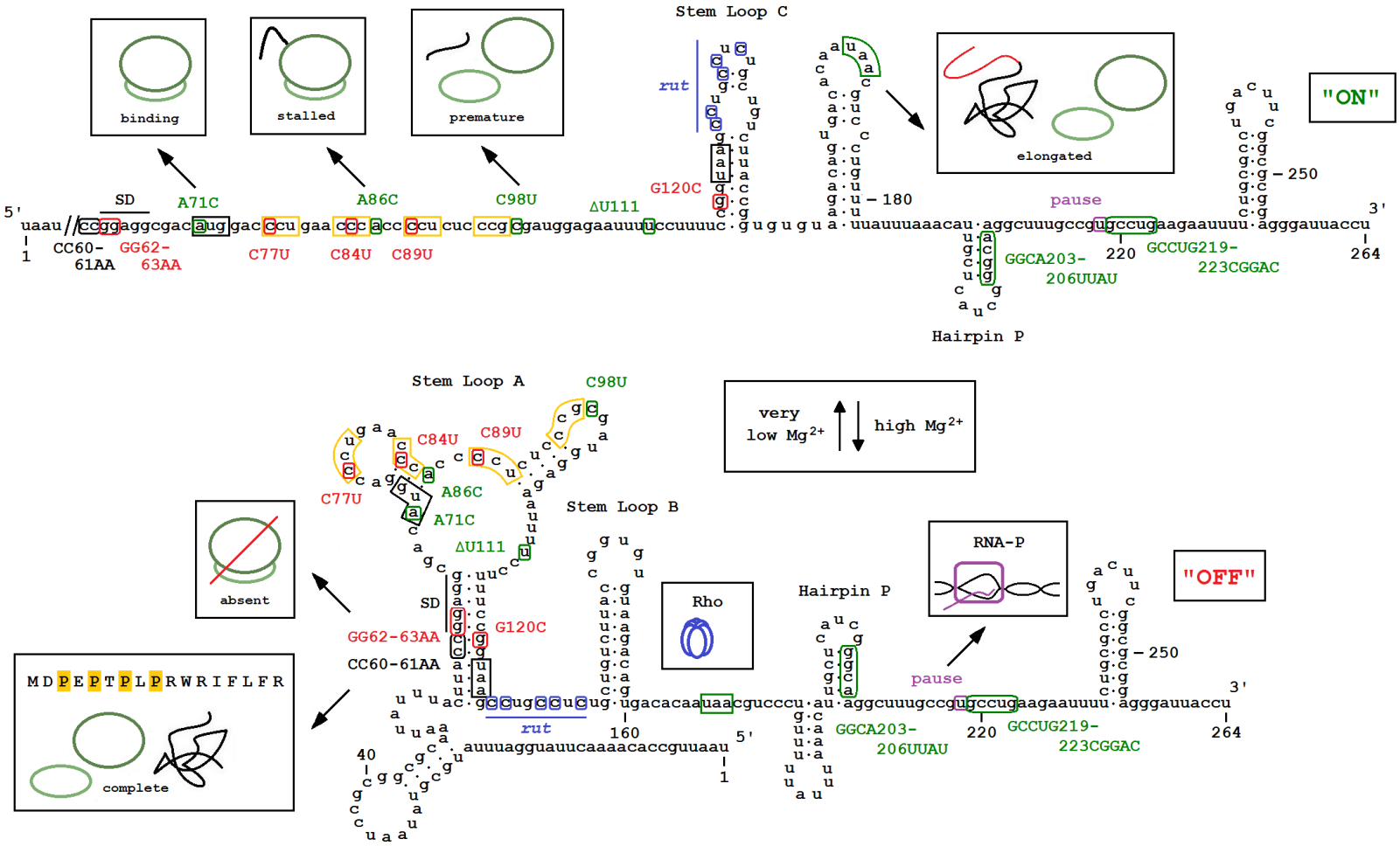
Stem Loop C
binding
stalled
premature
elongated
"ON"
rut
SD
A71C
A86C
C98U
ΔU111
G120C
pause
CC60-
61AA
GG62-
63AA
C77U
C84U
C89U
GGCA203-
206UUAU
GCCUG219-
223CGGAC
Hairpin P
Stem Loop A
Stem Loop B
very
low Mg2+
high Mg2+
absent
RNA-P
"OFF"
Rho
GG62-63AA
CC60-61AA
MDPEPTPLPRWRIFLFR
complete

Figure 4.2

4.2 Translation initiation of *mgtL*

Ribosomes bind to AG-rich sequences termed Shine-Dalgarno (SD) sites within mRNA transcripts and initiate translation at a nearby downstream start codon, both SD sites and start codons of which may vary in sequence, relying on species-specific nuances (Jacques and Dreyfus, 1990). In *E. coli*, the frequency of start codons is greatest for AUG (83%), then GUG (14%) and UUG (3%) (Blattner et al., 1997). The proline-rich, 17-codon leader peptide MgtL is encoded in the mutually-exclusive stem loops A and C, and translation terminates at the UAA stop codon upstream of stem loop B (Fig. 4.2). The *mgtL* SD site harbors a near-canonical consensus sequence and AUG start codon, specifying initiator $tRNA^{Met}$ (Fig. 4.2).

4.2.1 Lack of ribosome binding

We investigated the role of ribosome binding and translation initiation by constructing mutants that abrogate the SD site, start codon and neighboring mRNA. First, we constructed a SD site mutation (GG62-63AA) that alters the GGAGG consensus sequence of *mgtL* to AAAGG, which disrupts the left arm of stem loop A (Fig. 4.4A). Although it affects the base-pairing of the stem loop A arms, we hypothesized that the *5' LR* (GG62-63AA) mutation would affect *mgtA-lacZ* expression by impinging on ribosome-mediated regulation via *mgtL* translation, since the *mgtA* 5' LR mRNA retains ability to alternate between stem loops B and C (Fig. 4.2). Compared to the wild type, which was induced 10-fold by low Mg^{2+}, the *5' LR* (GG62-63AA) mutant exhibited constitutively low *mgtA-lacZ* expression (Fig. 4.3). This result suggests that either 1) disruption of stem loop A or 2) lack of ribosome binding facilitates transcription termination.

4.2.2 Disruption of RNA folding with wild-type translation

The question emerged whether constitutively low *mgtA-lacZ* expression in the *5' LR* (GG62-63AA) mutant was due to impaired stem loop A formation. Therefore, we constructed a second mutation (CC60-61AA) that abrogates the base-pairing of the stem loop A arms in a manner similar to the *5' LR* (GG62-63AA) mutation and yet retains the wild-type SD site (Fig. 4.2). The *5' LR* (CC60-61AA) mutant exhibited 8.8-fold induction by low Mg^{2+} similar to the wild type (Fig. 4.3). This result suggests that the constitutively "OFF" phenotype of the *5' LR* (GG62-63AA) mutant is due to elimination of *mgtL* translation and not impairment of stem loop A, implying that ribosome binding facilitates RNA folding in the wild type.

Figure 4.3

Effect of translation initiation mutations on *mgtA-lacZ* expression. Strains TL 5527 (*mgtL*$^{+}$ *mgtA-lacZ*), TL 5529 [*5' LR* (GG62-63AA) *mgtA-lacZ*], TL 5528 [*5' LR* (CC60-61AA) *mgtA-lacZ*], TL 5562 [*mgtL* (A71C) *mgtA-lacZ*], and TL 5569 (*5' LR* (GG62-63AA) *mgtL* (A71C) *mgtA-lacZ*) were grown to mid-exponential phase in minimal medium M63 containing high (1.6 mM) or low (0.016 mM) Mg^{2+} at 37°C. Shown are the mean and SD from at least three independent experiments. For panels 2 and 5, the activities were lower than the resolution of the figure following growth in high and low Mg^{2+}.

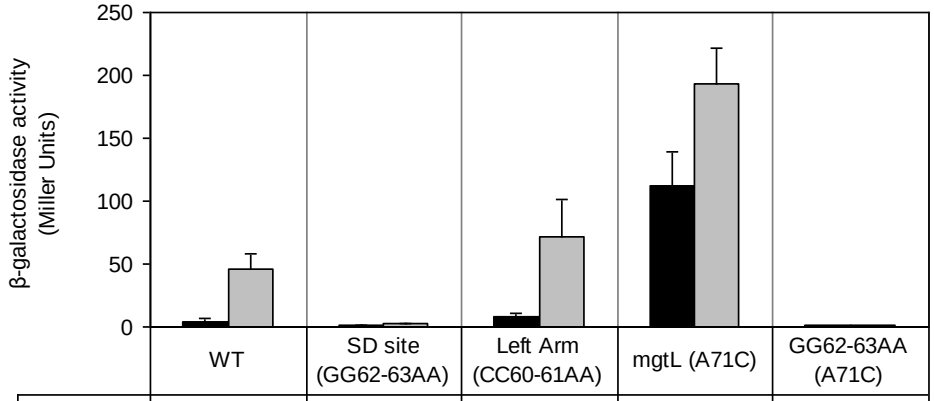

	WT	SD site (GG62-63AA)	Left Arm (CC60-61AA)	mgtL (A71C)	GG62-63AA (A71C)
■ 1.6 mM	4.5	1.2	8.2	111.8	1.1
□ 0.016 mM	46.6	3.1	71.3	192.8	1.3

Figure 4.3

Figure 4.4

Schematics and regulation of the *mgtA* 5' LR mRNA harboring **(A)** mutations that influence ribosome binding and translation initation, and **(B)** spontaneous premature translation (C85^A86), **(C)** extended translation (ΔT111), and **(D)** site-directed poly-Pro and stem loop B (A86C-G120C) mutations.

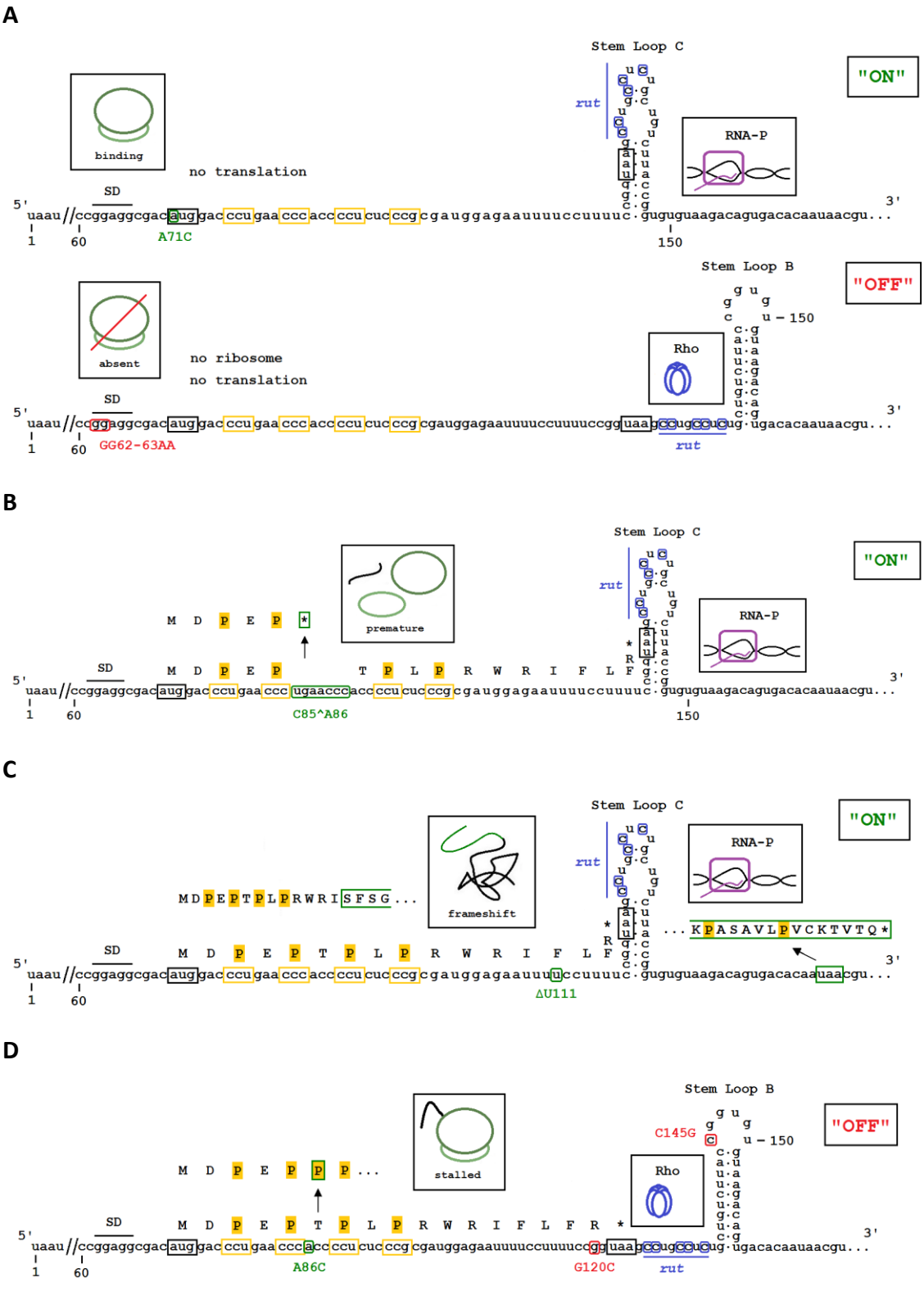
A
Stem Loop C
"ON"
binding
rut
RNA-P
no translation
SD
5'
3'
uaau//ccggaggcgacaaggacccugaacccacccccucuccgcgauggagaauuuuccuuuuc·gugugaagacagugacacaauaacgu...
1
60
A71C
150
Stem Loop B
"OFF"
absent
Rho
no ribosome
no translation
SD
uaau//ccggaggcgacaaggacccugaacccacccccucuccgcgauggagaauuuuccuuuuccgguaagccugccuc·ug·ugacacaauaacgu...
1
60
GG62-63AA
rut
B
Stem Loop C
"ON"
premature
rut
RNA-P
M D P E P *
SD
M D P E P T P L P R W R I F L F
uaau//ccggaggcgacaaggacccugaacccugaacccacccccucuccgcgauggagaauuuuccuuuuc·gugugaagacagugacacaauaacgu...
1
60
C85^A86
150
C
Stem Loop C
"ON"
frameshift
rut
RNA-P
MDPEPTPLPRWRISFSG...
...KPASAVLPVCKTVTQ*
SD
M D P E P T P L P R W R I F L F
uaau//ccggaggcgacaaggacccugaacccacccccucuccgcgauggagaauuuucccuuuuc·gugugaagacagugacacaauaacgu...
1
60
ΔU111
D
Stem Loop B
"OFF"
stalled
C145G
Rho
rut
M D P E P P P ...
SD
M D P E P T P L P R W R I F L F R *
uaau//ccggaggcgacaaggacccugaacccacccccucuccgcgauggagaauuuuccuuuuccgguaagccugccuc·ug·ugacacaauaacgu...
1
60
A86C
G120C
rut

Figure 4.4

4.2.3 Ribosome binding with lack of translation

We further investigated whether ribosome binding is necessary for unfolding the *mgtA* 5' LR mRNA by constructing a translation initiation mutant (A71C), in which the native AUG start codon was replaced with a CUG leucine (Fig. 4.4A). Here, the *mgtL* (A71C) mutant should retain ability of the ribosome to bind the SD site but eliminate translation initiation at the CUG codon. Compared to the wild type, the *mgtL* (A71C) mutant exhibited constitutively high *mgtA-lacZ* expression, unlike the constitutively "OFF" phenotype of the *5' LR* (GG62-63AA) mutant (Fig. 4.3). We investigated the combined effect of the *5' LR* (GG62-63AA) and *mgtL* (A71C) mutations on *mgtA-lacZ* expression, whether the A71C mutation exerts its effect on RNA folding or *mgtL* translation. Compared to the wild type, the double *5' LR* (GG62-63AA) *mgtL* (A71C) mutant exhibited the constitutively "OFF" phenotype like the single *5' LR* (GG62-63AA) mutant (Fig. 4.3). These results suggest that indeed both efficient ribosome binding and impaired translation of *mgtL* may influence RNA folding to adopt the stem loop C (anti-termination) conformation and transcription into the *mgtA* structural gene.

4.3 Translation termination of *mgtL*

Translation termination occurs when the ribosome reaches a stop codon on an mRNA transcript, and release factors recognize the unoccupied A-site stop codon, facilitating release of the nascent peptide from the exit tunnel and the ribosome from the mRNA transcript (Washburn and Gottesman, 2015). Three stop codons (UAA, UGA and UAG) specify translation termination signals with UAA occurring most frequently and UAG least (Povolotskaya et al., 2012). Ribosomes occupy a stretch of ~40 nucleotides (Beyer et al., 1994), and translation elongation occurs by the ribosome exhibiting helicase activity, unwinding the mRNA as it may fold onto itself (Washburn and Gottesman, 2015). Premature translation termination and inefficient ribosomal release often lead to aberrant proteins and events that stimulate mRNA degradation or frameshifting that extends translation into non-coding mRNA regions (Atkins and Björk, 2009; Deana and Belasco, 2005). Termination of *mgtL* translation at its native UAA stop codon generates the proline-rich, 17-amino acid leader peptide MgtL (Fig. 4.2).

4.3.1 Premature translation termination

We investigated the role of ribosome position as it relates to translation elongation. Of the more than 20 mutants, we characterized a spontaneous mutation (C85^A86), which inserted a repeat sequence (TGAACCC) between nucleotides C85 and A86, resulting in premature translation termination at the internally generated UAA stop codon (Fig. 4.4B). Despite inserting a 7-bp repeat sequence, the C85^A86 mutation does not significantly alter the predicted secondary structure of the *mgtA* 5' LR mRNA. The C85^A86 mutant exhibited constitutively high *mgtA-lacZ* expression, a 32.5-fold increase at high Mg^{2+} compared to wild type (Fig. 4.5). Here, translation termination and ribosomal release occur upstream of the native UAA stop codon, facilitating stem loop C formation that would otherwise be occluded by wild-type translation termination.

4.3.2 Frameshift translation

It has been shown that the protein-synthesis reading frame is maintained by the translation elongation factor EF-P (Gamper et al., 2015). In its absence, +1 frameshifting occurs, resulting in errors in protein synthesis (Qian and Björk, 1997). Given that the wild-type *mgtL* does not harbor contiguous Pro codons, our previous results for the Δ*efp::Cm*^{R} mutant suggest that deletion of EF-P may cause +1 frameshifting during translation of *mgtL*, leading to constitutively high *mgtA-lacZ* expression (see Chapter 3). Upon +1 frameshifting of *mgtL*, transcription may proceed into the *mgtA* structural gene by sequestering the *rut* site in stem loop C and antagonizing Rho-dependent transcription termination. To test this hypothesis, we constructed an *mgtL* (ΔT111) mutant, which generates a +1 frameshift by deletion of nucleotide T at position 111 and extends translation by an additional 15 codons past the native stop codon to the next available UAA stop codon downstream (Fig. 4.4C). We observed constitutively high *mgtA-lacZ* expression, a 10-fold increase at high Mg^{2+} compared to the wild type (Fig. 4.5). Using the Mfold web server (Zuker, 2003), we observed that the *mgtL* (ΔT111) mutation should not disrupt the secondary structure of the *mgtA* 5' LR mRNA (Fig. 4.4C); therefore, the main contribution for constitutively high *mgtA-lacZ* expression by the *mgtL* (ΔT111) mutation is ribosomal release downstream of the alternative stem loop structures.

Figure 4.5

Effect of translation termination mutations on *mgtA-lacZ* expression. Strains TL 4295 (*mgtL*$^{+}$ *mgtA-lacZ*), TL 4701 [*mgtL* (C85^A86) *mgtA-lacZ*], and TL 5634 [*mgtL* (ΔT111) *mgtA-lacZ*] were grown as described in Fig. 4.3. Shown are the mean and SD from at least three independent experiments.

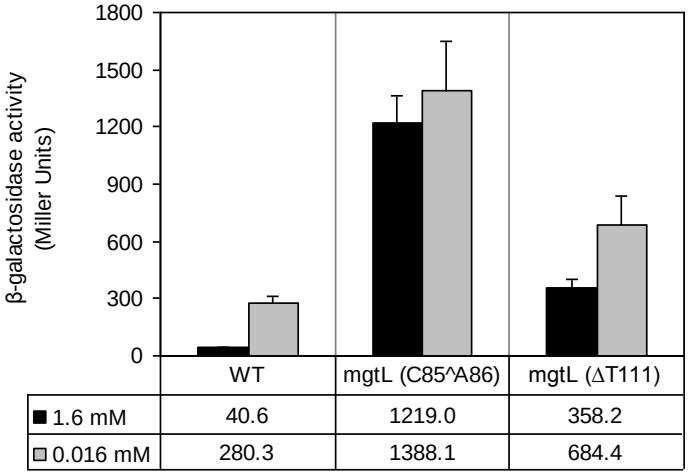

	WT	mgtL (C85^A86)	mgtL (ΔT111)
■ 1.6 mM	40.6	1219.0	358.2
□ 0.016 mM	280.3	1388.1	684.4

Figure 4.5

4.4 Transcription-translation coupling of *mgtA*

Transcription-translation coupling facilitates ribosome binding to an RNA-DNA transcription complex, allowing coexistent protein synthesis from their respective coding mRNA transcripts (Washburn and Gottesman, 2015). The number of extant copies of mRNA transcript limits translation, while multiple ribosomes may translate an mRNA transcript, forming a polysome complex of ribosomes tethered to the mRNA transcript (Qin and Fredrick, 2013).

Regulatory factors and events contribute to the transcription-translation coupling and occupy the same space on the *mgtA* 5' LR mRNA, including 1) RNA polymerase pausing, 2) translation of *mgtL*, 3) RNA folding and 4) Rho-dependent transcription termination. We investigated the interplay of these multiple regulatory factors and events by introducing combinations of compensatory mutations from each of the four categories into a strain harboring an *mgtA-lacZ* transcriptional or translational fusion at its chromosomal locus. Compensatory mutations involving Rho-dependent transcription termination will be discussed (see Sub-section 4.5.3).

4.4.1 RNA polymerase pausing vs. translation of *mgtL*

Analysis of the *mgtA* 5' LR mRNA revealed that RNA polymerase pauses for an extended period at a region downstream of *mgtL* and *rut* site by aid of a small stem loop structure (Hairpin P), resulting in termination at nucleotide +118 *in vitro* (Fig. 4.2) (Hollands et al., 2014). We investigated the interplay of RNA polymerase pausing and *mgtL* translation initiation to determine which event is limiting or more important for differential Mg^{2+}-sensing control. First, we constructed two mutants that harbored base-pair substitutions in the right arm of Hairpin P [GGCA(203-206)TTAT] and in a Pause Region [GCCTG(219-223)CGGAC], which resulted in disruption of the *mgtA* 5' LR mRNA (Fig. 4.2). Compared to the wild type, both mutants exhibited constitutively high *mgtA-lacZ* expression (Fig. 4.6), supporting the role of Hairpin P and the Pause Region in the regulation of *mgtA* expression, as described previously (Hollands et al., 2014).

Then, we monitored the Lac phenotype of a double mutant [GG62-63AA, GGCA(203-206)TTAT] harboring the translation initiation and Hairpin P mutations on MacConkey agar. Similar to the wild type,

the double mutant exhibited the Lac^{--} phenotype, de-activating *mgtA-lacZ* expression (Table 4.1). Despite ability to free RNA polymerase from the pause region, the *5' LR* (GG62-63AA) mutation constitutively favors the stem loop B conformation, leading to Rho-dependent transcription termination. Interestingly, this result demonstrates that Rho may catch up to RNA polymerase and unwind the RNA-DNA transcriptional complex.

4.4.2 RNA folding dynamics vs. translation of *mgtL*

Mutations that altered the preference for stem loops B or C were shown previously to affect *mgtA-lacZ* expression (Cromie et al., 2006). Single mutations in *mgtL* (G120C) or the *mgtA* 5' LR (C145G) that disrupted the arms of stem loop C resulted in constitutively low *mgtA-lacZ* expression, compared to the wild type (Cromie et al., 2006), by favoring stem loop B formation and Rho-dependent transcription termination (Fig. 4.4D) (Hollands et al., 2012). We corroborated the constitutively "OFF" phenotype of the G120C mutant (Fig. 4.7). In addition, the double *mgtL* (G120C) *5'LR* (C145G) mutation re-established the stem loop C conformation and regained differential Mg^{2+}-sensing control, similar to the wild type (Cromie et al., 2006).

Premature translation termination of *mgtL* by the C98T mutation has been shown to significantly increase *mgtA-lacZ* expression compared to the wild type, resulting in the constitutively "ON" phenotype (see Chapter 3) (Cromie et al., 2006; O'Connor et al., 2009). However, when the interplay of early translation termination and RNA folding was investigated by introducing both the nonsense and stem loop C mutations into *mgtL*, the double (*mgtL*-C98T, G120C) mutation resulted in constitutively low *mgtA-lacZ* expression, similar to the single *mgtL* (G120C) mutant (Cromie et al., 2006). Despite premature ribosomal release, RNA folding favored stem loop B and Rho-dependent transcription termination.

Therefore, we investigated the interplay of ribosome stalling and RNA folding by introducing both the poly-Pro and stem loop C mutations into a strain harboring the chromosomal *mgtA-lacZ* transcriptional fusion (Fig. 4.4D). The ribosome in the *mgtL* (A86C, G120C) mutant is predicted to remain bound longer to *mgtL* than in the double *mgtL* (C98T, G120C) mutant. We hypothesized that the poly-Pro mutation may differently regulate RNA folding than the premature translation termination mutation. Despite predicted ribosome stalling at the poly-Pro stretch, however, the *mgtL* (A86C) mutation was unable to overcome the

Figure 4.6

Effect of RNA polymerase pause region mutations on *mgtA-lacZ* expression. Strains TL 5527 (*mgtL*$^{+}$ *mgtA-lacZ*), TL 5563 {*5' LR* [GGCA(203-206)TTAT] *mgtA-lacZ*}, and TL 5565 {*5' LR* [GCCTG(219-223)CGGAC] *mgtA-lacZ*} were grown to mid-exponential phase in minimal medium M63 containing high (1.6 mM) or low (0.016 mM) Mg^{2+} at 37°C. Shown are the mean and SD from at least three independent experiments.

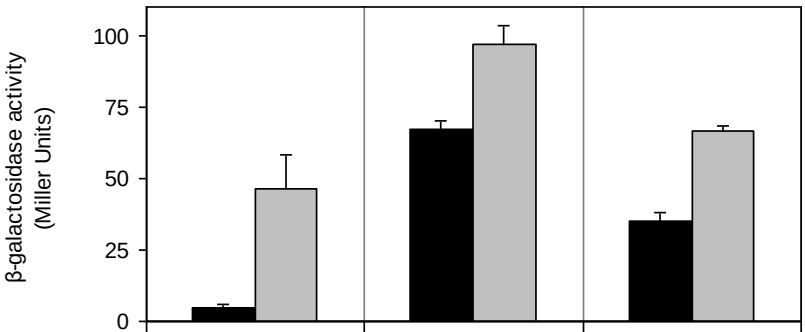

	WT	Hairpin P (GGCA-->TTAT)	Pause Region (GCCTG-->CGGAC)
■ 1.6 mM	4.5	67.4	35.2
□ 0.016 mM	46.6	97.1	66.7

Figure 4.6

silencing effect of the single *mgtL* (G120C) mutation in the double mutant, which exhibited the constitutively "OFF" phenotype, compared to the wild type (Fig. 4.7).

4.5 Transcription termination of *mgtA*

Bacteria employ two mechanisms of transcription termination: 1) factor-independent, or intrinsic, transcription termination and 2) factor-dependent transcription termination. The first mechanism involves a GC-rich stem loop structure followed by a poly-uracil stretch that functions to destabilize the RNA-DNA duplex, which releases the RNA polymerase from the transcription complex (Carafa et al., 1990). On the other hand, the second mechanism utilizes the ATP-dependent helicase Rho, which binds to cytosine-rich, single-stranded and untranslated regions of mRNA, termed *R*ho-*ut*ilization (*rut*) sites, and unwinds the RNA-DNA duplex until it releases RNA polymerase (Richardson, 2002).

Based on mutational analysis of the *mgtA* 5' LR and use of the Rho-specific inhibitor bicyclomycin, it has been shown that Rho factor functions to terminate *mgtA* transcription (Hollands et al., 2012). Immediately downstream of *mgtL*, a *rut* site is available for Rho binding in the event that RNA folding favors the stem loop B conformation; however, if stem loop C forms, then the *rut* site becomes sequestered in the hairpin structure (Fig. 4.2) (Hollands et al., 2012).

4.5.1 Rho helicase

To investigate the order and importance of Rho-dependent transcription termination in the regulation of *mgtA* expression, we obtained a mutant (Y80C) harboring a point mutation in the *rho* gene, which generates an RNA- and ATP-binding defect without temperature sensitivity for the protein (Chalissery et al., 2007). Given its essentiality, the Y80C-*rho* mutant exhibits a slow growth phenotype. Compared to the wild type, the Y80C-*rho* mutant exhibited constitutively high *mgtA-lacZ* expression (Fig. 4.9). Thus, we corroborated the involvement of Rho factor in the *mgtA* regulation, supporting its role in the previous model (Hollands et al., 2012).

Figure 4.7

Effect of RNA folding mutations on *mgtA-lacZ* expression. Strains TL 4295 (*mgtL*$^{+}$ *mgtA-lacZ*), TL 4576 [*mgtL* (A86C) *mgtA-lacZ*], TL 5139 [*mgtL* (G120C) *mgtA-lacZ*], and TL 5143 [*mgtL* (A86C-G120C) *mgtA-lacZ*] were grown to mid-exponential phase in minimal medium M63 containing high (1.6 mM) or low (0.016 mM) Mg^{2+} at 37°C. Shown are the mean and SD from at least three independent experiments. For panels 3 and 4, the activities were lower than the resolution of the figure following growth in high and low Mg^{2+}.

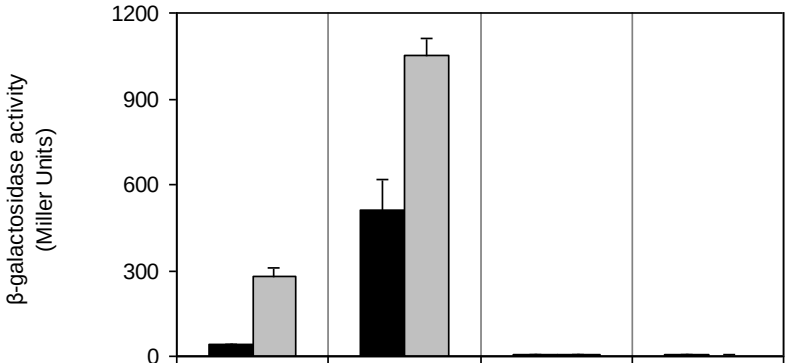

	WT	mgtL (A86C)	mgtL (G120C)	A86C-G120C
■ 1.6 mM	40.6	513.2	4.6	3.3
▫ 0.016 mM	280.3	1049.6	4.6	2.8

Figure 4.7

4.5.2 Cytosine-deficient *mgtL*

We hypothesized that the cytosine-rich *mgtL* functions partly or entirely as a *rut* site. We investigated Rho recognition by constructing a strain that harbors 10 out of 19 cytosine substitutions (C-deficient) but retains the wild-type MgtL amino acid sequence (Fig. 4.8). If *mgtL* functions as a *rut* site, then replacement of ~50% of cytosine content would be predicted to impair Rho binding and transcription termination, resulting in constitutively high *mgtA-lacZ* expression. Compared to the wild type, however, the C-deficient mutant exhibited constitutively low *mgtA-lacZ* expression (Fig. 4.9).

Using the Mfold web server (Zuker, 2003), we observed that the secondary structure of the C-deficient *mgtA* 5' LR mRNA is predicted to favor the stem loop B conformation (Fig. 4.8). Replacement of cytosines within *mgtL* disrupts formation of stem loop C conformation, leading to constitutive stem loop B formation. Had *mgtL* indeed functioned as a *rut* site for Rho recognition, then we would observe constitutively high *mgtA-lacZ* expression even if stem loop B formed constitutively. Therefore, we concluded that the cytosines of *mgtL* do not function as a *rut* site for Rho-dependent transcription termination.

4.5.3 Rho and compensatory mutations

Lastly, we investigated the interplay of translation of *mgtL*, RNA polymerase pausing and Rho-dependent transcription termination by introducing the Y80C-*rho* mutation into the SD site and Hairpin P mutant backgrounds and observing the Lac phenotypes of the various double mutants on MacConkey agar. We noted that Rho inhibition was able to de-repress *mgtA-lacZ* expression in the double *5'LR* (GG62-63AA) Y80C-*rho* mutant, which exhibited the Lac^+ phenotype (Table 4.1). In addition, Rho inhibition resulted in a synergistic increase in the Lac^+ phenotype of the double *5'LR* [GGCA(203-206)TTAT] Y80C-*rho* mutant compared to the single *5'LR* [GGCA(203-206)TTAT] rho^+ mutant (Table 4.1). These findings support the role of the helicase Rho as the final determining factor in *mgtA* expression. Despite the silencing effect of the SD mutation and besides de-repression by the Hairpin P mutation, the Lac^+ phenotypes of the double mutants suggest that efficient Rho-dependent transcription termination is the last, critical step in differential Mg^{2+}-sensing control.

Figure 4.8

Schematic of the *mgtA* 5' LR mRNA harboring replacement of cytosine and uracil nucleotides in *mgtL* that retain the wild-type amino acid sequence. Nucleotides C76, C92, C112, C113 and C118 were replaced with thymines, nucleotides C85, C88, C94, C98 and C119 were replaced with adenines, and nucleotide U115 was replaced with a guanine (not shown). Nucleotide substitutions are denoted with red boxes.

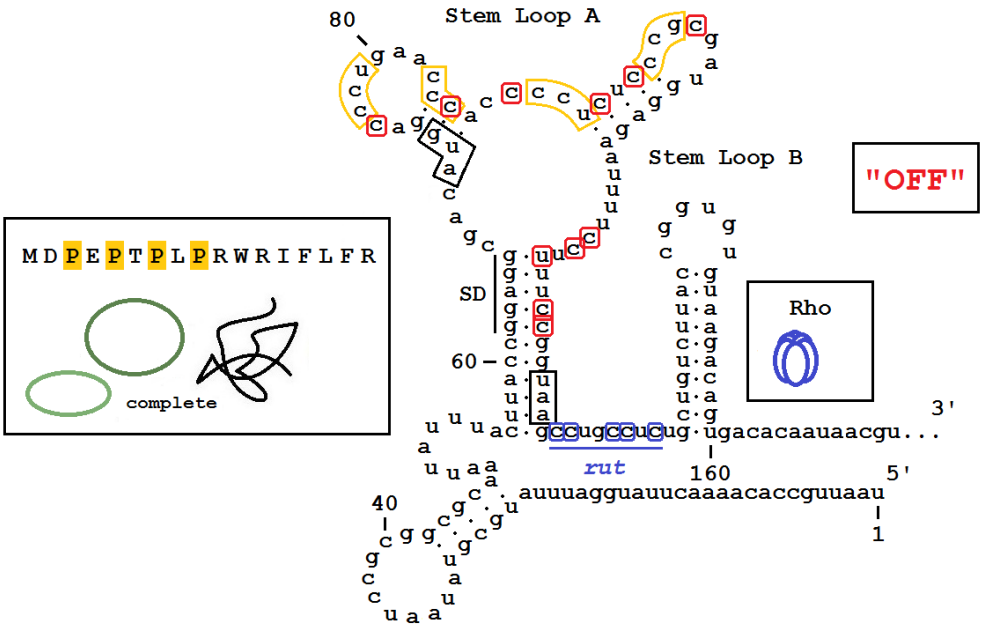
80
Stem Loop A
Stem Loop B
"OFF"
MDPEPTPLPRWRIFLFR
complete
SD
60
Rho
rut
160
5'
3'
40
1

Figure 4.8

Figure 4.9

Effect of transcription termination mutations on *mgtA-lacZ* expression. Strains TL 4295 (*mgtL*$^{+}$ *mgtA-lacZ*), TL 5573 (IG$^{[rhlB\text{-}trxA]}$::Tpop Y80C-*rho mgtA-lacZ*), and TL 5125 [*mgtL* (C-deficient) *mgtA-lacZ*] were grown to mid-exponential phase in minimal medium M63 containing high (1.6 mM) or low (0.016 mM) Mg^{2+} at 37°C. Shown are the mean and SD from at least three independent experiments.

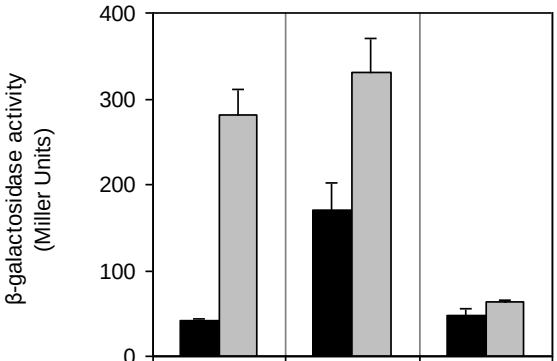

	WT	Y80C-rho	mgtL (C-def)
■ 1.6 mM	40.6	170.8	47.1
□ 0.016 mM	280.3	329.8	62.8

Figure 4.9

Table 4.1

Effect of compensatory mutations on *mgtA-lacZ* expression based on Lac phenotype. The Y80C-*rho* mutation was introduced into various wild-type and mutant backgrounds. Plus (+) and minus (--) denote red (Lac^{+}) and white (Lac^{--}) colonies on MacConkey agar, respectively.

Table 4.1

Strain	Genotype	Lac Phenotype	
		WT	Y80C-*rho*
TL 4295	*mgtA9226::MudJ* (wild-type transcriptional fusion)	--	+
TL 5527	*mgtA774::MudK* (wild-type translational fusion)	--	+
TL 5528	*5' LR* (CC60-61AA) *mgtA774::MudK*	--	+
TL 5529	*5' LR* (GG62-63AA) *mgtA774::MudK*	--	--
TL 5125	*mgtL* (C-deficient) *mgtA9226::MudA*	--	+
TL 5139	*mgtL* (G120C) *mgtA9226::MudJ*	--	+
TL 5571	*mgtL* (CC118-119AA) *mgtA774::MudK*	--	+
TL 5563	*5' LR* [GGCA(203-206)TTAT] *mgtA774::MudK*	+	++
TL 5567	*5' LR* [GG62-63AA, GGCA(203-206)TTAT] *mgtA774::MudK*	--	--

4.6 Concluding remarks

Based on previous models and recent experimental findings, we support an overall, comprehensive model that integrates both *cis*-acting and *trans*-acting factors into the regulation of *mgtA* expression (Fig. 4.2). Investigation of the independent steps of transcription of the *mgtA* 5' LR and translation of *mgtL* provided insights in the speculation of the order and importance of the regulatory events involved (Fig. 4.1). In addition, we examined the effect of combinations of compensatory mutations of both the *mgtA* 5' LR and *mgtL* to understand the mechanism of transcription-translation coupling that occurs (Tables 4.1 and 4.2).

Overall, we conclude that transcription activation by the PhoQP TCS under conditions of low extra-cytoplasmic Mg^{2+} and transcription termination by the ATP-dependent helicase Rho under conditions of high intracellular Mg^{2+} are undoubtedly essential in differential Mg^{2+}-sensing control. We establish that efficient translation initiation and accurate translation termination of *mgtL* influence folding of the *mgtA* 5' LR mRNA, determining whether the stem loop B (*rut* available) or stem loop C (*rut* blocked) conformation will be favored. In reviewing the two previously recognized models for the role of *mgtL*, we noted that increasing the length of the translated MgtL leader peptide by independently introducing nonsense mutations at increasing distances from the initiation codon increased the degree of differential Mg^{2+}-sensing control of the *mgtA* transcript (Park et al., 2010). This result indicates an important role of ribosomal position in differential Mg^{2+}-sensing, and together with our results, supports that the translating ribosome must reach the native stop codon to preclude stem loop C and favor stem loop B formation to permit Rho-dependent transcription termination. Therefore, as previously described, translation of *mgtL* is necessary to sense the Mg^{2+} signal (see Chapter 3), indicating the essential role of ribosome-mediated attenuation and transcription-translation coupling.

CHAPTER 5. PRELIMINARY EVIDENCE FOR ALTERNATIVE TRANSCRIPTION

5.1 Introduction

The PhoQP TCS regulates *mgtA* and other genes involved in Mg^{2+} homeostasis, pathogenicity, cell envelope composition and acid resistance (Groisman, 2001; Kato et al., 1999). Wild-type transcription activation of *mgtA* is dependent on the DNA-binding transcriptional regulator PhoP and the histidine sensor kinase PhoQ (this study) (Véscovi et al., 1996). Although the Rob protein has been shown to activate transcription of the *mgtA* gene at a site downstream of the wild-type PhoP-dependent TSS, deletion of the *rob* gene had little effect on induction of *mgtA-lacZ* expression by limiting Mg^{2+} (this study) (Barchiesi et al., 2008). The question of whether the PhoQP TCS is the only regulatory system involved in *mgtA* transcription activation arose when previously isolated, spontaneous Lac^+ mutants exhibited elevated *mgtA-lacZ* expression at high Mg^{2+} when the PhoQP TCS should be repressed (Castelli et al., 2000; Chamnongpol et al., 2003; Montagne et al., 2001).

Therefore, we investigated whether other regulators could activate transcription of the *mgtA* gene in the absence of PhoP and whether other sensor kinases could activate *mgtA* transcription via phosphorylation of PhoP in the absence of PhoQ. By screening two categories of mutants on MacConkey agar—ones that induce *mgtA-lacZ* expression in the absence of PhoP (*phoP::Cm*^{R}) and others in the absence of PhoQ (*phoQ::Tn10*)—we were able to isolate several spontaneous Lac^+ mutants that harbored independent mutations both linked and unlinked to the *mgtA-lacZ* transcriptional fusion. Most unlinked mutations are predicted to be located in genes already shown to be involved. Regardless of location, both linked and unlinked mutations provide insight and clarify the roles of Mg^{2+}, Pro and regulatory factors involved. Of several spontaneous Lac^+ mutants isolated, one (G138A) resulted in constitutively high *mgtA-lacZ* expression in the absence of the PhoP, PhoQ and Rob regulators. The *5'LR* (G138A) mutation is

located within the *mgtA* 5' LR downstream of *mgtL*. In this chapter, I focus on the *5'LR* (G138A) mutation and the potential role it may play in the regulation of *mgtA* expression.

5.2 Transcription activation of *mgtA*

5.2.1 PhoQP TCS

The PhoQP TCS regulates a diverse set of genes involved in pathogenesis, acid stress and antimicrobial peptide resistances, cell membrane composition, and Mg^{2+} transport (Groisman, 2001). The sensor kinase PhoQ responds to periplasmic Mg^{2+}, acid pH and antimicrobial peptides (Bader et al., 2005; Gunn and Richards, 2007; Soncini et al., 1996). PhoQ phosphorylates the DNA-binding transcriptional regulator PhoP under low Mg^{2+} conditions (Castelli et al., 2000; Chamnongpol et al., 2003; Montagne et al., 2001), and in turn, PhoP binds to a consensus sequence (T/G)GTTTA 5nt (T/G)GTTTA, termed the PhoP Box (Fig. 5.1A), either activating or repressing the transcription of target genes including activation of its own operon (Lejona et al., 2003; Zwir et al., 2012)

We investigated the contribution of PhoP in the activation of *mgtA* transcription by constructing a *phoP::Cm*^{R} mutant harboring a chromosomal *mgtA-lacZ* transcriptional fusion. Compared to the wild type, which exhibited a 7-fold induction by low Mg^{2+}, the *phoP::Cm*^{R} mutant exhibited constitutively low *mgtA-lacZ* expression (Fig. 5.3). In addition, we measured β-galactosidase activity of strains grown in "Mg^{2+}-free" M63 over time. Mg^{2+}-starvation was unable to induce the *phoP::Cm*^{R} mutant, while the wild-type exhibited a 7.6-fold increase in *mgtA-lacZ* expression at 6 hrs compared to 3 hrs (not shown). Under the conditions tested, both sets of results for the *phoP::Cm*^{R} mutant grown in defined and "Mg^{2+}-free" M63 confirm that transcription of the *mgtA* gene is dependent on PhoP (Véscovi et al., 1996).

5.2.2 Rob transcriptional activator

Rob is a member of the Sox/Mar subfamily of transcriptional regulators that functions in multidrug, heavy metal, superoxide and organic solvent resistance phenotypes (Duval and Lister, 2013). Bile salts and fatty acids increase Rob activity (Rosenberg et al., 2003), and glucose and phosphate starvation enhance expression of *rob* (Kakeda et al.). It has been shown that Rob binds to a region overlapping the PhoP-

Figure 5.1

Schematics of *mgtL* and the *mgtA* 5' LR with emphasis on regulatory features. **A)** Transcriptional regulation of the *mgtA* 5' LR (arrows denote activation; flathead arrows denote repression), emphasis on PhoB Box, Rob-binding site and *mgtA* 5' LR mRNA containing *mgtL* (black nucleotides), Pro codons (yellow boxes), start and stop codons (black boxes), mutations (red nucleotides denote repression; green nucleotides denote activation), *rut* site (blue boxes) and repeat sequences (purple boxes). **(B)** Mutation of the PhoP Box and deletions of the *mgtA* 5' LR (hash-marked boxes indicate mutation of the PhoP Box; black solid-filled boxes indicate repeat sequences).

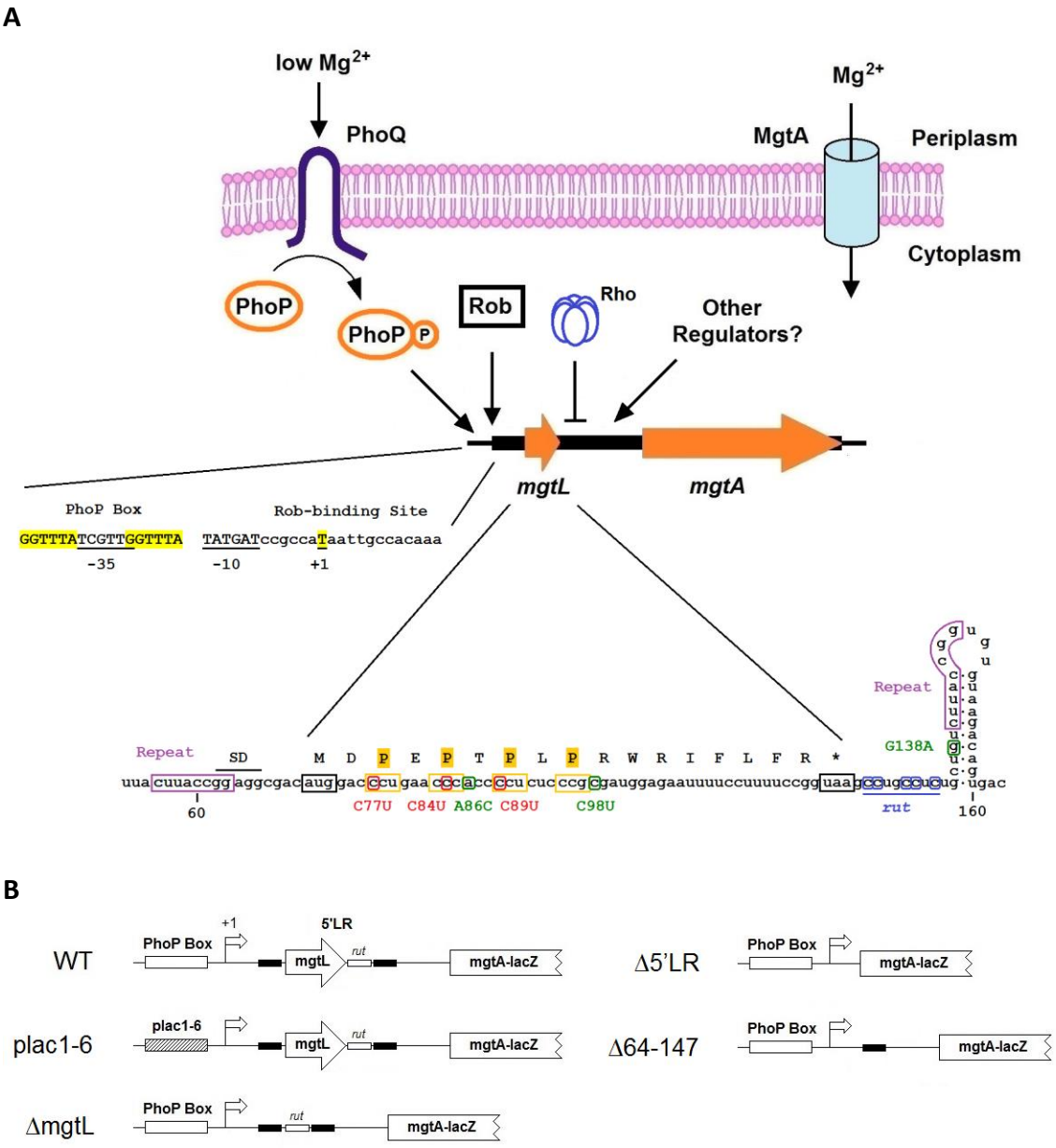
A
low Mg2+
PhoQ
Mg2+
MgtA
Periplasm
Cytoplasm
PhoP
PhoP P
Rob
Rho
Other Regulators?
mgtL
mgtA
PhoP Box
Rob-binding Site
GGTTTATCGTTGGTTTA
TATGATccgccaTaattgccacaaa
-35
-10
+1
Repeat
SD
M D P E P T P L P R W R I F L F R *
uua cuuaccgg aggcgac aug gac Ccu gaa ccc a cc ccu cuc ccg cgauggagaauuuuccuuuuccgg uaa gccugccugug
C77U C84U A86C C89U C98U
rut
60
160
G138A
B
WT
PhoP Box
+1
5'LR
mgtL
rut
mgtA-lacZ
Δ5'LR
plac1-6
ΔmgtL
Δ64-147

Figure 5.1

Figure 5.2

BLAST alignment of *mgtL* nucleotide and MgtL amino acid sequences. **(A)** Nucleotide alignment of *mgtL* or **(B)** amino acid alignment of MgtL from several Enteric bacteria (the number of nucleotides or amino acids in each line is located on the right; asterisks denote homology).

A

```
Salmonella Typhimurium    AUGGACCCUGAACCCACCCCUCUCCCGCGAUGGAGAAUUUUCCUUUUCCGGUAA 54
Salmonella Typhi          AUGGACCCUGAACCCACCCCUCUCCCGCGAUGGAGAAUUUUCCUUUUCCGGUAA 54
Enterobacter sp. 638      AUGGACCCUGAUCCCACCCCUCUCCCGCGAUGGAGAA---UCUCUUUCCGGUAA 51
Citrobacter koseri        AUGGAUCCCGAACCCACCCCUCUCCCGCGAUGGAGAAAUAGCCCUUUCCGGUAA 54
Citrobacter rodentium     AUGGAUCCCGAUCCCACCCCUCUCCCCCGAUGGAGAUACGUUUUUUUCCGGUAA 54
Klebsiella pneumoniae     AUGGACCCCGAUCCCACUCCUCAUCCUCGAUGGAGCAACCUUUCUUUCCGGUAA 54
Enterobacter cloacae      AUGGAUCCCGAUCCCACACCUCUCCUGACCAGGAGAACCCCUUCUUUCCGGUAA 54
                          ***** ** ** ***** ****  *      ****         **********
```

B

```
Salmonella Typhimurium    MDPEPTPLPRWRIFLFR 17
Salmonella Typhi          MDPEPTPLPRWRIFLFR 17
Enterobacter sp. 638      MDPDPTPLPRWRIS-FR 16
Citrobacter koseri        MDPEPTPLPRWRNSPFR 17
Citrobacter rodentium     MDPDPTPLPRWRYVFFR 17
Klebsiella pneumoniae     MDPDPTPHPRWSNLSFR 17
Enterobacter cloacae      MDPDPTPLLTRRTPSFR 17
                          *** ***        **
```

Figure 5.2

dependent *mgtA* transcription start site (Fig. 5.1A), and when over-expressed from a plasmid, Rob activates transcription of *mgtA* in a PhoP-independent manner (Barchiesi et al., 2008). In fact, Rob over-expression can complement de-activation of *mgtA* by a *phoP* knockout; however, Rob over-expression did not result in constitutively high *mgtA-lacZ* expression but preserved the differential Mg^{2+}-sensing control of the *mgtA* gene (Barchiesi et al., 2008).

We corroborated the contribution of Rob by constructing a *rob::Kn*^{R} mutant harboring the *mgtA-lacZ* transcriptional fusion. We observed a slight decrease in the basal levels of *mgtA-lacZ* expression for the *rob::Kn*^{R} mutant, compared to the wild type, under the conditions tested (Fig. 5.3). Because the *rob::Kn*^{R} mutant retained differential Mg^{2+}-sensing control of *mgtA*, we concluded that Rob might contribute to *mgtA* regulation under growth conditions that may not activate the PhoQP TCS.

5.2.3 PhoQ-independent transcription activation

PhoP-dependent transcription regulation of target genes may occur by 1) PhoQ-dependent phosphorylation or 2) PhoP over-expression, both of which facilitate PhoP self-association (Lejona et al., 2003; Montagne et al., 2001). It has been shown that mutation in the *phoP* gene resulting in an S93N substitution in the response regulator receive domain of PhoP mimics auto-phosphorylation in the absence of PhoQ (Chamnongpol and Groisman, 2000). Here, the mutant does not respond to extra-cytoplasmic Mg^{2+} but constitutively expresses the PhoP* protein despite lack of its cognate sensor kinase PhoQ (Chamnongpol and Groisman, 2000).

We corroborated the effect of PhoQ-independent PhoP-dependent transcription activation of the *mgtLA* promoter by introducing the missense and insertion (*phoP** *phoQ::Tn10*) mutations into a strain harboring the chromosomal *mgtA-lacZ* transcriptional fusion. Compared to the wild type, the *phoP** *phoQ::Tn10* mutant exhibited a 23-fold induction in *mgtA-lacZ* expression by low Mg^{2+} (Fig. 5.4). Despite constitutive transcription activation of the promoter, expression of *mgtA* responded to intracellular Mg^{2+}, confirming previous reports that the *mgtA* 5' LR retains ability to differentially regulate transcription into the *mgtA* structural gene (Chamnongpol and Groisman, 2000; Cromie et al., 2006; Spinelli et al., 2008).

Figure 5.3

Effect of transcription activation mutations on *mgtA-lacZ* expression. Strains TL 4295 (*mgtL*$^{+}$ *mgtA-lacZ*), TL 5198 (*phoP1028::Tn10d-Cm*^{R} *mgtA-lacZ*), and TL 4704 (*rob::Kn*^{R} *mgtA-lacZ*] were grown to mid-exponential phase in minimal medium M63 containing high (1.6 mM) or low (0.016 mM) Mg^{2+} at 37°C. Shown are the mean and SD from at least three independent experiments. For panel 2, the activity was lower than the resolution of the figure following growth in high and low Mg^{2+}.

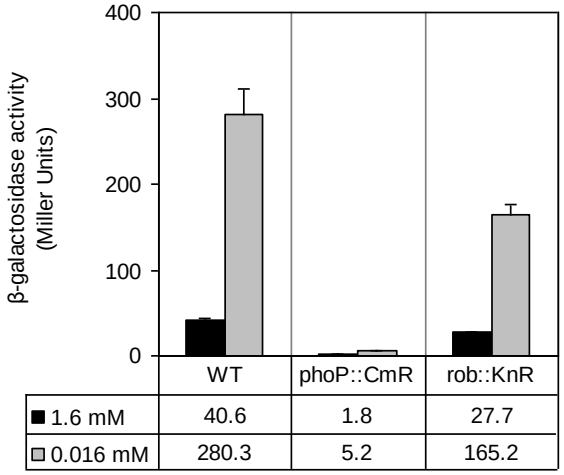
400
300
200
100
0
β-galactosidase activity
(Miller Units)
WT
phoP::CmR
rob::KnR
1.6 mM
40.6
1.8
27.7
0.016 mM
280.3
5.2
165.2

Figure 5.3

5.2.4 PhoP-independent promoter

The *mgtA* 5' LR was proposed to function as a Mg^{2+}-sensing riboswitch in which folding of the mRNA may adopt alternating stem loop structures that facilitate transcription into or termination upstream of the *mgtA* structural gene depending on the intracellular [Mg^{2+}] (Cromie et al., 2006). Previously, a strain harboring a PhoP-independent and Mg^{2+}-unresponsive promoter ($p_{lac1\text{-}6}$) was characterized (Cromie et al., 2006). We investigated the role of the *mgtA* 5' LR by constructing the $p_{lac1\text{-}6}$ mutant harboring a chromosomal *mgtA-lacZ* transcriptional fusion (Fig. 5.1B) and measured β-galactosidase activity of strains grown in minimal media M63 containing high or low Mg^{2+}. Compared to the wild type, the $p_{lac1\text{-}6}$ mutant exhibited 20-fold induction by low Mg^{2+} (Fig. 5.4). Although our model does not support the 5' LR as a Mg^{2+}-sensing riboswitch, our results corroborate the previous report that the 5' LR functions independently of the PhoQP TCS in differential Mg^{2+}-sensing control of *mgtA* expression (Cromie et al., 2006).

5.3 Leader region of *mgtA*

Based on previous results, the *mgtA* 5' LR functions to differentially regulate transcription into the *mgtA* structural gene by a ribosome-mediated mechanism involving Mg^{2+}-sensing via prolyl-bond formation during translation of *mgtL* (see Chapter 3). We investigated downstream regions that may contribute to the regulation by constructing site-directed deletions and isolating spontaneous mutations within the 5' LR.

5.3.1 Deletion of *mgtL*

We investigated the contribution of *mgtL* in differential Mg^{2+}-sensing control by deleting the entire *mgtL* ORF (Δ*71-124*, or Δ*mgtL*; Fig. 5.1B). The Δ*mgtL* mutant lacks stem loop A and cannot form stem loop C but retains ability to form stem loop B. Compared to the wild type, the Δ*mgtL* mutant exhibited constitutively low *mgtA-lacZ* expression (Fig. 5.5). In this case, with only ability to form stem loop B, Rho binding and transcription termination dominate the regulation of *mgtA* expression. This result emphasizes the need for translation of *mgtL* to antagonize Rho termination at low Mg^{2+}.

Figure 5.4

Effect of promoter mutations on *mgtA-lacZ* expression. Strains TL 4295 (*mgtL*$^{+}$ *mgtA-lacZ*), TL 5839 (S93N-*phoP phoQ::Tn10 mgtA-lacZ*), and TL 5176 (up-9251::Cm^{R} *plac*$_{1\text{-}6}$ *mgtA-lacZ*] were grown as described in Fig. 5.3. Shown are the mean and SD from at least three independent experiments.

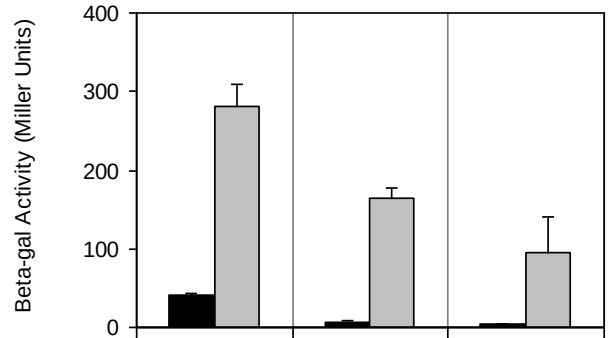

	WT	S93N-phoP phoQ::Tn10	plac1-6
■ 1.6 mM	40.6	7.2	4.7
□ 0.016 mM	280.3	164.8	95.8

Figure 5.4

5.3.2 Deletion of the *mgtA* 5' LR

We corroborated previous findings that deletion of the entire *mgtA* 5' LR (nucleotides 9-244) resulted in constitutively high *mgtA-lacZ* expression, compared to the wild type (Spinelli et al., 2008), by constructing the Δ*9-244* mutant (Δ*5' LR*) and measuring β-galactosidase activity (Fig. 5.1B). Here, the Δ*5' LR* mutant retains the native PhoP-dependent promoter and TSS but lacks the alternating stem loop structures; therefore, expression of the chromosomal *mgtA-lacZ* transcriptional fusion should correlate to the level of PhoP-dependent activation. Compared to the wild type, which exhibited a 7-fold induction by low Mg^{2+}, the Δ*5' LR* mutation resulted in constitutively high *mgtA-lacZ* expression (Fig. 5.5). Despite growth in high Mg^{2+}, which should turn "OFF" the PhoQP TCS, the Δ*5' LR* mutant exhibited the constitutively "ON" phenotype, suggesting that 1) PhoP-dependent activation of the *mgtLA* promoter is also constitutive and independent of the Mg^{2+} concentration and/or the Δ*5' LR* mutation 2) eliminates a negative regulatory site or 3) enhances a positive regulatory site (discussed further in Section 5.5).

5.3.3 Deletion of an *mgtA* 5' LR portion

We isolated a spontaneous Lac^{+} mutant harboring deletion of *mgtL* and part of the 5' LR (Fig. 5.1B). Apparently, the deletion resulted from excision of nucleotides 64-147 of the *mgtA* 5' LR by homologous recombination at two repeat sequences (CTTACCGG). Compared to the wild type, the Δ*64-147* mutant exhibited constitutively high *mgtA-lacZ* expression (Fig. 5.5). Before evidence of the *rut* site and Rho-dependent transcription termination was provided (Hollands et al., 2012), it was shown that deletion of stem loop B by the Δ*126-170* (Δ*SLB*) mutation resulted in constitutively high *mgtA-lacZ* expression (Spinelli et al., 2008). Here, deletion of the *rut* site by the Δ*SLB* mutation like in the Δ*64-147* mutant precludes ability to terminate transcription of the *mgtA* structural gene. At first glance, excision by the repeat sequences appeared unexceptional until considered more in depth (see Sub-section 5.5.2).

5.4 Spontaneous and compensatory mutations

To discover novel factors involved and growth conditions that induce *mgtA* expression, we selected for spontaneous mutants on MacConkey agar that 1) exhibited the Lac^+ phenotype at repressing Mg^{2+} conditions and 2) overcame repression by the *mgtL* (3Pro-) and *phoP::Cm*^{R} mutations.

5.4.1 Isolation of constitutive mutations of *mgtA*

We isolated two spontaneous Lac^+ mutants on MacConkey agar (A86C and C98T) that harbored mutations in *mgtL* (see Chapter 3). The *mgtL* (A86C) mutation resulted in a threonine-to-proline codon substitution, generating three contiguous Pro codons within *mgtL* (Fig. 5.1A). On the other hand, the *mgtL* (C98T) mutation resulted in an arginine-to-nonsense codon substitution and premature translation termination of *mgtL* (Fig. 5.1A). Both leader ORF mutants exhibited constitutively high *mgtA-lacZ* expression compared to the wild type (see Chapter 3). In addition, we isolated a novel, spontaneous Lac^+ mutant of the *mgtA* 5' LR, which generated a point mutation (G138A) located downstream of both *mgtL* and the *rut* site but upstream of the *mgtA* structural gene (Fig. 5.1A). Compared to the wild type, the *5' LR* (G138A) mutation resulted in constitutively high *mgtA-lacZ* expression (Fig. 5.6).

5.4.2 De-repression of silencing mutations of *mgtA*

Rapid, complete translation of the *mgtL* (3Pro-) mutant is predicted to favor stem loop B, constitutively exposing the *rut* site and facilitating Rho-dependent transcription termination of *mgtA* (see Chapter 3). We investigated whether mutations that result in constitutively "ON" phenotype could overcome the silencing effects of the *mgtL* (3Pro-) mutation by isolating spontaneous Lac^+ mutants starting with the *mgtL* (3Pro-) strain (Fig. 5.1A). Of several spontaneous mutants, surprisingly, we re-isolated the *5' LR* (G138A) mutation in the *mgtL* (3Pro-) background. Here, the double *5' LR* (G138A) *mgtL* (3Pro-) mutant exhibited constitutively high *mgtA-lacZ* expression compared to the wild type, contrary to the single *mgtL* (3Pro-) mutant, which exhibited the constitutively "OFF" phenotype (Fig. 5.6).

We investigated whether the *mgtL* (A86C), *mgtL* (C98T) and *5' LR* (G138A) mutants were dependent on PhoP activation by introducing the *phoP::Cm*^{R} mutation into their respective backgrounds and

Figure 5.5

Effect of leader region mutations on *mgtA-lacZ* expression. Strains TL 4295 (*mgtL*$^{+}$ *mgtA-lacZ*), TL 5135 (*mgtL* (Δ71-124) *mgtA-lacZ*), TL 5453 [*5' LR* (Δ64-147) *mgtA-lacZ*], and TL 4697 (*5' LR* (Δ9-244) *mgtA-lacZ*] were grown as described in Fig. 5.3. Shown are the mean and SD from at least three independent experiments.

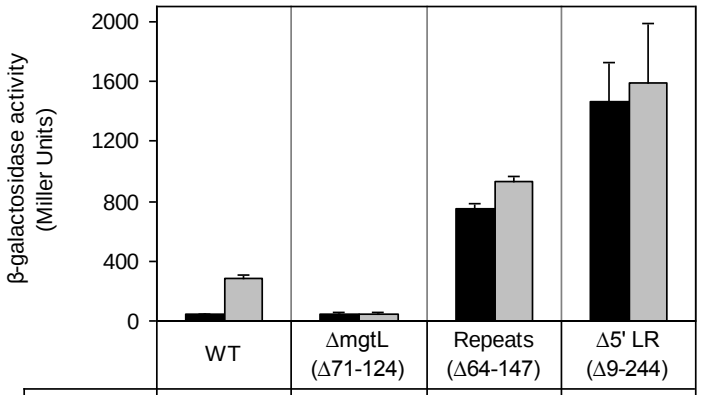

	WT	ΔmgtL (Δ71-124)	Repeats (Δ64-147)	Δ5' LR (Δ9-244)
■ 1.6 mM	40.6	47.0	754.8	1467.6
□ 0.016 mM	280.3	40.6	930.2	1590.5

Figure 5.5

measuring β-galactosidase activity or observing the Lac phenotype of the independent double mutants on MacConkey agar. Both the double *mgtL* (A86C) *phoP::Cm*^{R} and the double *mgtL* (C98T) *phoP::Cm*^{R} mutants exhibited the Lac^{--} phenotype similar to the single *mgtL*$^+$ *phoP::Cm*^{R} mutant (Table 5.1), indicating that these two mutations require PhoP. Interestingly, however, the double *5' LR* (G138A) *phoP::Cm*^{R} mutant exhibited constitutively high *mgtA-lacZ* expression similar to the single *5' LR* (G138A) *phoP*$^+$ mutant (Fig. 5.6). The double *5' LR* (G138A) *phoQ::*Tn*10* and triple *5' LR* (G138A) *phoP::Cm*^{R} *phoQ::*Tn*10* mutants retained the Lac$^+$ phenotype of the single *5' LR* (G138A), *phoP*$^+$ *phoQ*$^+$ mutant (Table 5.1). Lastly, we investigated whether the *mgtL* (A86C), *mgtL* (C98T) and *5' LR* (G138A) mutants were dependent on Rob transcription activation by introducing the *rob::Kn*^{R} mutation into their respective backgrounds and performing the same analysis as described above. Despite lack of the Rob transcriptional activator, the double *mgtL* (A86C) *rob::Kn*^{R}, double *mgtL* (C98T) *rob::Kn*^{R} and double *5' LR* (G138A) *rob::Kn*^{R} mutants retained the Lac$^+$ phenotype similar to their respective single *rob*$^+$ mutant counterparts (Table 5.1). In this case, these three mutations do not require a transcript generated by Rob but only PhoP.

At first glance, the *5' LR* (G138A) mutation, which is located within the left arm of stem loop B, was predicted to disrupt stem loop B and favor stem loop C based on RNA folding dynamics (Fig. 5.1A). However, the *5' LR* (G138A) mutation induces *mgtA* expression by a mechanism independent of translation of *mgtL* [e.g., *mgtL* (3Pro-) background] and PhoP-dependent transcription activation [e.g., *phoP::Cm*^{R} background]. These results indicate that *5' LR* (G138A) may regulate *mgtA* expression downstream of the native *mgtLA* promoter by 1) creating a new promoter, 2) destroying a negative regulatory site or 3) enhancing a positive regulatory site.

5.5 Alternative transcription activation of *mgtA*

In addition to sigma factor-dependent transcription activation of bacterial genes and operons, regulatory proteins may bind promoter regions, facilitating RNA polymerase in forming an RNA-DNA complex (Ruff et al., 2015). DNA-binding transcriptional regulators may modulate transcription, generating multiple TSSs that lead to differential regulation of their 5' LRs and respective structural genes (Narlikar, 2014). The *mgtLA* promoter region harbors a consensus sequence [(T/G)GTTTA 5nt (T/G)GTTTA] termed the PhoP

Figure 5.6

Effect of spontaneous and compensatory mutations on *mgtA-lacZ* expression. Strains TL 4295 (*mgtL*$^{+}$ *mgtA-lacZ*), TL 5055 (*5' LR* (G138A) *mgtA-lacZ*), TL 5540 [*mgtL* (3Pro-) *mgtA-lacZ*], TL 5716 [*mgtL* (3Pro-) *5' LR* (G138A) *mgtA-lacZ*], TL 5198 (*phoP1028::Tn10d-Cm*^{R} *mgtA-lacZ*], and TL 5493 [*phoP1028::Tn10d-Cm*^{R} *5' LR* (G138A) *mgtA-lacZ*] were grown as described in Fig. 5.3. Shown are the mean and SD from at least three independent experiments. For panels 3 and 5, the activities were lower than the resolution of the figure following growth in high and low Mg^{2+}.

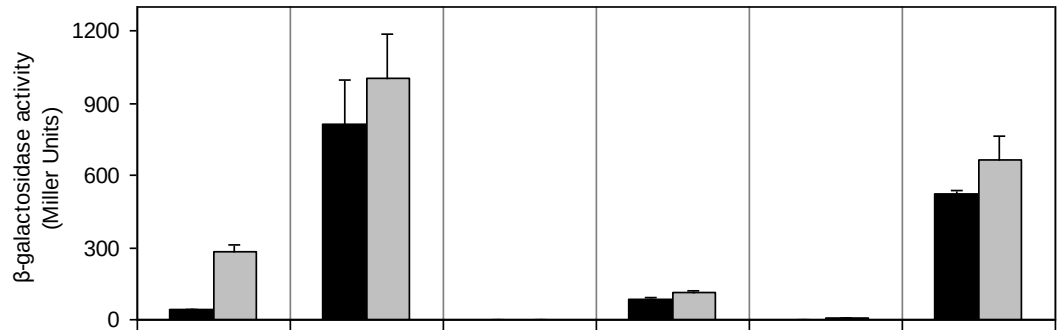

	WT	5' LR (G138A)	mgtL (3Pro-)	5' LR (G138A) mgtL (3Pro-)	phoP::CmR	phoP::CmR 5' LR (G138A)
■ 1.6 mM	40.6	809.5	0.2	86.1	1.8	522.0
□ 0.016 mM	280.3	1003.4	0.2	112.9	5.2	665.9

Figure 5.6

Table 5.1

Effect of transcriptional activator mutations on the Lac phenotype of various mutants. The *phoP::Cm*^{R}, *phoQ::Tn10* and *rob::Kn*^{R} mutations were introduced independently into various wild-type and mutant backgrounds. Plus (+) and minus (--) denote red (Lac$^+$) and white (Lac$^-$) colonies on MacConkey agar, respectively. ND denotes the Lac phenotypes that were not determined.

Table 5.1

Strain	Genotype	Lac Phenotype			
		WT	*phoP*$^{--}$	*phoQ*$^{--}$	*rob*$^{--}$
TL 4295	*mgtA9226::MudJ* (wild-type transcriptional fusion)	--	--	--	--
TL 4575	*mgtL* (C98T) *mgtA9226::MudJ*	+	--	ND	ND
TL 4576	*mgtL* (A86C) *mgtA9226::MudJ*	+	--	ND	+
TL 5055	*5′ LR* (G138A) *mgtA9226::MudJ*	+	+	+	+
TL 5527	*mgtA774::MudK* (wild-type translational fusion)	--	ND		
TL 5540	*mgtL* (3Pro-) *mgtA774::MudK*	--	ND		
TL 5716	*mgtL* (3Pro-) *5′ LR* (G138A) *mgtA774::MudK*	+	+		
TL 5135	*ΔmgtL* (Δ71-124) *mgtA9226::MudA*	--	ND		
TL 5453	*5′ LR* (Δ64-147) *mgtA9226::MudJ*	+	--		
TL 4697	*Δ5′ LR* (Δ9-244) *mgtA9226::MudJ*	+	--		

Box for PhoP-dependent transcription activation and a binding site (ACCGCCTAATTGCCACAAA) for Rob transcription activation with the PhoP-activated TSS underlined (Fig. 5.1A). The locations of the PhoP- and Rob-activated TSSs differ, though both generate a similar *mgtA* 5' LR and common *mgtA* structural gene. We investigated the hypothesis that, unlike mutations in *mgtL* that result in constitutively "ON" phenotypes in a PhoP-dependent manner, the *5' LR* (G138A) mutation uncovers a novel function of the *mgtA* 5' LR in regulating *mgtA* independently of Rob and the PhoQP TCS.

5.5.1 SMARTer 5' RACE analysis of the *mgtA* 5' LR

As described in Materials and Methods, we investigated whether the *5' LR* (G138A) mutation excites an alternative TSS by using the SMARTer® RACE 5'/3' Kit (Clontech Laboratories, Inc.) to analyze the *mgtA* 5' LR mRNA transcripts generated from the single *5' LR* (G138A) *phoP*$^{+}$ and double *5' LR* (G138A) *phoP::Cm*^{R} mutants (Fig. 5.7A). Based on preliminary SMARTer 5'RACE analysis of the single *5' LR* (G138A) *phoP*$^{+}$ mutant, DNA sequencing revealed a 5' end at nucleotide +149, while in the double *5' LR* (G138A) *phoP::Cm*^{R} mutant, the 5' end was generated at nucleotide +151 (Fig. 5.7B). These independent results could represent the same TSS based on DNA sequencing errors; yet, finding the location of these 5' ends within two nucleotides distance is promising. Whether these TSSs have any role in the regulation of *mgtA* expression, the wild type needs to be determined. Given its location between the *rut* site and the *mgtA* structural gene, and based on its ability to retain constitutively high *mgtA-lacZ* expression in the *phoP::Cm*^{R} background, we hypothesized that the *5' LR* (G138A) mutation affects the DNA-binding site for an unidentified, transcriptional regulator.

5.5.2 Potential protein-binding site in the *mgtA* 5' LR mRNA

As discussed above, we isolated a spontaneous mutation of the *mgtA* 5' LR (Δ*64-147*) that excised both *mgtL* and the *rut* site (Fig. 5.1A). The Δ*64-147* mutation resulted in constitutively high *mgtA-lacZ* expression, compared to the wild type (Fig. 5.5). Initially, we attributed the constitutively "ON" phenotype to loss of the *rut* site and Rho-dependent transcription termination. Analysis of the *mgtA* 5' LR revealed a repeat sequence (CTTACCGG) that may have facilitated this deletion by homologous recombination (Fig.

Figure 5.7

Detailed flow chart of 5’ RACE and preliminary results for G138A mutants. **(A)** Re-drawn schematic from the SMARTer® RACE 5’/3’ Kit (Clontech Laboratories, Inc) and **(B)** Sanger Sequencing results from the Low Throughput Laboratory (Purdue University) for the 5’ ends of cDNA generated from the single *5’ LR* (G138A) *phoP*$^{+}$ and double *5’ LR* (G138A) *phoP::Cm*^{R} mutants.

A

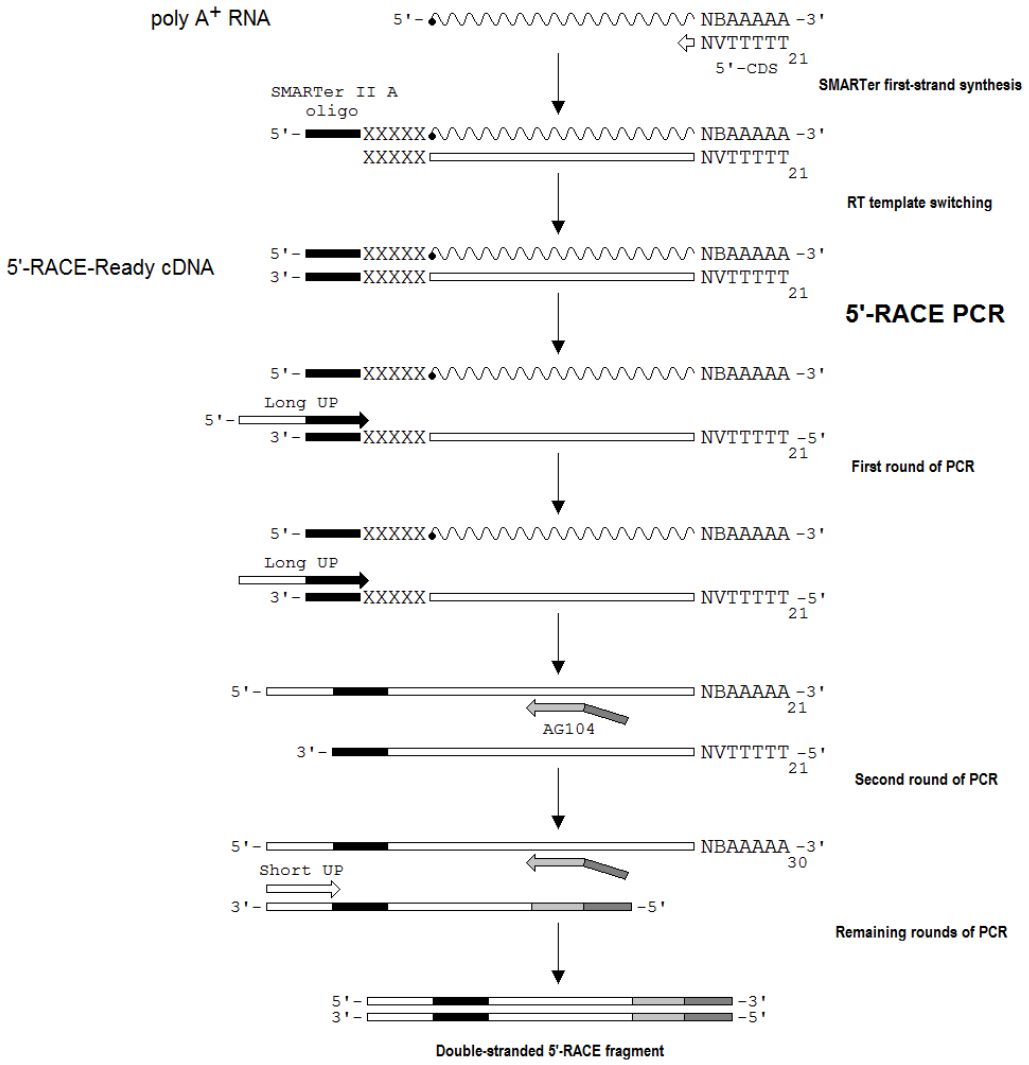

B

G138A *phoP*$^{+}$ +149 GTGTAAGACAGTGACACAATAACGT...

G138A *phoP::Cm*^{R} +151 GTAAGACAGTGACACAATAACGT...

Figure 5.7

5.1A). The presence of this repeat sequence raises the possibility that it may function as a binding site for a regulatory protein.

Using the bioinformatics web server PRODORIC (Grote et al., 2009), we analyzed the *mgtLA* promoter region and 5' LR for potential promoters and protein-binding sites. Based on the virtual footprint, we observed that CTTACCGG showed slight sequence similarity to the protein-binding site for the DNA-binding transcriptional regulator RhlR of *Pseudomonas aeruginosa* (Fig. 5.8). In response to auto-inducers such as *N*-acylhomoserine lactones (AHLs), RhlR activates transcription of its own operon (*rhlABR*) that harbors genes involved in rhamnolipid production, which plays an important role in the quorum-sensing response (QSR) (Medina et al., 2003a; Medina et al., 2003b; Ochsner et al., 1994). Based on protein-protein BLAST analysis, the QSR transcriptional regulator SdiA (suppressor of cell division inhibitor) of *Salmonella enterica* is similar to RhlR, especially the C-terminal DNA-binding domain of LuxR-like proteins (Fig. 5.9). A member of the LuxR family, SdiA activates expression of genes involved in cell division and *ydiV*, which is involved in the interaction with the cyclic AMP (cAMP) receptor protein CRP (Ahmer et al., 1998).

5.5.3 Search for transcriptional regulators of *mgtA*

In *Pseudomonas*, *E. coli* and *Salmonella*, the PhoBR TCS regulates genes involved in phosphate homeostasis (Baek et al., 2007; Crépin et al., 2011; Filloux et al., 1988) and is involved in *E. coli* virulence (Crépin et al., 2011). Similar to the Mg^{2+} response of the PhoQP TCS, low phosphate activates the sensor kinase PhoR, which in turn phosphorylates the DNA-binding transcriptional regulator PhoB (Gardner et al., 2015). Activation of genes involved in uptake and metabolism occurs when PhoB binds to a region, termed the PHO box, harboring two 7-bp direct repeats (CTGTCAT) separated by a variable-length segment (Blanco et al., 2002; Makino et al., 1986). In *Pseudomonas aeruginosa*, PhoB contributes to the transcription activation of the *rhlR* gene via biosynthesis of quorum-sensing secondary metabolites (Jensen et al., 2006). Based on gene expression profiling of a *phoB::Cm*^{R} mutant under acidic conditions, PhoB may activate transcription of the *phoQ* gene in *E. coli* (Marzan et al., 2012). In addition, PhoP was shown to activate transcription of the *psiD* gene, whose expression phosphate availability also regulates (Groisman et al., 1989).

Figure 5.8

Sequence logo derived from RhlR- and LasR-regulated genes and the *mgtA* 5' LR. **(A)** Sequence logo derived from the RhlR-regulated *rhlAB*, *phzA*, *acpP*, and *pa1L* genes and the LasR-regulated *hcnABC*, *lasB*, *acpP*, *phzA*, *lasL*, *rhlL*, *rsaL*, and *rhlR* genes. **(B)** Portion of the *mgtA* 5' LR from +136 to +151 including nucleotide G138 (underlined).

A

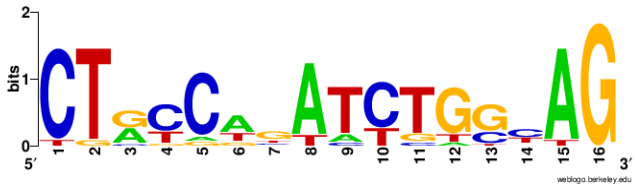

B

mgtA 5' LR +136 **CTGTCTTACCGGTGTG** +151

Figure 5.8

Figure 5.9

BLAST alignment of *Salmonella* SdiA and *Pseudomonas* RhlR transcriptional regulators. Exact matches are denoted by abbreviated amino acids in-between BLAST alignments. Similar amino acids based on charge are denoted by plus (+).

```
SdiA    M-QENDFFTWRRAMLLRFQEMAAAEDVYTELQYQTQRLEFDYYALCVRHPVPFTRPKISLRT  62
           +  F  W   +    Q +  ++ V+  L+ + +RL FDYYA  VRH +PFTRPK  +
RhlR    MRNDGGFLLWWDGLRSEMQPIHDSQGVFAVLEKEVRRLGFDYYAYGVRHTIPFTRPKTEVHG  64

SdiA    TYPPAWVTHYQSENYFAIDPVLKPENFRQGHLHWDDVLFHEAKAMWDAAQRFGLRRGVTQ  122
        TYP AW+  YQ +NY A+DP +         + W D LF +++ +W+ A+ +GL  G T
RhlR    TYPKAWLERYQMQNYGAVDPAILNGLRSSEMVVWSDSLFDQSRMLWNEARDWGLCVGATL  124

SdiA    CVMLPNRALGFLSFSRSSLRCSSFTYDEVELRLQLLARESLSALTRFEDDMVMAPEMRFS  182
         +  PN  L  LS +R     SSF  +E+ LRL+ +       LT  E  M+M+  +  S
RhlR    PIRAPNNLLSVLSVARDQQNISSFEREEIRLRLRCMIELLTQKLTDLEHPMLMSNPVCLS  184

SdiA    KREKEILKWTAEGKTSSEIAIILSISENTVNFHQKNMQKKFNAPNKTQIACYAAATGLI  241
         RE+EIL+WTA+GK+S EIAIILSISE+TVNFH KN+QKKF+APNKT  A YAAA GLI
RhlR    HREREILQWTADGKSSGEIAIILSISESTVNFHHKNIQKKFDAPNKTLAAAYAAALGLI  243
```

Figure 5.9

Therefore, we investigated PhoB, PhoR and SdiA as potential novel regulators of *mgtA* expression by independently introducing *phoB::Cm*^{R}, *phoR::Cm*^{R} and *sdiA::Cm*^{R} mutations (Porwollik et al., 2014) into the wild-type, single *5' LR* (G138A) *phoP*$^+$ and double *5' LR* (G138A) *phoP::Cm*^{R} mutant backgrounds and observing their Lac phenotypes on MacConkey agar. Both sets of double and triple mutants harboring the *phoB::Cm*^{R}, *phoR::Cm*^{R} and *sdiA::Cm*^{R} mutations retained the Lac$^+$ phenotype, while all three single mutations were unable to increase the Lac phenotype of the wild-type background on MacConkey agar but retained the Lac^{--} phenotype (Table 5.2). Based on these results, neither PhoB nor SdiA facilitate transcription activation via the *5' LR* (G138A) mutation or repression of *mgtA* in the wild-type background. We investigated the possibility that PhoB, PhoR and/or SdiA facilitate transcription repression of *mgtA* by introducing the *phoB::Cm*^{R}, *phoR::Cm*^{R} and *sdiA::Cm*^{R} mutations into the wild-type background harboring an *mgtA-lacZ* transcriptional fusion. However, we observed the Lac^{--} phenotype for all constructs (Table 5.2), indicating that neither PhoB, PhoR nor SdiA facilitate transcription repression of *mgtA* in the wild-type background. As a last attempt, we will introduce both *phoB::Cm*^{R} and *phoR::Cm*^{R} mutations into a double *5' LR* (G138A) *phoP::Tc*^{R} mutant background, since the PhoBR TCS may require both PhoB and PhoR for regulation (Baek et al., 2007).

Table 5.2

Effect of regulator mutations on the Lac phenotype of the wild type and G138A mutants. The *sdiA::Kn*^{R}, *phoB::Kn*^{R} and *phoR::Kn*^{R} mutations were introduced independently into various wild-type and mutant backgrounds. Plus (+) and minus (--) denote red (Lac$^+$) and white (Lac$^-$) colonies on MacConkey agar, respectively. ND denotes the Lac phenotypes that were not determined.

Table 5.2

Strain	Genotype	Lac Phenotype			
		WT	*sdiA*$^{--}$	*phoB*$^{--}$	*phoR*$^{--}$
TL 4295	*mgtA9226::MudJ* (wild-type transcriptional fusion)	--	--	--	--
TL 5055	*5′ LR* (G138A) *mgtA9226::MudJ*	+	+	+	+
TL 5493	*5′ LR* (G138A) *mgtA9226::MudJ phoP::Cm*^{R}	+	+	+	+
TL 5877	*mgtA9226::MudJ phoP::Tc*^{R} *phoR::Cm*^{R}	+	ND	ND	
TL 5933	*5′ LR* (G138A) *mgtA9226::MudJ phoP::Tc*^{R} *phoR::Cm*^{R}	+	ND	ND	

CHAPTER 6. PRELIMINARY EVIDENCE FOR THE REGULATION OF SUCCINATE METABOLISM BY MAGNESIUM, PROLINE AND REGULATORY PROTEINS

6.1 Introduction

Salmonella experiences diverse environmental conditions and exposure to a wide range of nutrients during infection of host epithelial cells and macrophages (Eisenreich et al., 2010). Sensory regulators and TCSs can monitor environmental cues and intracellular signals to maintain cell growth and proliferation (Rychlik and Barrow, 2005). In particular, stationary phase sigma factor RpoS and the PhoQP TCS function coordinately to adapt to stresses and nutrient starvation and to maintain intracellular Mg^{2+} homeostasis, respectively (Schellhorn, 2014; Véscovi et al., 1996). The sigma factor RpoS regulates genes involved in nutrient uptake and metabolism, cell membrane permeability and other important cellular processes when cells experience stress and nutrient starvation (Schellhorn, 2014).

It was shown previously that *Salmonella* strains deficient in the stationary phase sigma factor RpoS or the translation factor EF-P, which rescues ribosomes stalled during translation of peptides containing poly-Pro stretches, experience increased rates of growth (decreased doubling times) when sub-cultured into minimal media supplemented with succinate as the sole carbon source compared to their respective parental strains (Navarre et al., 2015). A C4-dicarboxylic acid, succinate is one of the intermediate sugars of the Tricarboxylic Acid (TCA) cycle and functions as the poorest, secondary carbon source compared to glucose, glycerol, acetate, and citrate, in order based on growth rate of *E. coli* in aerobic conditions (Paliy and Gunasekera, 2007).

In addition, supplementation of cultures with exogenous Pro, an osmoprotectant, decreased the lag phase growth of *Salmonella* on succinate (Navarre et al., 2015). Apparently, RpoS represses transcription of *dctA*, a gene encoding a necessary transporter for C4-dicarboxylates such as malate, fumarate and succinate under aerobic conditions, and thus an RpoS-deficient strain showed an increase in *dctA*

expression (Navarre et al., 2015). In addition, RpoS down-regulates expression of the succinate dehydrogenase complex, encoded by the *sdhCDBA* operon, genes encoding the ATP synthase and cytochromes involved in electron transport (Lévi-Meyrueis et al., 2015). EF-P was hypothesized to aide RpoS-mediated adjustments in metabolism by preventing cytoplasmic acidification when *Salmonella* proliferates within the phagosome of the macrophage (Navarre et al., 2015). However, involvement of Pro and EF-P in affecting growth on succinate remains a mystery.

We corroborated the effects of *Salmonella* strains deficient in RpoS and EF-P and supplementing minimal medium M63 with exogenous Pro. Interestingly, we found that a strain deficient in PhoP also experienced a decrease in the doubling time compared to the wild type, similar to single *rpoS::Ap*^{R} and Δ*efp::Cm*^{R} mutants. In the PhoQP TCS, acid pH, APs and low Mg^{2+} activate the sensor kinase PhoQ, which in turn phosphorylates its cognate DNA-binding transcriptional regulator PhoP (Bader et al., 2005; Prost et al., 2007; Soncini et al., 1996). In Mg^{2+} homeostasis, PhoP activates transcription of the *mgtA* gene and the *mgtCBR* operon, both of which encode P-type ATPase transporters MgtA and MgtB to mediate Mg^{2+} influx (Papp-Wallace and Maguire, 2008). As discussed above, we showed that EF-P regulates transcription of the *mgtA* gene via translation of *mgtL* (see Chapter 3). Because strains deficient in PhoP and EF-P result in similar phenotypes when grown on succinate and yet regulate *mgtA* expression in opposite manners (see Chapter 3), we investigated further the contributions of Pro availability the Mg^{2+} transporters MgtA and MgtB to better understand the cross-regulation of Mg^{2+} transport, Pro and succinate metabolism.

6.2 Succinate metabolism

Succinate is converted to fumarate by SdhDCBA, which generates $FADH_2$ during the TCA cycle and transfers electrons via ubiquinol to the cytochrome *bo* complex during aerobic respiration (Fig. 6.1) (Ingledew and Poole, 1984). We investigated the effect of several, independent mutations on the growth of *Salmonella* strains on succinate as the sole carbon source by measuring cell density over time of subcultures grown aerobically with shaking at 37°C in minimal medium M63 supplemented with 20 mM succinate.

6.2.1 Regulation by transcription and translation factors

Based on the slopes of a logarithmic graph with cell density plotted over time, we observed decreases in the exponential-phase doubling times for the *phoP::Cm*^{R}, *rpoS::Ap*^{R} and Δ*efp::Cm*^{R} mutants, compared to the wild type (Fig. 6.2). In addition, we observed a significant decrease in the lag phase growth of the parental strain on 20 mM succinate when supplemented with 1 mM Pro (<6 hrs) compared to its absence (~38 hrs) and a slight decrease in the doubling time in the presence of Pro compared to its absence (Fig. 6.3).

6.2.2 Involvement of Pro and metabolic enzymes

The question of how exogenous Pro may dramatically decrease the lag phase growth of *Salmonella* on succinate arose, whether Pro metabolism plays a role in the TCA cycle via the translation factor EF-P. PutA is an enzyme that converts L-proline to L-glutamate in a 2-step process (Fig. 6.1) (Servet et al., 2012). ProA, ProB and ProC are essential enzymes that convert L-glutamate into L-proline in a 3-step process for the biosynthesis of Pro (Fig. 6.1) (Adams and Frank, 1980). Deletion of one of these three genes results in Pro auxotrophy, requiring exogenous Pro to complement the growth defect. In addition, PutA contains a Proline-Proline-Glycine (PPG) motif of that may be recognized by the translation factor EF-P, and therefore, EF-P may assist translation of PutA (Doerfel et al., 2013). We hypothesized that deletion of the *efp* gene should decrease PutA protein levels, which may increase intracellular Pro levels and simultaneously decrease intracellular glutamate levels. Deletion of the *putA* gene is hypothesized to result in a similar phenotype as the Δ*efp::Cm*^{R} mutant.

We investigated the contribution of intracellular Pro in succinate utilization, whether Pro itself increases growth rate, by measuring cell density of *Salmonella* strains that harbor deletion of the *putA* gene or in which plasmid-borne expression of a *proBA-74* mutation results in a dramatic increase in intracellular Pro levels (Csonka, 1981). Compared to the wild type, we found that the *putA*$^{--}$ mutant, deficient in Pro degradation, exhibited a decreased doubling time on succinate (Fig. 6.2). Deficiency in PutA is more reminiscent of addition of exogenous Pro than deficiency in EF-P in its effect on succinate metabolism. Compared to the wild type, the *proBA-74* mutant exhibited a decreased doubling time but a slightly

Figure 6.1

Biochemical reactions, enzymes and substrates in succinate and Pro metabolisms. Succinate metabolism utilitzes the SdhDCBA (succinate dehydrogenase) complex and the cytochrome *bo* complex during aerobic respiration. Proline metabolism comprises degradation via PutA-mediated conversion of L-proline to L-glutamate in a 2-step process, and biosynthesis of L-proline from L-glutamate by the ProA, ProB and ProC enzymes in a 3-step process. Parentheses enclose enzmes, substrates or electron carriers.

Succinate Metabolism

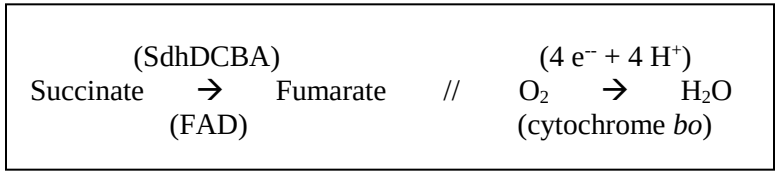

Proline Metabolism

Degradation

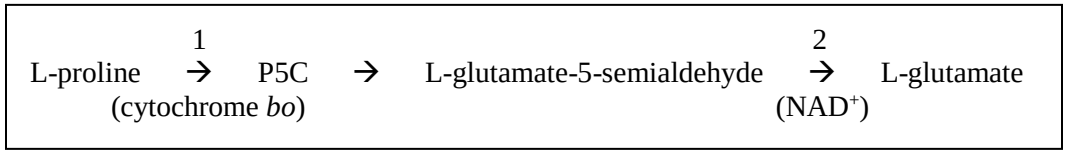

Biosynthesis

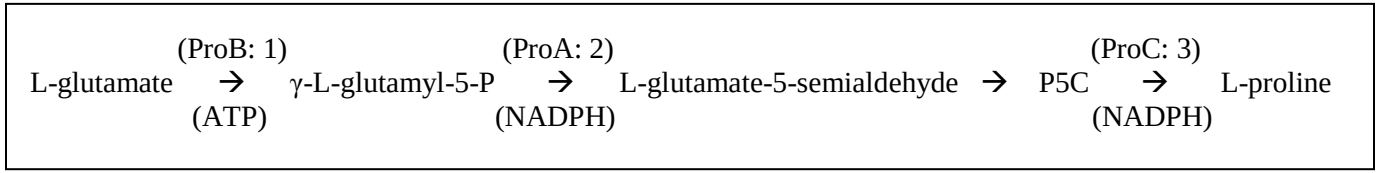

Figure 6.1

increased lag phase (Fig. 6.3). Over-production of intracellular Pro appears to negatively influence cell division but eventually increases the growth rate similar to deficiencies of PhoP, RpoS, and EF-P.

6.2.3 Involvement of Mg^{2+} transport

The P-type ATPase transporters MgtA and MgtB mediate influx of Mg^{2+} by hydrolyzing ATP (Maguire). We investigated the effect of Mg^{2+} transport on succinate metabolism, whether intracellular Mg^{2+} is the main contributor, by measuring the growth of *Salmonella* strains deficient in Mg^{2+} transport (*mgtA*$^{--}$ and *mgtB*$^{--}$) and that over-express MgtA and MgtB (*mgtA*$^{++}$ and *mgtB*$^{++}$) in minimal medium M63 supplemented with 20 mM succinate. Compared to the wild type, all mutants exhibited slight decreases in doubling times, though not as significant as deficiencies of PhoP, RpoS, and EF-P (Figs. 6.2 and 6.4). Interestingly, we observed a pattern in which deficiency in MgtA or MgtB did not affect the lag phase growth compared to the wild type; however, over-expression of MgtA and MgtB independently increased the lag phase growth on succinate (Fig. 6.4).

6.3 Concluding remarks

We corroborated previous findings that implicated the response regulator RpoS and translation factor EF-P in dynamics of the TCA cycle, specifically succinate metabolism under aerobic conditions. RpoS represses transcription of the *dctA* gene, encoding the C4-dicarboxylate transporter, which takes up succinate into the cell under aerobic conditions, and yet, expression of *dctA* increases in stationary phase (Davies et al., 1999). Therefore, RpoS deficiency results in de-repression of the *dctA* gene, and in turn, increased levels of DctA facilitate succinate transport, thus decreasing doubling time.

Based on preliminary findings, we implicated the PhoQP TCS in succinate metabolism by observing a decrease in doubling time, compared to the wild type. We investigated the contribution of the PhoQP TCS, finding support in literature for cross-regulation and dicarboxylic acid transport. First, the PhoQP TCS and RpoS are interconnected by a complex regulatory system of protein stabilizers and anti-adaptors. The RpoS-specific anti-adaptor protein RssB facilitates turnover of RpoS by ClpXP-mediated proteolysis (Hengge, 2009). PhoP activates transcription of two independent genes, encoding stabilizer proteins IraM

Figure 6.2

Effect of regulator mutations on the growth of *Salmonella* strains on succinate. Strains TL 1 (wild-type *Salmonella* LT2), TL 3331 (*rpoS::Ap*^{R}), TL 4299 (*phoP::Cm*^{R}) and TL 5638 (Δ*efp::Cm*^{R}) were grown over time in minimal medium M63 containing 20 mM succinate at 37°C. Shown is cell density (OD_{600}) plotted on a logarithmic scale against time in hours for one independent experiment. Below are the approximate doubling times in hours for each strain.

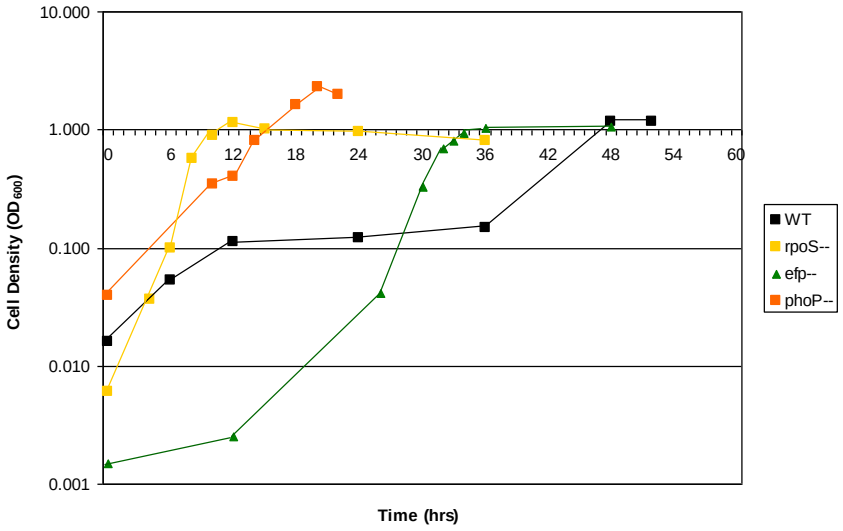

	WT	***rpoS*⁻⁻**	***phoP*⁻⁻**	***efp*⁻⁻**
Doubling Time (hrs)	7.3	1.1	1.6	1.6

Figure 6.2

Figure 6.3

Effect of Pro and related mutations on the growth of *Salmonella* strains on succinate. Strains TL 1 (wild-type *Salmonella* LT2), TL 1 supplemented with 1 mM proline, MS 1202 (*putA::MudJ*) and TL 126 (*F'128 proBA-74*) were grown as described in Fig. 6.2. Shown is cell density (OD_{600}) plotted on a logarithmic scale against time in hours for one independent experiment. Below are the approximate doubling times in hours for each strain.

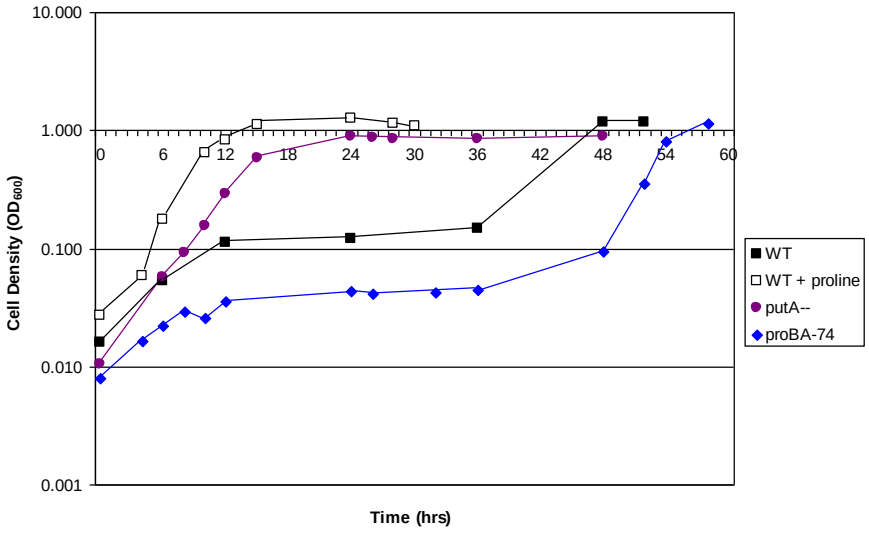

	WT	WT + Pro	*putA*$^{--}$	*proBA-74*
Doubling Time (hrs)	7.3	1.1	2.6	2.0

Figure 6.3

Figure 6.4

Effect of Mg^{2+} transport mutations on the growth of *Salmonella* strains on succinate. Strains TL 1 (wild-type *Salmonella* LT2), TL 4295 (*mgtA::MudJ*), TL 4523 [*mgtL* (C98T) *mgtA*$^+$], TL 4646 (*mgtB::MudJ*), and TL 3360 (*chr-2 mgtB*$^+$) were grown as described in Fig. 6.2. Shown is cell density (OD_{600}) plotted on a logarithmic scale against time in hours for one independent experiment. Below are the approximate doubling times in hours for each strain.

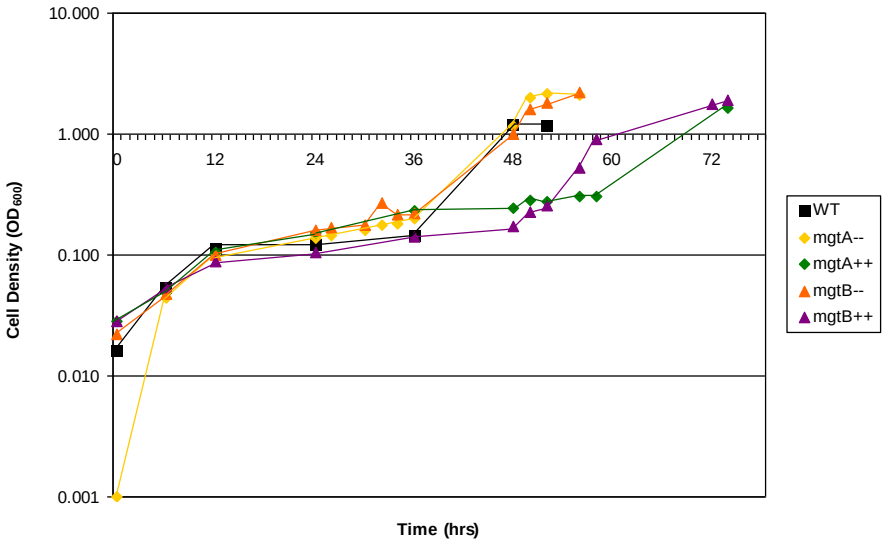

	WT	*mgtA*$^{--}$	*mgtA*$^{++}$	*mgtB*$^{--}$	*mgtB*$^{++}$
Doubling Time (mins)	7.3	4.4	7.1	5.1	4.3

Figure 6.4

and IraP, which results in IraM- and IraP-mediated inhibition of RssB and thus stabilizes the RpoS protein (Eguchi et al., 2011; Tu et al., 2006). In low Mg^{2+}, IraP is produced in a PhoP-dependent manner in both *Salmonella* and *E. coli*, and during phosphate starvation, IraP is produced in a PhoP-independent manner in *E. coli*, both growth conditions of which increase RpoS levels (Tu et al., 2006). Thus, deficiency in PhoP may result in decreased RpoS levels, indirectly affecting succinate metabolism via RpoS-mediated *dctA* regulation.

Second, based on microarray analysis for potential target genes, PhoP may repress transcription of the *dcuD* gene, encoding a putative C4-dicarboxylate transporter in *E. coli*; however, DcuD may not be significantly expressed, or it functions under conditions other than succinate metabolism (Janausch and Unden). Based on protein-protein BLAST results, *Salmonella* encodes a similar transporter, DcuC, which mediates C4-dicarboxylate uptake under anaerobic conditions (Zientz et al., 1996). Expression of the *dcuC* gene is repressed under aerobic conditions (Zientz et al., 1999). The *dcuC* promoter may harbor a PhoP Box overlapping the -35 element (not shown). Therefore, if PhoP represses transcription of *dcuC* under aerobic conditions, then deficiency of PhoP may increase *dcuC* expression, facilitating DcuC-mediated succinate uptake and indirectly expedite succinate metabolism.

We obtained preliminary results for a network implicating Pro and Mg^{2+} homeostasis in succinate metabolism. We found that addition of exogenous Pro decreased both the doubling time and lag phase growth of a *Salmonella* strain in minimal medium M63 supplemented with succinate as the sole carbon source. We investigated the effect of exogenous Pro on succinate utilization by examining two aspects of Pro metabolism—degradation and biosynthesis of L-proline—and found that a *putA*$^{--}$ mutant, deficient in conversion of L-proline to L-glutamate, exhibited decreased doubling time, compared to the wild type. Both the SdhDCBA and PutA enzymes utilize cytochrome *bo* complex during aerobic respiration to function according to their respective metabolic reactions; therefore, we hypothesized that intracellular Pro degradation may regulate succinate metabolism via competition for access to the cytochrome *bo* complex. One reason is that an increase in intracellular Pro by plasmid-borne expression of the *proBA-74* mutation in the wild-type background resulted in a pattern of growth different from addition of exogenous Pro and the *putA*$^{--}$ mutant. Biosynthesis of L-proline from L-glutamate via the ProBAC enzymes requires ATP

hydrolysis (Csonka and Leisinger, 2007), and therefore, overproduction of Pro by the *proBA-74* mutation is hypothesized to result in a high ATP demand by the Pro biosynthesis enzymes. Two areas to further investigate are 1) entry into the TCA cycle via α-ketoglutarate, which can be formed by conversion from L-glutamate by GdhA and combined effort by GlnA and the GltBD complex (Yan, 2007), and 2) the contribution of Pro transport.

Lastly, we found that deficiency in the MgtA and MgtB Mg^{2+} transport genes (*mgtA*$^{--}$ and *mgtB*$^{--}$) had little effect on the growth on succinate, compared to the wild type. However, we hypothesized two patterns: 1) one Mg^{2+} transporter could complement deficiency of the other, or CorA is sufficient to complement either deficiency, and 2) over-expression of either Mg^{2+} transporter negatively influenced lag phase growth, resulting in a dramatic increase, compared to the wild type. Over-expression of the P-type ATPase Mg^{2+} transporters is hypothesized to burden the cell by a high ATP demand similar to overproduction of intracellular Pro by the *proBA-74* mutation. Initially, it appears that Mg^{2+} may not have a role in succinate metabolism unlike Pro in regards to doubling time. Therefore, further investigation is needed to distinguish whether the effect of MgtA and MgtB over-expression is due to increased intracellular Mg^{2+} or decreased intracellular ATP. One approach is to measure cell density over time in cultures grown in minimal medium M63 supplemented with 20 mM succinate containing high or low Mg^{2+}. In this case, we may conclude or exclude regulation of succinate metabolism by intracellular Mg^{2+}.

Figure 6.5

Schematic of the TCA cycle with emphasis on factors involved in succinate metabolism. Stationary phase sigma factor, RpoS, represses transcription of the *dctA* gene, PutA represses transcription of the *putP* gene, and PhoP may repress transcription of the *dcuC* gene. Both *dctA* and *dcuC* encode C4-dicarboxylic acid transporters, and *putP* encodes the Na+-proline symporter. EF-P may assist translation of AceK, AstD, GltB, and PutA based on motif sequences containing contiguous Pro residues in each protein.

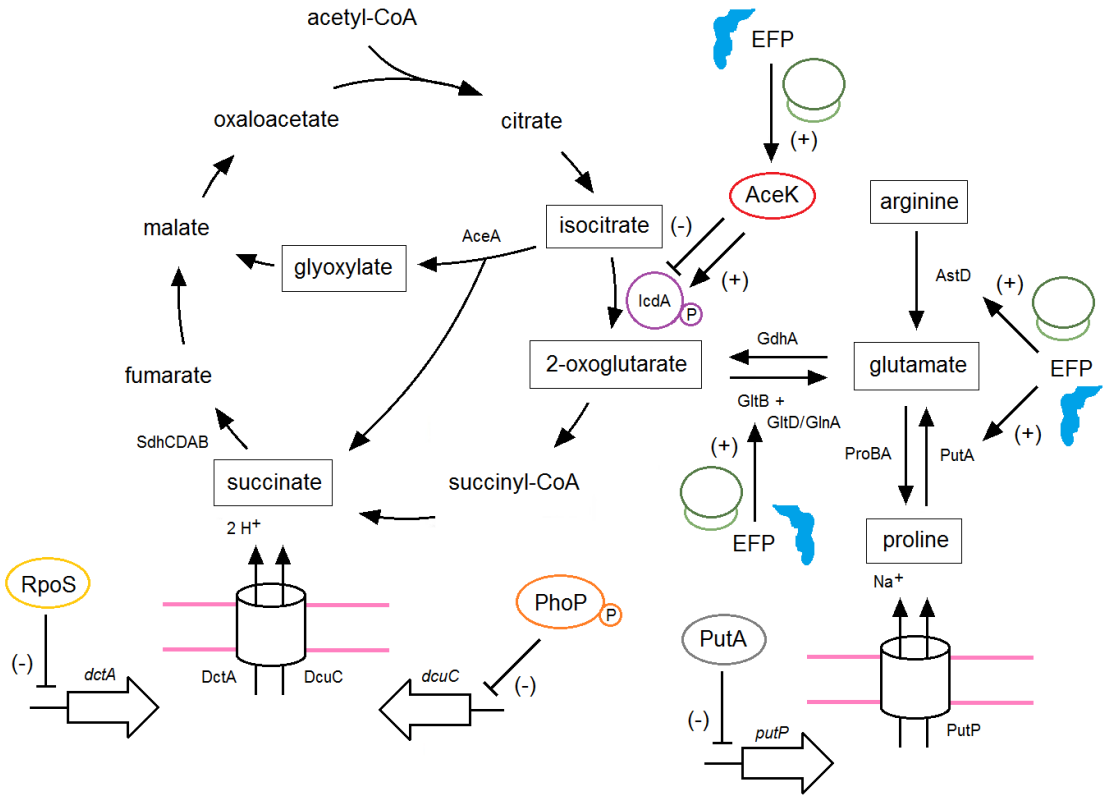
acetyl-CoA
citrate
isocitrate
AceK
EFP
(+)
(-)
arginine
AstD
malate
oxaloacetate
glyoxylate
AceA
IcdA
P
2-oxoglutarate
GdhA
GltB +
GltD/GlnA
glutamate
fumarate
SdhCDAB
succinate
succinyl-CoA
ProBA
PutA
proline
2 H+
Na+
RpoS
dctA
DctA
DcuC
dcuC
PhoP
putA
putP
PutP

Figure 6.5

CHAPTER 7. DISCUSSION

7.1 Evaluation of previous models for *mgtA* regulation

Transport and homeostasis of the divalent cation Mg^{2+} are important areas of research in bacteria such as *Salmonella*, a food-borne pathogen, given the role of Mg^{2+} in facilitating enzymatic reactions, stabilization of proteins, lipids and nucleic acids and potential virulence (Silver, 1996). In *Salmonella*, three Mg^{2+} transporters mediate homeostasis—CorA is a constitutive, bidirectional transporter, and MgtA and MgtB are P-type ATPase transporters that mediate influx of Mg^{2+} (Papp-Wallace and Maguire, 2008). In response to environmental Mg^{2+}, the PhoQP TCS regulates transcription of genes involved in acid stress, AP resistance and cell membrane permeability (Bader et al., 2005; Prost et al., 2007; Soncini et al., 1996), including activation of the *mgtA* gene and *mgtCBR* operon, which encodes a virulence factor MgtC and a regulatory protein MgtR (Heithoff et al., 1999; Smith et al., 1998; Tao et al., 1998; Véscovi et al., 1996).

The *mgtA* gene harbors a 264-nucleotide 5' LR that contains an 18-codon ORF, termed *mgtL*, which encodes a proline-rich, 17-amino acid peptide. Over the past decade, an increasing number of regulatory factors that contribute to *mgtA* expression has been discovered, with several models proposed to explain the multiple levels of regulation, namely transcription initiation, elongation and termination, post-transcription and post-translation regulation, and transporter activity (Choi et al., 2012; Cromie et al., 2006; Hollands et al., 2012; Hollands et al., 2014; Park et al., 2010; Park and Groisman, 2014; Spinelli et al., 2008; Subramani et al., 2016; Zhao et al., 2011).

Although each model attempted to explain a unique aspect of *mgtA* regulation, we highlighted five models in particular that share common features and yet do not account for artifacts and newly discovered mutations. Specifically, we emphasize the Riboswitch Model (Cromie et al., 2006), Proline Model (Park et al., 2010) and Shine-Dalgarno Model (Zhao et al., 2011), providing review, comments, comparison and contrast. In addition, we corroborated the Rho Model (Hollands et al., 2012) and Pause Model (Hollands et

al. 2014) with experimental findings. Note that each model is provided with a unique name that is not recognized by its original source.

7.1.1 Riboswitch Model

In the Riboswitch Model, the 5' LR of the *mgtA* mRNA has an unspecified Mg^{2+} binding site, and binding of this divalent cation influences the folding of the mRNA, which in turn regulates whether transcription is terminated before *mgtA* or RNA polymerase enters into the structural gene. In this model, low Mg^{2+} facilitates the formation of stem loop C, leading to transcription into the *mgtA* structural gene, while high Mg^{2+} facilitates the formation of stem loops A and B, leading to transcription termination within the *mgtA* 5' LR (Fig. 7.1) (Cromie et al., 2006).

The mFold web server (Zuker, 2003) and *in vitro* analysis of the *mgtA* 5' LR mRNA by RNase T probing at different Mg^{2+} concentrations provided evidence for a predicted secondary structure of the *mgtA* 5' LR mRNA based on hybridization energies and supporting data for alternative stem loop structures, respectively (Cromie et al., 2006). In addition, site-directed mutations that altered the *mgtA* 5' LR mRNA detailed the conformations of stem loops A, B and C (Cromie et al., 2006).

In our Proposed Model, Mg^{2+} does not regulate RNA folding by directly binding the *mgtA* 5' LR mRNA and alternate stem loop structures. However, we provided evidence corroborating the role of Mg^{2+}-independent RNA folding by constructing a site-directed mutation (CC118-119AA) that disrupts the right arm of stem loop C and favors formation of stem loop B. The CC118-119AA mutation resulted in constitutively low *mgtA-lacZ* expression based on the Lac^{--} phenotype on MacConkey agar (Table 4.1). Here, abrogation of stem loop C (anti-termination) and preference of stem loop B (termination) by the CC118-119AA mutation supports the role of RNA folding in the regulation of *mgtA* expression.

A spontaneous mutation (C98T) located within a single-stranded region of the *mgtA* 5' LR was previously characterized as increasing the tolerance of *Salmonella* to heat-killing by constitutively expressing the *mgtA* gene (O'Connor et al., 2009). Despite its ability to adopt the stem loop B conformation (termination), the C98T mutant exhibited the constitutively "ON" phenotype (O'Connor et

Figure 7.1

Comparison and contrast of the previous models for *mgtA* regulation. Note: the Proline and Pause Models have the same role for Mg^{2+} as in the Riboswitch Model; Hairpin P formation is Mg^{2+}-independent and equated with the Long pause in the Pause Model.

Riboswitch Model (Cromie et al., 2006)

[Mg^{2+}]		**RNA folding**		***mgtA***
High	→	stem loop B (terminator)	→	"OFF"
Low	→	stem loop C (anti-terminator)	→	"ON"

Proline Model (Park et al., 2010)

[Proline]		***mgtL***		**RNA folding**		***mgtA***
High	→	Complete translation	→	stem loop B (terminator)	→	"OFF"
Low	→	Ribosome stalling	→	stem loop C (anti-terminator)	→	"ON"

Shine-Dalgarno Model (Zhao et al., 2011)

[Mg^{2+}]		**RNA folding**		***mgtL***		**RNA folding**		***mgtA***
High	→	Hairpin A1 (SD available)	→	Complete translation	→	stem loop B (terminator)	→	"OFF"
Low	→	stem loop D (SD blocked)	→	No translation	→	stem loop C (anti-terminator)	→	"ON"

Rho Model (Hollands et al., 2012)

[Mg^{2+}]		**RNA folding**		**Rho**		**Transcription**		***mgtA***
High	→	stem loop B (terminator)	→	*rut* available	→	Termination	→	"OFF"
Low	→	stem loop C (anti-terminator)	→	*rut* blocked	→	Elongation	→	"ON"

Pause Model (Hollands et al., 2014)

RNA-P		**[Mg^{2+}]**		**RNA folding**		**Rho**		**Transcription**		***mgtA***
Long pause	→	High	→	stem loop B (terminator)	→	*rut* available	→	Termination	→	"OFF"
		Low	→	stem loop C (anti-terminator)	→	*rut* blocked	→	Elongation	→	"ON"

Figure 7.1

al., 2009), suggesting a different mode instead of riboswitch-mediated regulation, since the C98U mRNA substitution is not predicted to significantly alter the secondary structure of the *mgtA* 5' LR mRNA.

7.1.2 Proline Model

After the Riboswitch Model was proposed, two groups independently showed that the *mgtA* 5' LR contains the sequence for a short, 18-codon ORF, termed *mgtL*, that encodes a highly conserved leader peptide (Park et al., 2010; Zhao et al., 2011). A second model was proposed in which the *mgtA* 5' LR employs translation of *mgtL* to regulate transcription of *mgtA*. In the Proline Model, abundant intracellular Pro facilitates complete translation of *mgtL*, which would favor stem loop B formation and transcription termination upstream of the *mgtA* structural gene. On the other hand, limiting Pro would decrease intracellular levels of Pro-charged $tRNA^{Pro}$, which would lead to ribosome stalling and formation of stem loop C, resulting in transcription into the *mgtA* structural gene (Fig. 7.1) (Park et al., 2010). In this case, translation of *mgtL* may regulate folding of the *mgtA* 5' LR mRNA by a ribosome-mediated mechanism and in turn transcription into the *mgtA* structural gene. In the Proline Model, the role of Mg^{2+} is the same as in the Riboswitch Model—a signal for the Mg^{2+}-sensing riboswitch. The role of Pro is to directly regulate translation efficiency by charging $tRNA^{Pro}$ and indirectly regulate folding of the *mgtA* 5' LR mRNA via the ribosome. However, in this model, it is not clear what physiological connection there is between the availability of Mg^{2+} and Pro. Furthermore, the model does not explain how the intracellular Mg^{2+} and Pro concentrations may simultaneously regulate *mgtA* expression.

We provided evidence corroborating the Proline Model in part by introducing mutations of the Pro biosynthesis (Δ*proBA*) and transport genes (Δ*putPA* and *proP1654*) into a strain harboring the chromosomal *mgtA-lacZ* transcriptional fusion. ProA, ProB and ProC catalyze biosynthesis of L-proline from L-glutamate (Csonka and Leisinger, 2007), and the Na^+-Pro and H^+-Pro symporters, PutP and ProP, transport extra-cytoplasmic Pro into the cell (Jung et al., 2012; MacMillan et al., 1999). Single (Δ*proBA* *putP*$^+$ *proP*$^+$), double (Δ*proBA* *putP*$^+$ *proP*$^{--}$) and triple (Δ*proBA* Δ*putPA* *proP1654*) mutants were grown in minimal medium M63 containing high (2 mM) or low (0.4 mM) Pro to complement Pro auxotrophy, and β-galactosidase activity was measured. Similar to the wild type, both the single and combination of double

mutants exhibited no significant effect on *mgtA-lacZ* expression between the Pro concentrations (Fig. 4.10). However, the triple Pro biosynthesis and transport mutant showed a significant induction, resulting in constitutively high *mgtA-lacZ* expression (Fig. 4.10). Hence, starvation of intracellular Pro must occur before Pro has a regulatory role in the translation of *mgtL* and transcription of *mgtA*.

Although we show that Pro availability may regulate transcription of *mgtA*, intracellular Pro appears to have a second-order effect compared to Mg^{2+}, which does not require severe starvation conditions to induce the *mgtA* gene. Pro starvation induces the *mgtA-lacZ* transcriptional fusion to levels that µM Mg^{2+} does. Based on previous findings, the level of intracellular Pro may not be as variable for macrophage-containing *Salmonella* (Eriksson et al., 2003), and therefore, the regulatory role of Pro may be minor. In addition, as Park et al. (2010) observed, we noted that replacement of the combinations and numbers of Pro codons in *mgtL* resulted in a substantial decrease in the degree of differential Mg^{2+}-sensing control (fold change of high/low Mg^{2+}) of *mgtA* expression, compared to the wild type. Substitutions of the Pro codons should not significantly alter the secondary structure of the *mgtA* 5' LR mRNA (Park et al., 2010), so the loss of Mg^{2+}-induction due to replacement of *mgtL* Pro codons suggests a greater role of translation in differential Mg^{2+}-sensing control.

7.1.3 Shine-Dalgarno Model

Independent discovery of *mgtL* within the 5' LR of *mgtA* led to a disparate conclusion about the roles of Pro and RNA folding than in the Proline Model. In the Shine-Dalgarno Model (Zhao et al., 2011), the role of Mg^{2+} is similar as in the Riboswitch Model; however, Pro was shown to have no regulatory role contrary to the Proline Model (as described above). In addition, the order of events in regulating translation of *mgtL* and RNA folding is different from the Proline Model. In the Shine-Dalgarno Model, the role of Mg^{2+} is to directly facilitate folding of the 5' LR mRNA, which in turn regulates ribosome binding to the SD site and indirectly regulates translation of *mgtL*. In this model, two sets of stem loop structures regulate translation of *mgtL* and transcription into the *mgtA* structural gene. stem loop A and Hairpin A1 favor translation of *mgtL* by exposing the SD site, and stem loop B favors termination of transcription; other the other hand, stem loop D sequesters the SD site, precluding translation of *mgtL*, and stem loop C facilitates transcription

into the *mgtA* structural gene (Fig. 7.1) (Zhao et al., 2011). Note that RNA folding first regulates translation of *mgtL* in the Shine-Dalgarno Model, and then the ribosome further regulates RNA folding.

In reviewing the predicted secondary structure and mutations of the *mgtA* 5' LR mRNA in this model, we noted three discrepancies in RNA folding and translation of *mgtL*. First, stem loop A contains a small hairpin structure, termed Hairpin A1. The left arm of Hairpin A1 is reported to function as an anti-SD sequence, blocking translation of *mgtL* by complementary base-pairing to the SD site and forming a stem loop D structure (Zhao et al., 2011). stem loops A and D are mutually-exclusive structures. On the other hand, the right arm of Hairpin A1 is reported to function as an anti-anti-SD sequence, exposing the SD site when it complementary base-pairs to the left arm of Hairpin A1. In this model, stem loop A and Hairpin A1 expose the SD site, facilitating translation of *mgtL*, whereas Stem loop D sequesters the SD site, blocking translation of *mgtL* (Zhao et al., 2011). Mutation of the left arm of Hairpin A1 (sub 91-95) by replacing nucleotides with ones anti-complementary to the right arm of Hairpin A1 repressed *mgtA-lacZ* expression by disrupting the anti-SD sequence and stem loop D formation, which favors translation of *mgtL* (Cromie et al., 2006; Zhao et al., 2011). Double mutation of the left and right arms of Hairpin A1 (rev 91-95, 102-106), which restores ability to form Hairpin A1, resulted in differential Mg^{2+}-sensing control of *mgtA-lacZ* expression similar to the wild type (Cromie et al., 2006; Zhao et al., 2011). Based on the Shine-Dalgarno Model, stem loop D must form to sequester the SD site and block translation of *mgtL* and in turn induce *mgtA* expression. However, the double mutant cannot form stem loop D, because the Hairpin A1 (sub 91-95) mutation should expose the SD site and facilitate translation of *mgtL*, the opposite mechanism of proposed regulation (Zhao et al., 2011). Therefore, the results by Zhao et al. (2011) cannot support the claim that RNA folding regulates availability of the SD site.

Second, levels of MgtL peptide were undetected previously, suggesting that the peptide is quickly degraded following translation (Park et al., 2010). Plasmid-borne expression of FLAG-tagged MgtL was monitored at high and low Mg^{2+} in an *E. coli* strain under UV irradiation to increase the yield of MgtL-FLAG protein (Zhao et al., 2011). In high Mg^{2+}, level of MgtL-FLAG protein increased as the time of exposure to UV irradiation increased, while no product was detected in low Mg^{2+} (Zhao et al., 2011). However, we noted that no control was performed to verify whether low Mg^{2+} is sufficient to facilitate

plasmid-borne expression of MgtL-FLAG protein. We suggest that the observation of no detected product was a false negative result for two reasons: 1) the C98T nonsense mutation in *mgtL*, which is not predicted to affect folding of the *mgtA* 5' LR mRNA, results in high *mgtA-lacZ* expression even at high Mg^{2+} (see Chapter 3), and 2) expression of the *mgtL-lacZ* translational fusion at its chromosomal locus occurs at low Mg^{2+} (see Chapter 3). These results confirm that MgtL is produced at both high and low Mg^{2+}, in disagreement with the Shine-Dalgarno Model.

Lastly, we noted that replacement of the combinations and numbers of Pro codons in *mgtL* resulted in decreases in the degree of differential Mg^{2+}-sensing control (fold change of high/low Mg^{2+}) of *mgtA* expression (Zhao et al., 2011). As discussed above, we found that Pro regulates transcription of *mgtA* via translation of *mgtL*, albeit with a second-order effect (see Chapter 4), in disagreement with the Shine-Dalgarno Model.

7.1.4 Rho Model

In the Rho Model, the regulatory role of Mg^{2+} is the same as in the Riboswitch Model—a signal for the Mg^{2+}-sensing riboswitch. Mutational analysis of the *mgtA* 5' LR and use of the Rho-specific inhibitor bicyclomycin demonstrated that the ATP-dependent helicase Rho binds to two exposed *R*ho-*ut*ilization (*rut*) sites (R1 and R2) when the stem loop B conformation is favored (Hollands et al., 2012). On the other hand, stem loop C and another stem loop structure sequester the R1 and R2 *rut* sites, respectively, and therefore block Rho binding, facilitating transcription into the *mgtA* structural gene (Hollands et al., 2012). The role of Rho helicase is to recognize the *rut* site and directly facilitate transcription termination in a manner interdependent on translation of *mgtL* and RNA folding.

Based on mutational analysis of the *mgtA* 5' LR mRNA, the R1 *rut* site was disrupted by single base-pair substitutions that replaced cytosine nucleotides, which resulted in constitutively high *mgtA-lacZ* expression, compared to the wild type (Hollands et al., 2012). However, the proposed R2 *rut* site was mutated and yet retained ability to differentially regulate *mgtA-lacZ* expression (Hollands et al., 2012). Based on their results, we concluded that the R2 *rut* site may not facilitate Rho-dependent transcription termination but only the R1 *rut* site (referred to, hereafter, as "the *rut* site").

We provided confirmatory evidence for the Rho Model by introducing a *rho* mutation (Y80C-*rho*) into a strain harboring an *mgtA-lacZ* transcriptional fusion at its chromosomal locus. Resulting in a slow-growth phenotype, the Y80C-*rho* mutant is defective in ATP binding with decreased ability to unwind mRNA and facilitate transcription termination (Chalissery et al., 2007). Compared to the wild type, the Y80C-*rho* mutant exhibited constitutively high *mgtA-lacZ* expression (Fig. 4.9), supporting the role of Rho in transcription termination of *mgtA*, thus corroborating the Rho Model in part.

7.1.5 Pause Model

In the Pause Model, the regulatory role of Mg^{2+} is the same as in the Riboswitch Model—a signal for the Mg^{2+}-sensing riboswitch (Hollands et al., 2014). Mutational analysis of the *mgtA* 5' LR demonstrated that RNA polymerase pauses at nucleotide +218 by aid of Hairpin P, a stem loop structure neighboring a region of nucleotides, termed the Pause Region (Hollands et al., 2014). The role of RNA polymerase pausing is to provide adequate time for Rho helicase to recognize the *rut* site, unwind and release the *mgtA* 5' LR from the RNA-DNA transcription complex, resulting in transcription termination.

We provided evidence corroborating the Pause Model in part by constructing two strains harboring mutations in the right arm of Hairpin P [GGCA(203-206)TTAT] and the Pause Region [GCCTG(219-223)CGGAC] immediately downstream of nucleotide +218 of the *mgtA* 5' LR (Fig. 4.2). Compared to the wild type, both the Hairpin P and Pause Region mutations resulted in the constitutively "ON" phenotype (Fig. 4.6), supporting the roles of Hairpin P and the Pause Region in transcription attenuation of *mgtA*.

7.2 Updated model of transcription-translation coupling of *mgtA*

We showed that Mg^{2+} directly regulates translation of *mgtL*, thereby facilitating folding of the *mgtA* 5' LR mRNA and whether transcription will proceed into the *mgtA* structural gene (see Chapter 3). Including multiple regulatory factors, we propose an overall, comprehensive model that explains the mechanism of transcription-translation coupling and speculate the order of events involved. We provided evidence to substantiate the interplay of five areas that governs *mgtA* expression: 1) PhoP-dependent transcription activation, 2) RNA polymerase pausing, 3) translation of *mgtL*, 4) RNA folding and 5) Rho-dependent

transcription termination. Note that both EF-P and TrmD were shown to affect translation of *mgtL* but independently of the differential Mg^{2+}-sensing of translation of *mgtL* (see Chapter 3).

7.2.1 PhoP-dependent transcription activation of *mgtA*

The first step in *mgtA* expression is activation of transcription of the 264-nucleotide *mgtA* 5' LR by the PhoQP TCS (Véscovi et al., 1996). Absence of PhoP by a *phoP::Cm*^{R} mutation resulted in constitutively low *mgtA-lacZ* expression (Fig. 5.3), indicating its essential role in activation of the *mgtLA* promoter. In addition, a *phoQ::*Tn*10 phoP*$^+$ mutant exhibited the same phenotype (not shown). These results confirm PhoP-dependent transcription activation in the regulation of *mgtA* expression. Note that the contribution of Rob in transcription activation has a second-order effect (see Chapter 5).

7.2.2 RNA polymerase pausing in the *mgtA* 5' LR

During transcription of the *mgtA* 5' LR, the RNA-DNA transcription complex reaches a region downstream of *mgtL* and the *rut* site that facilitates RNA polymerase pausing for an extended time at nucleotide +218 by aid of Hairpin P and a Pause Region (Hollands et al., 2014). We corroborated the roles of Hairpin P and the Pause Region as described above (Fig. 4.6). In addition, introduction of the *phoP::Cm*^{R} mutation into the Hairpin P mutant background de-activated expression of *mgtA* based on the Lac phenotype on MacConkey agar (not shown). This result supports that transcription activation of the *mgtA* 5' LR by PhoP occurs before RNA polymerase pausing upstream of the *mgtA* structural gene.

7.2.3 Translation of *mgtL*

In the third step of *mgtA* expression, transcription of the left arm of stem loop A exposes the SD site, facilitating ribosome binding and initation of translation of *mgtL*. Mutations in *mgtL* (A86C and C98T) result in constitutively high *mgtA-lacZ* expression (Figs. 3.2 and 3.5A). These results indicate that activation of the *mgtLA* promoter must occur not only at low Mg^{2+} but also high Mg^{2+}. We showed that high Mg^{2+} facilitates prolyl-bond formation during translation of *mgtL*, while low Mg^{2+} results in ribosome stalling, leading to termination or transcription of *mgtA* expression, respectively (see Chapter 3).

7.2.4 Folding of the *mgtA* 5' LR mRNA

In the fourth step of *mgtA* expression, stem loops A and B are mutually-exclusive to stem loop C based on hybridization energies (Zuker, 2003). Once the left arm of stem loop A is transcribed and exposes the SD site, translation of *mgtL* occurs and in turn ribosome-mediated folding of the *mgtA* 5' LR mRNA. Mutation of the SD site (GG62-63AA), which eliminates ribosome binding, results in constitutively low *mgtA-lacZ* expression (Fig. 4.3). This result suggests that ribosome binding to the SD site normally favors stem loop C formation, possibly by occluding the left arm of stem loop A. In the absence of ribosome binding, constitutive formation of stem loop B must occur in the GG62-63AA mutant, exposing the *rut* site, which leads to Rho-dependent transcription termination. In addition, mutation of the left arm of stem loop A (CC60-61AA), which disrupts formation of stem loop A like the GG62-63AA mutation but retains ribosome binding and translation of *mgtL*, does not disrupt differential regulation of *mgtA* expression (Fig. 4.4A). This result supports that ribosome occlusion and translation of *mgtL* are essential in activating and repressing *mgtA* expression, respectively.

Furthermore, mutation of the start codon (A71C) results in constitutively high *mgtA-lacZ* expression (Fig. 4.3). Although opposite of the *5' LR* (GG62-63AA) mutation, this result for the *mgtL* (A71C) mutation supports how ribosome occlusion in the absence of translation of *mgtL* facilitates transcription into the *mgtA* structural gene by favoring stem loop C formation. Based on the analysis of compensatory mutations in *mgtL* (A86C) and the *mgtA* 5' LR (G120C) (Fig. 4.7), translation of *mgtL* and RNA folding are interdependent, in which translation of *mgtL* dictates folding of the *mgtA* 5' LR mRNA, and the final structure—either stem loop B or C—determines expression of the *mgtA* structural gene. Overall, ribosome binding initiates folding of the *mgtA* 5' LR mRNA, in which complete translation of *mgtL* favors stem loop B formation in high Mg^{2+} or ribosome stalling favors stem loop C formation in low Mg^{2+}, leading to termination or transcription into the *mgtA* structural gene, respectively.

Lastly, ribosomal release is an important determinant in RNA folding based on the constitutively "ON" phenotypes of the *mgtL* (C98T) and *mgtL* (ΔT111) mutants. Premature translation termination with the *mgtL* (C98T) mutation (see Chapter 3) and extended translation by frameshift with the *mgtL* (ΔT111) mutation (Fig. 4.4C) indicated that ribosomal release upstream and downstream of the native UAA stop

codon, respectively, antagonizes Rho-dependent transcription termination by favoring stem loop C formation. As in the wild type, if ribosomal release occurs at the native UAA stop codon, then stem loop B is favored, facilitating Rho binding at the *rut* site and in turn termination of transcription.

7.2.5 Rho-dependent transcription termination of *mgtA*

In the last step of *mgtA* expression, the alternative stem loop B or C structure may expose the *rut* site and facilitate Rho-dependent transcription termination or sequester the *rut* site and facilitate transcription into the *mgtA* structural gene, respectively (Hollands et al., 2014). Following binding to the *rut* site, Rho traces along the *mgtA* 5' LR mRNA and unwinds the RNA-DNA transcription complex, leading to termination of *mgtA* expression. We corroborated the role of Rho helicase in transcription attenuation by observing constitutively high *mgtA-lacZ* expression in a Y80C-*rho* mutant (Fig. 4.9). In addition, we introduced the Y80C-*rho* mutation into the *5' LR* (GG62-63AA) and Hairpin P [GGCA(203-206)TTAT] mutant backgrounds and observed the Lac^+ phenotype on MacConkey agar (Table 4.1). As the *mgtA* 5' LR is transcribed, the SD site is exposed before the *rut* site, facilitating ribosome binding and translation of *mgtL* before Rho binding occurs. Despite constitutive exposure of the *rut* site, inhibition of Rho termination de-represses *mgtA* expression by allowing the paused RNA polymerase in the double Y80C-*rho 5' LR* (GG62-63AA) mutant to continue transcribing into the *mgtA* structural gene. Lastly, we introduced the Y80C-*rho* mutation into the Hairpin P [GGCA(203-206)TTAT] background and observed a synergistic increase in the Lac^+ phenotype on MacConkey agar (Table 4.1). Because inhibition of Rho termination further induced *mgtA* expression, this result suggests that residual RNA polymerase pausing may still occur despite disruption of the Hairpin P structure. Overall, these results support that Rho helicase is the last determining factor in the differential Mg^{2+}-sensing control of *mgtA* expression, since the effect of Rho inhibition was dominant over all previous steps of regulation, except PhoP-dependent transcription activation, of course.

7.3 Evaluation of regulatory factors and growth conditions

Salmonella enterica experiences diverse environmental conditions that affect its growth and replication (Eisenreich et al., 2010). We discuss 1) the contribution of the PhoQP TCS to the regulation of *mgtA*

expression, 2) growth conditions that may activate Rob-dependent transcription of *mgtA* and 3) speculate other regulatory factors and growth conditions that may regulate *mgtA* expression.

7.3.1 PhoQP TCS and Mg^{2+}-starvation

As discussed above, the PhoQP TCS responds to several regulatory signals including changes in pH, Mg^{2+} and APs (Bader et al., 2005; Prost et al., 2007; Soncini et al., 1996). Specifically, low Mg^{2+} (μM levels) and high Mg^{2+} (mM levels) has been proposed to activate and inactivate the PhoQP TCS, respectively (Véscovi et al., 1996). When *Salmonella* is present within extracellular fluids, the PhoQP TCS should be repressed by the range of 0.7-1.0 mM Mg^{2+} in the serum, and once inside a host cell, *Salmonella* is exposed to 0.5 mM Mg^{2+} in the cytosol (Reinhart, 1988). The extra-cytoplasmic concentration of Mg^{2+} for *Salmonella* that reside within membrane-bound vacuoles, termed phagosomes, of epithelial cells have been estimated to be <50 μM (Portillo et al., 1992). At this concentration of Mg^{2+}, the sensor kinase PhoQ is predicted to auto-phosphorylate and in turn activate its cognate DNA-binding transcriptional regulator PhoP, which activates the *mgtA* structural gene and *mgtCBR* operon (Castelli et al., 2000; Chamnongpol et al., 2003; Heithoff et al., 1999; Montagne et al., 2001; Tao et al., 1998; Véscovi et al., 1996).

Attenuation of *Salmonella* virulence occurs in the absence of the PhoQP TCS (Thompson et al., 2011). *Salmonella* mutants harboring deletions of the *mgtA*, *mgtB* or *mgtC* gene experience decreased survival during infection (Blanc-Potard and Groisman, 1997). Although the bidirectional transporter CorA is constitutively active, absence of either MgtA or MgtB results in growth defects in Mg^{2+}-limiting environments (not shown). We noted that the *mgtA-lacZ* transcriptional fusion was expressed at high levels in minimal medium M63 containing 1.6 mM Mg^{2+} in a large number of mutants that were obtained, including strains harboring the *mgtL* (A86C and C98T; Fig. 2A) and *rpmA* (G23A; Fig. 2B) mutations and others. These phenotypes are inconsistent with the suggestion that the PhoQP TCS is completely inactivated at high Mg^{2+} concentrations. Previously, our lab showed that transcription from the native *mgtLA* promoter was dependent on the PhoQP TCS even in the *mgtA* constitutive mutants (O'Connor et al., 2009). Thus, although expression of *mgtA* requires the transcriptional activator PhoP under the conditions tested, the phosphorylation state of this protein appears to be adequate even at the high (1.6 mM)

concentration of Mg^{2+} to drive transcription of the *mgtA* structural gene. If this is correct, then the role of Mg^{2+} in controlling the PhoQP regulon in pathogenesis may need reevaluation. Our results suggest that the main contributor for the differential Mg^{2+}-sensing control of *mgtA* expression is translation of *mgtL*, and regulation by the PhoQP TCS may be a second-order effect.

7.3.2 Rob and phosphate starvation

The MarA/SoxS-like transcriptional regulator Rob functions in resistance to antibiotics, superoxide and heavy metals (Duval and Lister, 2013). We showed that Rob activates *mgtA* expression with a second-order effect to the PhoQP TCS (Fig. 5.3). In minimal medium M63 containing high or low Mg^{2+}, a *rob::Kn*^{R} mutant exhibited decreased basal levels, and yet, Mg^{2+} retained ability to differentially regulate *mgtA-lacZ* expression similar to the wild type (Fig. 5.3). Despite the defined Mg^{2+} conditions that do not necessarily induce its activity, Rob was able to activate transcription of *mgtA* in a PhoP-independent manner.

Growth conditions that may not activate the PhoQP TCS may induce *mgtA* expression via Rob transcription activation. Not only do bile salts and fatty acids increase the activity of Rob as with the PhoQP TCS (Rosenberg et al., 2003), but also glucose and phosphate starvation enhance expression of *rob* (Kakeda et al.). Coincidentally, phosphate starvation activates transcription of the *phoQ* gene in a PhoB-dependent manner (Marzan et al., 2012). In addition, EF-P may assist translation of the *phoR* gene based on regulation of the signature PPP and PPG motifs both found in the protein (Doerfel et al., 2013). These preliminary findings suggest that phosphate starvation may induce transcription of the *mgtA* structural gene via Rob directly or the PhoBR TCS indirectly.

7.3.3 Alternative transcription by a 5’ LR mutation

We provided evidence that suggests alternative transcription activation exists amid the multi-tiered regulation of *mgtA* expression. We isolated and characterized spontaneous mutations in both *mgtL* and the *mgtA* 5’ LR that resulted in high *mgtA-lacZ* expression at high Mg^{2+}. Because *mgtA* expression is dependent on the PhoQP TCS, we investigated how spontaneous mutations may de-repress transcription of the *mgtA* gene at repressing Mg^{2+} concentrations by constructing site-directed mutations of the *mgtA* 5’ LR

and by isolating mutations in the *mgtL* (3Pro-) and *phoP::Cm*^{R} mutant backgrounds. Initial analysis of the *mgtA* 5' LR suggested that the nucleotide region downstream of *mgtL* and the *rut* site may be important in regulating *mgtA* expression in an Mg^{2+}-independent manner.

Isolation of the *5' LR* (G138A) mutation that resulted in constitutively high *mgtA-lacZ* expression in the absence of the PhoQP TCS and Rob suggests that another transcription factor could regulate *mgtA* expression (see Chapter 5). In this case, the *5' LR* (G138A) mutation may function to either enhance a positive regulatory site or disrupt a negative regulatory site, both under growth conditions that may not have been tested. We observed that two 8-bp repeat sequences are located within the *mgtA* 5' LR. Using the Virtual Footprint and PRODORIC prediction web server (Grote et al., 2009), further analysis revealed that each repeat sequence resembles the protein-binding motif of the DNA-binding transcriptional regulator RhlR of *Pseudomonas aeruginosa*. RhlR functions in rhamnolipid production and the quorum-sensing response (QSR) (Medina et al., 2003a; Medina et al., 2003b; Ochsner et al., 1994). Based on BLAST analysis of the amino acid sequence, RhlR is homologous to the DNA-binding transcriptional regulator SdiA of *Salmonella enterica*, which activates transcription of cell division genes and an intermediary in the CRP-mediated cAMP response (Ahmer et al., 1998). In addition, we noted that the PhoBR TCS, which regulates phosphate homeostasis, contributes to transcription activation of the *rhlR* gene in *Pseudomonas aeurginosa* (Jensen et al., 2006) and might activate transcription of the *phoQ* gene in *E. coli*, a close relative of *Salmonella* (Marzan et al., 2012).

Two interesting, physiological connections may exist between magnesium homeostasis via the PhoQP TCS and phosphate homeostasis via the PhoBR TCS or the RhlR-like quorum-sensing regulator SdiA. When we investigated the contributions of PhoB, PhoR and SdiA in the regulation of *mgtA* expression, however, we found that none had a role in transcription activation or repression of *mgtA* under the conditions tested. In addition, based on genome-wide analysis by ChIP-sequencing, the PhoBR regulon did not include the Mg^{2+} transport genes (Yang et al., 2012). Nonetheless, the constitutively "ON" phenotype of the *5' LR* (G138A) mutant indicates that an unknown regulatory factor does indeed regulate *mgtA* expression by a PhoP- and Rob-independent mechanism, and it is plausible that phosphate starvation may induce transcription of the *mgtA* gene via an unknown regulatory factor.

Not only does low extra-cytoplasmic Mg^{2+} induce transcription of the *mgtLA* promoter via the PhoQP TCS, but also intracellular Mg^{2+} regulates transcription into the *mgtA* structural gene via translation of *mgtL* (see Chapter 3), but also an unidentified protein may regulate transcription of the *mgtA* 5' LR in an Mg^{2+}-independent and PhoQP-independent manner. Alternative transcription downstream of the *rut* site can activate *mgtA* expression independently of the PhoQP TCS, *mgtL* translational control and Rho-dependent transcription termination, and in this case, the inducing signal may induce *mgtA* transcription directly without these regulatory barriers. Two questions arise that require further investigation: in the absence of an active PhoQP TCS, 1) what environmental signal may activate *mgtA* expression, and 2) what is the transcriptional regulator that mediates this physiological response, whether or not it utilizes the potential repeat sequences as a binding site?

7.3.4 Other regulatory factors and growth conditions

We noted that the PhoQP TCS is interconnected with other systems and overlaps in regulation with other regulatory factors. We provided preliminary evidence and found evidence in scientific literature for overlapping regulation of Pro and succinate metabolisms involved in the TCA cycle by the PhoQP TCS, RpoS and EF-P. In addition, we investigated the role of Mg^{2+} transport and found a potential negative correlation with intracellular Mg^{2+} and succinate utilization. We discuss the areas of Pro and succinate metabolisms in which Mg^{2+} homeostasis and transport may be involved either directly or indirectly.

7.3.4.1 TCA cycle and succinate metabolism

In response to changes in environmental conditions, *Salmonella* modulates pathways that alternatively regulate energy and nutrient metabolism to maintain or improve growth and replication (Rychlik and Barrow, 2005). During aerobic respiration of bacteria, the TCA cycle generates electron carriers ($FADH_2$ and NADH) that facilitate redox reactions and efflux of H^+ ions across the inner membrane, and the F_1F_0-ATP synthase generates ATP by influx of H^+ ions into the cytoplasm and reduction of O_2 to H_2O (Unden and Bongaerts, 1997). An incomplete TCA cycle was shown to increase survival of *Salmonella* inside resting and active macrophages (Bowden et al., 2010). Specifically, deletion of the *sdhCDAB* operon,

encoding succinate dehydrogenase that catalyzes the conversion of succinate to fumarate in the TCA cycle, resulted in increased percentages of *Salmonella* compared to the initial inoculum (Bowden et al., 2010).

Regulation of the overall metabolism of succinate may occur at multiple levels, particularly expression of genes involved in succinate transport and catabolism. Multiple proteins mediate transport of the C4-dicarboxylic acids malate, fumarate and succinate. In both *E. coli* and *Salmonella*, RpoS represses transcription of the *dctA* gene, encoding the C4-dicarboxylic acid transporter DctA during aerobic respiration (Navarre et al., 2015), and in *Salmonella*, PhoP may repress transcription of the *dcuD* gene, which is homologous to the *dcuC* gene, encoding the C4-dicarboxylic acid transporter DcuC of *E. coli* during anaerobic respiration (Zientz et al., 1996). An active PhoQP TCS is hypothesized to promote pathogenicity upon infection not only by expressing genes involved in virulence but also stabilization of RpoS and repression of genes involved in the TCA cycle (e.g., succinate transport).

In addition, the elongation factor EF-P may assist translation of the *aceK* gene based on regulation of the signature PPP motif found in the protein (Doerfel et al., 2013). AceK regulates the activity of the IcdA enzyme, which catalyzes the conversion of isocitrate to 2-oxoglutarate in the TCA cycle (Walsh and Koshland, 1984). In the absence of IcdA, an increase in the glyoxylate shunt via AceA occurs (Walsh and Koshland, 1985), resulting in an incomplete TCA cycle that bypasses flux through succinate. Transcript levels for the *sdhCAB* and *sucCD* genes increased in *Corynebacterium glutamicum* in response to succinate; however, transcript levels for the *aceA* and *aceB* genes did not change, compared to growth on glucose, indicating that the glyoxylate shunt has a minor role during utilization of succinate as the sole carbon source (Han et al., 2008). Therefore, EF-P may promote virulence via regulation of the TCA cycle.

7.3.4.2 Pro and succinate metabolisms

Pro homeostasis is connected to succinate metabolism via the inter-conversion of L-glutamate to α-ketoglutarate, a TCA cycle intermediate, and factors including RpoS, PhoP and possibly EF-P. Glutamate biosynthesis occurs by several pathways involving conversion from 2-oxoglutarate or catabolism of the amino acids L-proline, L-arginine or L-glutamine. The GltBD complex and GlnA or GdhA only catalyze the conversion of L-glutamate to 2-oxoglutarate (Yan, 2007). In Pro biosynthesis, ProA, ProB and ProC are

essential enzymes that catalyze the conversion of L-glutamate to L-proline in a 3-step process, while PutA catalyzes the reverse reaction in Pro biosynthesis, converting L-proline to L-glutamate in a 2-step process (see Chapter 3) (Servet et al., 2012). In addition, several enzymes mediate conversion of L-arginine to L-glutamate, including AstD (Schneider et al., 1998).

We noted that EF-P may assist translation of the *gltB* gene based on regulation of the signature PPP motif found in the protein and the signature PPG motifs found in the AstD and PutA proteins (Doerfel et al., 2013). Deletion of the *astD* and *putA* genes or the *gltBD* genes do not result in glutamate auxotrophy or impairment of the TCA cycle, respectively, while deletion of the *proBAC* genes results in Pro auxotrophy. In the absence of EF-P, however, we hypothesize a decrease in the expressions of any one of these gene products may occur, given its role in ribosome rescue of proteins containing poly-Pro stretches (Doerfel et al., 2013). Therefore, another role for EF-P in promoting virulence is in assisting translation of gene products that regulate amino acid biosynthesis and degradation, and in turn, entry into the TCA cycle.

Based on preliminary results for *Salmonella* strains harboring independent mutations, we found that the growth rate on succinate as the sole carbon source increased for *rpoS::Ap*^{R}, *phoP::Cm*^{R} or Δ*efp::Cm*^{R} mutants, compared to the wild type (Fig. 6.2). In addition, we found that supplementation with exogenous Pro decreased the lag phase growth on succinate (Fig. 6.3), and a *putA*$^{--}$ mutant exhibited increased growth rate, compared to the wild type (Fig. 6.3), supporting a connection between Pro and succinate metabolisms.

The *putA*$^{--}$ mutation is hypothesized to increase the growth rate by 1) increasing the availability of the cytochrome *bo* oxidase to the SdhCDAB complex and/or 2) increasing the levels of intracellular Pro by decreasing conversion to L-glutamate. In the former instance, SdhCDAB and PutA utilize the cytochrome *bo* complex during aerobic respiration and Pro degradation, respectively (Ingledew and Poole, 1984; Servet et al., 2012). The *putA*$^{--}$ mutation is likely to increase availability of the cytochrome *bo* complex for succinate catabolism by SdhCDAB. In the latter instance, deficiency of PutA may or may not affect levels of L-glutamate; however, the *putA*$^{--}$ mutation is predicted to increase intracellular Pro, which somehow positively affects succinate metabolism (see above for details). Although PutA represses transcription of *putP*, encoding the Na^+-Pro transporter, deficiency of PutP had no effect on growth on succinate (not shown), ruling out the involvement of Pro transport via PutP. In the event that *Salmonella* experiences Pro

starvation during infection, it can be understood that decreased intracellular Pro may promote survival and virulence by inhibiting succinate metabolism and dynamics of the TCA cycle.

7.3.4.3 Mg^{2+} transport and succinate metabolism

Lastly, we observed a potential negative correlation between Mg^{2+} transport and succinate utilization. Over-expression of the MgtA or MgtB transporters increased the lag phase growth and slightly decreased the growth rate on succinate (Fig. 6.4). On the other hand, deletion of either the *mgtA* or *mgtB* gene had little effect on the growth on succinate, compared to the wild type (Fig. 6.4). Three possibilities arise that may explain these results: increased Mg^{2+} transport decreases intracellular ATP via 1) excessive ATP hydrolysis during Mg^{2+} transport or 2) inhibition of the F_1F_0-ATP synthase by the virulence factor MgtC, and/or 3) increased intracellular Mg^{2+} inhibits succinate utilization. MgtC, encoded in the *mgtCBR* operon, was shown to inhibit the ATP synthase by direct binding to the F_0 subunit a, encoded by the *atpB* gene, decreasing ATP production (Lee et al., 2013). The *mgtB*$^{++}$ mutation is predicted to increase expression of the operon, including the *mgtC* gene. If decreased intracellular ATP is the main reason for decreased growth rate on succinate via either Mg^{2+} transport or inhibition of the ATP synthase, then increased ATP production is hypothesized to complement the growth defects in the *mgtA*$^{++}$ and *mgtB*$^{++}$ mutants.

Preventing cytoplasmic acidification by influx of H^+ during ATP production is important during proliferation within the phagosomes of macrophages. EF-P may assist translation of the *atpA* and *atpB* genes, encoding subunits of the ATP synthase, based on regulation of the signature PPG motifs found in both proteins (Doerfel et al., 2013). In the absence of EF-P, levels of ATP synthase may decrease, which may explain in part the slow growth phenotype of the Δ*efp::Cm*^{R} mutant (not shown). In addition, succinate production was previously shown to enhance in a strain over-expressing the Mg^{2+} transport genes, *mgtA* and *mgtB*, and the virulence factor gene *mgtC* (Wang et al., 2014). Therefore, Mg^{2+} may promote *Salmonella* survival and virulence in hosts during infection similar to Pro availability by a mechanism that inhibits the TCA cycle and acidification of the bacterial cytoplasm.

REFERENCES

LIST OF REFERENCES

Adams, E., and Frank, L. (1980). Metabolism of Proline and the Hydroxyprolines. Annual Review of Biochemistry *49*, 1005-1061.

Ahmer, B.M.M., van Reeuwijk, J., Timmers, C.D., Valentine, P.J., and Heffron, F. (1998). *Salmonella* typhimurium Encodes an SdiA Homolog, a Putative Quorum Sensor of the LuxR Family, That Regulates Genes on the Virulence Plasmid. Journal of Bacteriology *180*, 1185-1193.

Alix, E., and Blanc-Potard, A.-B. (2008). Peptide-assisted degradation of the *Salmonella* MgtC virulence factor. EMBO J *27*, 546-557.

Alpuche Aranda, C.M., Swanson, J.A., Loomis, W.P., and Miller, S.I. (1992). *Salmonella typhimurium* activates virulence gene transcription within acidified macrophage phagosomes. Proceedings of the National Academy of Sciences of the United States of America *89*, 10079-10083.

Atkins, J.F., and Björk, G.R. (2009). A Gripping Tale of Ribosomal Frameshifting: Extragenic Suppressors of Frameshift Mutations Spotlight P-Site Realignment. Microbiology and Molecular Biology Reviews : MMBR *73*, 178-210.

Bader, M.W., Sanowar, S., Daley, M.E., Schneider, A.R., Cho, U., Xu, W., Klevit, R.E., Le Moual, H., and Miller, S.I. (2005). Recognition of Antimicrobial Peptides by a Bacterial Sensor Kinase. Cell *122*, 461-472.

Baek, J.H., Kang, Y.J., and Lee, S.Y. (2007). Transcript and protein level analyses of the interactions among PhoB, PhoR, PhoU and CreC in response to phosphate starvation in *Escherichia coli*. FEMS Microbiology Letters *277*, 254-259.

Barchiesi, J., Castelli, M.E., Soncini, F.C., and Véscovi, E.G. (2008). *mgtA* Expression Is Induced by Rob Overexpression and Mediates a *Salmonella enterica* Resistance Phenotype. Journal of Bacteriology *190*, 4951-4958.

Battesti, A., Tsegaye, Y.M., Packer, D.G., Majdalani, N., and Gottesman, S. (2012). H-NS Regulation of IraD and IraM Antiadaptors for Control of RpoS Degradation. Journal of Bacteriology *194*, 2470-2478.

Belon, C., Soscia, C., Bernut, A., Laubier, A., Bleves, S., and Blanc-Potard, A.-B. (2015). A Macrophage Subversion Factor Is Shared by Intracellular and Extracellular Pathogens. PLoS Pathogens *11*, e1004969.

Beyer, D., Skripkin, E., Wadzack, J., and Nierhaus, K.H. (1994). How the ribosome moves along the mRNA during protein synthesis. Journal of Biological Chemistry *269*, 30713-30717.

Björk, G.R., and Isaksson, L.A. (1970). Isolation of mutants of Escherichia coli lacking 5-methyluracil in transfer ribonucleic acid or 1-methylguanine in ribosomal RNA. Journal of Molecular Biology *51*, 83-100.

Björk, G.R., Ericson, J.U., Gustafsson, C.E.D., Hagervall, T.G., Jonsson, Y.H., and Wikstrom, P.M. (1987). Transfer RNA Modification. Annual Review of Biochemistry *56*, 263-285.

Blanc-Potard, A.B., and Groisman, E.A. (1997). The *Salmonella selC* locus contains a pathogenicity island mediating intramacrophage survival. The EMBO Journal *16*, 5376-5385.

Blanco, A.G., Sola, M., Gomis-Rüth, F.X., and Coll, M. (2002). Tandem DNA Recognition by PhoB, a Two-Component Signal Transduction Transcriptional Activator. Structure *10*, 701-713.

Blattner, F.R., Plunkett, G., Bloch, C.A., Perna, N.T., Burland, V., Riley, M., Collado-Vides, J., Glasner, J.D., Rode, C.K., Mayhew, G.F., *et al.* (1997). The Complete Genome Sequence of *Escherichia coli* K-12. Science *277*, 1453-1462.

Bowden, S.D., Ramachandran, V.K., Knudsen, G.M., Hinton, J.C.D., and Thompson, A. (2010). An Incomplete TCA Cycle Increases Survival of *Salmonella* Typhimurium during Infection of Resting and Activated Murine Macrophages. PLoS ONE *5*, e13871.

Bubunenko, M., Court, D.L., Refaii, A.A., Saxena, S., Korepanov, A., Friedman, D.I., Gottesman, M.E., and Alix, J.-H. (2013). Nus Transcription Elongation Factors and RNase III Modulate Small Ribosome Subunit Biogenesis in E. coli. Molecular Microbiology *87*, 382-393.

Carafa, Y.d.A., Brody, E., and Thermes, C. (1990). Prediction of rho-independent *Escherichia coli* transcription terminators: A statistical analysis of their RNA stem-loop structures. Journal of Molecular Biology *216*, 835-858.

Castelli, M.a.E., Véscovi, E.G.a., and Soncini, F.C. (2000). The Phosphatase Activity Is the Target for Mg^{2+} Regulation of the Sensor Protein PhoQ in *Salmonella*. Journal of Biological Chemistry *275*, 22948-22954.

Chalissery, J., Banerjee, S., Bandey, I., and Sen, R. (2007). Transcription Termination Defective Mutants of Rho: Role of Different Functions of Rho in Releasing RNA from the Elongation Complex. Journal of Molecular Biology *371*, 855-872.

Chamnongpol, S., Cromie, M., and Groisman, E.A. (2003). Mg^{2+} Sensing by the Mg^{2+} Sensor PhoQ of *Salmonella enterica*. Journal of Molecular Biology *325*, 795-807.

Chamnongpol, S., and Groisman, E.A. (2000). Acetyl phosphate-dependent activation of a mutant PhoP response regulator that functions independently of its cognate sensor kinase. Journal of Molecular Biology *300*, 291-305.

Chan, C.L., and Landick, R. (1989). The *Salmonella typhimurium* his operon leader region contains an RNA hairpin-dependent transcription pause site. Mechanistic implications of the effect on pausing of altered RNA hairpins. Journal of Biological Chemistry *264*, 20796-20804.

Chevance, F.F.V., Le Guyon, S., and Hughes, K.T. (2014). The Effects of Codon Context on In Vivo Translation Speed. PLoS Genetics *10*, e1004392.

Choi, E., Lee, K.-Y., and Shin, D. (2012). The MgtR regulatory peptide negatively controls expression of the MgtA Mg^{2+} transporter in *Salmonella enterica* serovar Typhimurium. Biochemical and Biophysical Research Communications *417*, 318-323.

Christian, T., Evilia, C., Williams, S., and Hou, Y.-M. (2004). Distinct Origins of tRNA(m1G37) Methyltransferase. Journal of Molecular Biology *339*, 707-719.

Coornaert, A., Chiaruttini, C., Springer, M., and Guillier, M. (2013). Post-Transcriptional Control of the *Escherichia coli* PhoQ-PhoP Two-Component System by Multiple sRNAs Involves a Novel Pairing Region of GcvB. PLoS Genet *9*, e1003156.

Coornaert, A., Lu, A., Mandin, P., Springer, M., Gottesman, S., and Guillier, M. (2010). MicA sRNA links the PhoP regulon to cell envelope stress. Molecular Microbiology *76*, 467-479.

Crépin, S., Chekabab, S.-M., Le Bihan, G., Bertrand, N., Dozois, C.M., and Harel, J. (2011). The Pho regulon and the pathogenesis of *Escherichia coli*. Veterinary Microbiology *153*, 82-88.

Cromie, M.J., Shi, Y., Latifi, T., and Groisman, E.A. (2006). An RNA Sensor for Intracellular Mg^{2+}. Cell *125*, 71-84.

Csonka, L., and Leisinger, T. (2007). Biosynthesis of Proline. EcoSal Plus.

Csonka, L.N. (1981). Proline over-production results in enhanced osmotolerance in *Salmonella typhimurium*. Molecular & General Genetics *1*, 82-86.

Datsenko, K.A., and Wanner, B.L. (2000). One-step inactivation of chromosomal genes in *Escherichia coli* K-12 using PCR products. Proceedings of the National Academy of Sciences *97*, 6640-6645.

Davies, S.J., Golby, P., Omrani, D., Broad, S.A., Harrington, V.L., Guest, J.R., Kelly, D.J., and Andrews, S.C. (1999). Inactivation and Regulation of the Aerobic C(4)-Dicarboxylate Transport (dctA) Gene of *Escherichia coli*. Journal of Bacteriology *181*, 5624-5635.

Davis R.W., Botstein D., Roth J.R. (1980). Advanced Bacterial Genetics. Cold Spring Harbor Lab Press, Plainview, NY.

Deana, A., and Belasco, J.G. (2005). Lost in translation: the influence of ribosomes on bacterial mRNA decay. Genes & Development *19*, 2526-2533.

Dijl, J.M., Bergh, R., Reversma, T., Smith, H., Bron, S., and Venema, G. Molecular cloning of the *Salmonella typhimurium* lep gene in *Escherichia coli*. Molecular and General Genetics MGG *223*, 233-240.

Doerfel, L.K., and Rodnina, M.V. (2013). Elongation factor P: Function and effects on bacterial fitness. Biopolymers *99*, 837-845.

Doerfel, L.K., Wohlgemuth, I., Kothe, C., Peske, F., Urlaub, H., and Rodnina, M.V. (2013). EF-P Is Essential for Rapid Synthesis of Proteins Containing Consecutive Proline Residues. Science *339*, 85-88.

Doerfel, L.K., Wohlgemuth, I., Kubyshkin, V., Starosta, A.L., Wilson, D.N., Budisa, N., and Rodnina, M.V. (2015). Entropic Contribution of Elongation Factor P to Proline Positioning at the Catalytic Center of the Ribosome. Journal of the American Chemical Society *137*, 12997-13006.

Duval, V., and Lister, I.M. (2013). MarA, SoxS and Rob of *Escherichia coli* – Global regulators of multidrug resistance, virulence and stress response. International journal of biotechnology for wellness industries *2*, 101-124.

Eguchi, Y., Ishii, E., Hata, K., and Utsumi, R. (2011). Regulation of Acid Resistance by Connectors of Two-Component Signal Transduction Systems in *Escherichia coli*. Journal of Bacteriology *193*, 1222-1228.

Eisenreich, W., Dandekar, T., Heesemann, J., and Goebel, W. (2010). Carbon metabolism of intracellular bacterial pathogens and possible links to virulence. Nat Rev Micro *8*, 401-412.

Eistetter, A.J., Butler, P.D., Traut, R.R., and Fanning, T.G. (1999). Characterization of *Escherichia coli* 50S ribosomal protein L31. FEMS Microbiology Letters *180*, 345-349.

Elseviers, D., Petrullo, L.A., and Gallagher, P.J. (1984). Novel *E. coli* mutants deficient in biosynthesis of 5-methylaminomethyl-2-thiouridine. Nucleic Acids Research *12*, 3521-3534.

Eriksson, S., Lucchini, S., Thompson, A., Rhen, M., and Hinton, J.C.D. (2003). Unravelling the biology of macrophage infection by gene expression profiling of intracellular *Salmonella enterica*. Molecular Microbiology *47*, 103-118.

Filloux, A., Bally, M., Soscia, C., Murgier, M., and Lazdunski, A. (1988). Phosphate regulation in Pseudomonas aeruginosa: Cloning of the alkaline phosphatase gene and identification of *phoB*- and *phoR*-like genes. Molecular and General Genetics MGG *212*, 510-513.

Gamper, H.B., Masuda, I., Frenkel-Morgenstern, M., and Hou, Y.-M. (2015). Maintenance of protein synthesis reading frame by EF-P and m^1G37-tRNA. Nat Commun *6*.

Garai, P., Gnanadhas, D.P., and Chakravortty, D. (2012). *Salmonella enterica* serovars Typhimurium and Typhi as model organisms: Revealing paradigm of host-pathogen interactions. Virulence *3*, 377-388.

García-del Portillo, F., Núñez-Hernández, C., Eisman, B., and Ramos-Vivas, J. (2008). Growth control in the *Salmonella*-containing vacuole. Current Opinion in Microbiology *11*, 46-52.

Gardner, S.G., Miller, J.B., Dean, T., Robinson, T., Erickson, M., Ridge, P.G., and McCleary, W.R. (2015). Genetic analysis, structural modeling, and direct coupling analysis suggest a mechanism for phosphate signaling in *Escherichia coli*. BMC Genetics *16*, S2-S2.

Graifer, D.M., Babkina, G.T., Matasova, N.B., Vladimirov, S.N., Karpova, G.G., and Vlassov, V.V. (1989). Structural arrangement of tRNA binding sites on Escherichia coli ribosomes, as revealed from data on affinity labelling with photoactivatable tRNA derivatives. Biochimica et Biophysica Acta (BBA) - Gene Structure and Expression *1008*, 146-156.

Groisman, E.A. (1998). The ins and outs of virulence gene expression: Mg^{2+} as a regulatory signal. BioEssays *20*, 96-101.

Groisman, E.A. (2001). The Pleiotropic Two-Component Regulatory System PhoP-PhoQ. Journal of Bacteriology *183*, 1835-1842.

Groisman, E.A., Chiao, E., Lipps, C.J., and Heffron, F. (1989). *Salmonella typhimurium phoP* virulence gene is a transcriptional regulator. Proceedings of the National Academy of Sciences of the United States of America *86*, 7077-7081.

Grote, A., Klein, J., Retter, I., Haddad, I., Behling, S., Bunk, B., Biegler, I., Yarmolinetz, S., Jahn, D., and Münch, R. (2009). PRODORIC (release 2009): a database and tool platform for the analysis of gene regulation in prokaryotes. Nucleic Acids Research *37*, D61-D65.

Gunn, J.S., and Richards, S.M. (2007). Recognition and Integration of Multiple Environmental Signals by the Bacterial Sensor Kinase PhoQ. Cell Host & Microbe *1*, 163-165.

Hammarlöf, D.L., and Hughes, D. (2008). Mutants of the RNA-processing enzyme RNase E reverse the extreme slow-growth phenotype caused by a mutant translation factor EF-Tu. Molecular Microbiology *70*, 1194-1209.

Han, S.O., Inui, M., and Yukawa, H. (2008). Effect of carbon source availability and growth phase on expression of *Corynebacterium glutamicum* genes involved in the tricarboxylic acid cycle and glyoxylate bypass. Microbiology *154*, 3073-3083.

Heithoff, D.M., Conner, C.P., Hentschel, U., Govantes, F., Hanna, P.C., and Mahan, M.J. (1999). Coordinate Intracellular Expression of *Salmonella* Genes Induced during Infection. Journal of Bacteriology *181*, 799-807.

Hengge-Aronis, R. (2002). Signal Transduction and Regulatory Mechanisms Involved in Control of the σ(S) (RpoS) Subunit of RNA Polymerase. Microbiology and Molecular Biology Reviews *66*, 373-395.

Hengge, R. (2009). Proteolysis of σ^S (RpoS) and the general stress response in *Escherichia coli*. Research in Microbiology *160*, 667-676.

Hensel, R.G.a.M. (2007). *Salmonella* pathogenicity island in host specificity, host pathogen-interactions and antibiotics resistance of *Salmonella enterica*. Berl Münch Tierärztl Wochenschr *120*, 4234-4242.

Hollands, K., Proshkin, S., Sklyarova, S., Epshtein, V., Mironov, A., Nudler, E., and Groisman, E.A. (2012). Riboswitch control of Rho-dependent transcription termination. Proceedings of the National Academy of Sciences *109*, 5376-5381.

Hollands, K., Sevostiyanova, A., and Groisman, E.A. (2014). Unusually long-lived pause required for regulation of a Rho-dependent transcription terminator. Proceedings of the National Academy of Sciences *111*, E1999-E2007.

Hou, Y.-M., and Perona, J.J. (2010). Stereochemical mechanisms of tRNA methyltransferases. FEBS Letters *584*, 278-286.

Hughes, D. (1990). Both genes for EF-Tu in *Salmonella typhimurium* are individually dispensable for growth. Journal of Molecular Biology *215*, 41-51.

Ingledew, W.J., and Poole, R.K. (1984). The respiratory chains of *Escherichia coli*. Microbiological Reviews *48*, 222-271.

Jacques, N., and Dreyfus, M. (1990). Translation initiation in *Escherichia coli*: old and new questions. Molecular Microbiology *4*, 1063-1067.

Janausch, G.I., and Unden, G. The *dcuD* (former *yhcL*) gene product of *Escherichia coli* as a member of the DcuC family of C4-dicarboxylate carriers: lack of evident expression. Archives of Microbiology *172*, 219-226.

Jensen, V., Löns, D., Zaoui, C., Bredenbruch, F., Meissner, A., Dieterich, G., Münch, R., and Häussler, S. (2006). RhlR Expression in *Pseudomonas aeruginosa* Is Modulated by the *Pseudomonas* Quinolone Signal via PhoB-Dependent and -Independent Pathways. Journal of Bacteriology *188*, 8601-8606.

Jung, H., Hilger, D., and Raba, M. (2012). The Na^+/L-proline transporter PutP. In Front Biosci (Landmark Ed), pp. 745-759.

Kakeda, M., Ueguchi, C., Yamada, H., and Mizuno, T. An *Escherichia coli* curved DNA-binding protein whose expression is affected by the stationary phase-specific sigma factor σ^S. Molecular and General Genetics MGG *248*, 629-634.

Kato, A., and Groisman, E.A. (2004). Connecting two-component regulatory systems by a protein that protects a response regulator from dephosphorylation by its cognate sensor. Genes & Development *18*, 2302-2313.

Kato, A., Tanabe, H., and Utsumi, R. (1999). Molecular Characterization of the PhoP-PhoQ Two-Component System in *Escherichia coli* K-12: Identification of Extracellular Mg^{2+}-Responsive Promoters. Journal of Bacteriology *181*, 5516-5520.

Katz, A., Solden, L., Zou, S.B., Wiley Navarre, W., and Ibba, M. (2013). Molecular evolution of protein-RNA mimicry as a mechanism for translational control. Nucleic Acids Research.

Kavaliauskas, D., Nissen, P., and Knudsen, C.R. (2012). The Busiest of All Ribosomal Assistants: Elongation Factor Tu. Biochemistry *51*, 2642-2651.

Kehres, D.G., and Maguire, M.E. (2002). Structure, properties and regulation of magnesium transport proteins. Biometals *15*, 261-270.

Keiler, K.C. (2015). Mechanisms of ribosome rescue in bacteria. Nat Rev Micro *13*, 285-297.

Kofoid, E. (1996). Standard PCR, E. Kofoid, ed.

Kox, L.F.F., Wösten, M.M.S.M., and Groisman, E.A. (2000). A small protein that mediates the activation of a two-component system by another two-component system. The EMBO Journal *19*, 1861-1872.

Landick, R., Yanofsky, C., Choo, K., and Phung, L. (1990). Replacement of the *Escherichia coli trp* operon attenuation control codons alters operon expression. Journal of Molecular Biology *216*, 25-37.

Lawrence, J. Genetics - How Green Plates Work, E. Kofoid, ed.

Lee, E.-J., Choi, J., and Groisman, E.A. (2014). Control of a *Salmonella* virulence operon by proline-charged $tRNA^{Pro}$. Proceedings of the National Academy of Sciences *111*, 3140-3145.

Lee, E.-J., and Groisman, E.A. (2010). An antisense RNA that governs the expression kinetics of a multifunctional virulence gene. Molecular Microbiology *76*, 1020-1033.

Lee, E.-J., and Groisman, E.A. (2012a). Control of a *Salmonella* virulence locus by an ATP-sensing leader messenger RNA. Nature *486*, 271-275.

Lee, E.-J., and Groisman, E.A. (2012b). Tandem attenuators control expression of the *Salmonella mgtCBR* virulence operon. Molecular Microbiology *86*, 212-224.

Lee, E.-J., Pontes, M.H., and Groisman, E.A. (2013). A Bacterial Virulence Protein Promotes Pathogenicity by Inhibiting the Bacterium's Own F_1F_o ATP Synthase. Cell *154*, 146-156.

Lejona, S., Aguirre, A., Cabeza, M.L., Véscovi, E.G., and Soncini, F.C. (2003). Molecular Characterization of the Mg^{2+}-Responsive PhoP-PhoQ Regulon in Salmonella enterica. Journal of Bacteriology *185*, 6287-6294.

Lévi-Meyrueis, C., Monteil, V., Sismeiro, O., Dillies, M.-A., Kolb, A., Monot, M., Dupuy, B., Duarte, S.S., Jagla, B., Coppée, J.-Y., *et al.* (2015). Repressor activity of the RpoS/σ^S-dependent RNA polymerase requires DNA binding. Nucleic Acids Research *43*, 1456-1468.

MacMillan, S.V., Alexander, D.A., Culham, D.E., Kunte, H.J., Marshall, E.V., Rochon, D., and Wood, J.M. (1999). The ion coupling and organic substrate specificities of osmoregulatory transporter ProP in *Escherichia coli*. Biochimica et Biophysica Acta (BBA) - Biomembranes *1420*, 30-44.

Maguire, M.E. MgtA and MgtB: Prokaryotic P-type ATPases that mediate Mg^{2+} influx. Journal of Bioenergetics and Biomembranes *24*, 319-328.

Makino, K., Shinagawa, H., Amemura, M., and Nakata, A. (1986). Nucleotide sequence of the *phoB* gene, the positive regulatory gene for the phosphate regulon of *Escherichia coli* K-12. Journal of Molecular Biology *190*, 37-44.

March, P.E., and Inouye, M. (1985). GTP-binding membrane protein of *Escherichia coli* with sequence homology to initiation factor 2 and elongation factors Tu and G. Proceedings of the National Academy of Sciences of the United States of America *82*, 7500-7504.

Marzan, L.W., Hasan, C.M.M., and Shimizu, K. (2012). Effect of acidic condition on the metabolic regulation of *Escherichia coli* and its *phoB* mutant. Archives of Microbiology *195*, 161-171.

Masuda, I., Sakaguchi, R., Liu, C., Gamper, H., and Hou, Y.-M. (2013). The Temperature Sensitivity of a Mutation in the Essential tRNA Modification Enzyme tRNA Methyltransferase D (TrmD). Journal of Biological Chemistry *288*, 28987-28996.

Medina, G., Juárez, K., and Soberón-Chávez, G. (2003a). The *Pseudomonas aeruginosa rhlAB* Operon Is Not Expressed during the Logarithmic Phase of Growth Even in the Presence of Its Activator RhlR and the Autoinducer N-Butyryl-Homoserine Lactone. Journal of Bacteriology *185*, 377-380.

Medina, G., Juárez, K., Valderrama, B., and Soberón-Chávez, G. (2003b). Mechanism of *Pseudomonas aeruginosa* RhlR Transcriptional Regulation of the *rhlAB* Promoter. Journal of Bacteriology *185*, 5976-5983.

Miller, JH. (1991). A Short Course in Bacterial Genetics: A Laboratory Manual and Handbook for *Escherichia coli* and Related Bacteria. Cold Spring Harbor Lab Press, Plainview, NY.

Mitrophanov, A.Y., and Groisman, E.A. (2008). Signal integration in bacterial two-component regulatory systems. Genes & Development *22*, 2601-2611.

Monsieurs, P., Keersmaecker, S., Navarre, W.W., Bader, M.W., Smet, F., McClelland, M., Fang, F.C., Moor, B., Vanderleyden, J., and Marchal, K. (2005). Comparison of the PhoPQ Regulon in *Escherichia coli* and *Salmonella typhimurium*. Journal of Molecular Evolution *60*, 462-474.

Montagne, M., Martel, A., and Le Moual, H. (2001). Characterization of the Catalytic Activities of the PhoQ Histidine Protein Kinase of *Salmonella enterica* Serovar Typhimurium. Journal of Bacteriology *183*, 1787-1791.

Muto, H., and Ito, K. (2008). Peptidyl-prolyl-tRNA at the ribosomal P-site reacts poorly with puromycin. Biochemical and Biophysical Research Communications *366*, 1043-1047.

Nakatogawa, H., and Ito, K. (2002). The Ribosomal Exit Tunnel Functions as a Discriminating Gate. Cell *108*, 629-636.

Narlikar, L. (2014). Multiple novel promoter-architectures revealed by decoding the hidden heterogeneity within the genome. Nucleic Acids Research *42*, 12388-12403.

Navarre, W.W., Hersch, S., Radan, B., and Watson, A. (2015). Metabolic Adaptations Controlled by RpoS and EF-P Limit Cytoplasmic Acidification in *Salmonella enterica*. In Molecular Genetics of Bacteria and Phages Meeting (Madison, Wisconsin), pp. 20.

O'Connor, K., Fletcher, S.A., and Csonka, L.N. (2009). Increased expression of Mg^{2+} transport proteins enhances the survival of *Salmonella enterica* at high temperature. Proceedings of the National Academy of Sciences *106*, 17522-17527.

Ochsner, U.A., Koch, A.K., Fiechter, A., and Reiser, J. (1994). Isolation and characterization of a regulatory gene affecting rhamnolipid biosurfactant synthesis in *Pseudomonas aeruginosa*. Journal of Bacteriology *176*, 2044-2054.

Paliy, O., and Gunasekera, T. (2007). Growth of *E. coli* BL21 in minimal media with different gluconeogenic carbon sources and salt contents. Appl Microbiol Biotechnol *73*, 1169-1172.

Papp-Wallace, K., and Maguire, M. (2008). Magnesium Transport and Magnesium Homeostasis. EcoSal Plus.

Papp-Wallace, K.M., Nartea, M., Kehres, D.G., Porwollik, S., McClelland, M., Libby, S.J., Fang, F.C., and Maguire, M.E. (2008). The CorA Mg^{2+} Channel Is Required for the Virulence of *Salmonella enterica* serovar Typhimurium. Journal of Bacteriology *190*, 6517-6523.

Park, S.-Y., Cromie, M.J., Lee, E.-J., and Groisman, E.A. (2010). A Bacterial mRNA Leader that Employs Different Mechanisms to Sense Disparate Intracellular Signals. Cell *142*, 737-748.

Park, S.-Y., and Groisman, E.A. (2014). Signal-specific temporal response by the *Salmonella* PhoP/PhoQ regulatory system. Molecular Microbiology *91*, 135-144.

Pavlov, M.Y., Watts, R.E., Tan, Z., Cornish, V.W., Ehrenberg, M., and Forster, A.C. (2009). Slow peptide bond formation by proline and other N-alkylamino acids in translation. Proceedings of the National Academy of Sciences of the United States of America *106*, 50-54.

Pech, M., Karim, Z., Yamamoto, H., Kitakawa, M., Qin, Y., and Nierhaus, K.H. (2011). Elongation factor 4 (EF4/LepA) accelerates protein synthesis at increased Mg^{2+} concentrations. Proceedings of the National Academy of Sciences *108*, 3199-3203.

Perez, J.C., Shin, D., Zwir, I., Latifi, T., Hadley, T.J., and Groisman, E.A. (2009). Evolution of a Bacterial Regulon Controlling Virulence and Mg^{2+} Homeostasis. PLoS Genetics *5*, e1000428.

Peters, J.M., Mooney, R.A., Kuan, P.F., Rowland, J.L., Keleş, S., and Landick, R. (2009). Rho directs widespread termination of intragenic and stable RNA transcription. Proceedings of the National Academy of Sciences of the United States of America *106*, 15406-15411.

Portillo, F.G.d., Foster, J.W., Maguire, M.E., and Finlay, B.B. (1992). Characterization of the micro-environment of *Salmonella typhimurium*–containing vacuoles within MDCK epithelial cells. Molecular Microbiology *6*, 3289-3297.

Porwollik, S., Santiviago, C.A., Cheng, P., Long, F., Desai, P., Fredlund, J., Srikumar, S., Silva, C.A., Chu, W., Chen, X., *et al.* (2014). Defined Single-Gene and Multi-Gene Deletion Mutant Collections in *Salmonella enterica* sv Typhimurium. PLoS ONE *9*, e99820.

Povolotskaya, I.S., Kondrashov, F.A., Ledda, A., and Vlasov, P.K. (2012). Stop codons in bacteria are not selectively equivalent. Biology Direct *7*, 30-30.

Prost, L.R., Daley, M.E., Le Sage, V., Bader, M.W., Le Moual, H., Klevit, R.E., and Miller, S.I. (2007). Activation of the Bacterial Sensor Kinase PhoQ by Acidic pH. Molecular cell *26*, 165-174.

Prost, L.R., and Miller, S.I. (2008). The *Salmonellae* PhoQ sensor: mechanisms of detection of phagosome signals. Cellular Microbiology *10*, 576-582.

Purta, E., van Vliet, F., Tricot, C., De Bie, L.G., Feder, M., Skowronek, K., Droogmans, L., and Bujnicki, J.M. (2005). Sequence–structure–function relationships of a tRNA (m^7G46) methyltransferase studied by homology modeling and site-directed mutagenesis. Proteins: Structure, Function, and Bioinformatics *59*, 482-488.

Qian, Q., and Björk, G.R. (1997). Structural alterations far from the anticodon of the $tRNA^{GGG}$ Proof *Salmonella typhimurium* induce +1 frameshifting at the peptidyl-site. Journal of Molecular Biology *273*, 978-992.

Qin, D., and Fredrick, K. (2013). Chapter Eight - Analysis of Polysomes from Bacteria. In Methods in Enzymology, L. Jon, ed. (Academic Press), pp. 159-172.

Rahman, T., Hosen, I., and Chakraborty, S. (2013). A Rapid Glimpse on Typhoid Fever: An Updated Mini Review. Journal of Life Medicine *1*, 83-92.

Ranaei-Siadat, E., Fabret, C., Seijo, B., Dardel, F., Grosjean, H., and Nonin-Lecomte, S. (2013). RNA-methyltransferase TrmA is a dual-specific enzyme responsible for C(5)-methylation of uridine in both tmRNA and tRNA. RNA Biology *10*, 572-578.

Rang, C., Alix, E., Felix, C., Heitz, A., Tasse, L., and Blanc-Potard, A.-B. (2007). Dual role of the MgtC virulence factor in host and non-host environments. Molecular Microbiology *63*, 605-622.

Reinhart, R.A. (1988). Magnesium metabolism: A review with special reference to the relationship between intracellular content and serum levels. Archives of Internal Medicine *148*, 2415-2420.

Richardson, J.P. (2002). Rho-dependent termination and ATPases in transcript termination. Biochimica et Biophysica Acta (BBA) - Gene Structure and Expression *1577*, 251-260.

Rosenberg, E.Y., Bertenthal, D., Nilles, M.L., Bertrand, K.P., and Nikaido, H. (2003). Bile salts and fatty acids induce the expression of *Escherichia coli* AcrAB multidrug efflux pump through their interaction with Rob regulatory protein. Molecular Microbiology *48*, 1609-1619.

Ruff, E.F., Record, M.T., and Artsimovitch, I. (2015). Initial Events in Bacterial Transcription Initiation. Biomolecules *5*, 1035-1062.

Rychlik, I., and Barrow, P.A. (2005). *Salmonella* stress management and its relevance to behaviour during intestinal colonisation and infection. FEMS Microbiology Reviews *29*, 1021-1040.

Sakaguchi, R., Lahoud, G., Christian, T., Gamper, H., and Hou, Y.-M. (2014). A Divalent Metal Ion-Dependent N^1-Methyl Transfer to G37-tRNA. Chemistry & biology *21*, 1351-1360.

Schellhorn, H.E. (2014). Elucidating the function of the RpoS regulon. Future Microbiology *9*, 497-507.

Schneider, B.L., Kiupakis, A.K., and Reitzer, L.J. (1998). Arginine Catabolism and the Arginine Succinyltransferase Pathway in *Escherichia coli*. Journal of Bacteriology *180*, 4278-4286.

Sen, R., Chalissery, J., and Muteeb, G. (2008). Nus Factors of *Escherichia coli*. EcoSal Plus.

Servet, C., Ghelis, T., Richard, L., Zilberstein, A., and Savoure, A. (2012). Proline dehydrogenase: a key enzyme in controlling cellular homeostasis. In Front Biosci (Landmark Ed), pp. 607-620.

Silver, S. (1996). *Escherichia coli* and *Salmonella typhimurium*: Cellular and Molecular Biology, 2nd ed. Washington, DC, Am Soc Microbiol.

Smith, R.L., Kaczmarek, M.T., Kucharski, L.M., and Maguire, M.E. (1998). Magnesium transport in *Salmonella typhimurium*: regulation of *mgtA* and *mgtCB* during invasion of epithelial and macrophage cells. Microbiology *144*, 1835-1843.

Snavely, M.D., Gravina, S.A., Cheung, T.T., Miller, C.G., and Maguire, M.E. (1991). Magnesium transport in *Salmonella typhimurium*. Regulation of *mgtA* and *mgtB* expression. Journal of Biological Chemistry *266*, 824-829.

Soncini, F.C., García Véscovi, E., Solomon, F., and Groisman, E.A. (1996). Molecular basis of the magnesium deprivation response in *Salmonella typhimurium*: identification of PhoP-regulated genes. Journal of Bacteriology *178*, 5092-5099.

Spinelli, S.V., Pontel, L.B., García Véscovi, E., and Soncini, F.C. (2008). Regulation of magnesium homeostasis in *Salmonella*: Mg^{2+} targets the *mgtA* transcript for degradation by RNase E. FEMS Microbiology Letters *280*, 226-234.

Subramani, S., Perdreau-Dahl, H., and Morth, J.P. (2016). The magnesium transporter A is activated by cardiolipin and is highly sensitive to free magnesium in vitro. eLife *5*, e11407.

Tanner, D.R., Cariello, D.A., Woolstenhulme, C.J., Broadbent, M.A., and Buskirk, A.R. (2009). Genetic Identification of Nascent Peptides That Induce Ribosome Stalling. Journal of Biological Chemistry *284*, 34809-34818.

Tao, T., Grulich, P.F., Kucharski, L.M., Smith, R.L., and Maguire, M.E. (1998). Magnesium transport in *Salmonella typhimurium*: biphasic magnesium and time dependence of the transcription of the *mgtA* and *mgtCB* loci. Microbiology *144*, 655-664.

Tao, T., Snavely, M.D., Farr, S.G., and Maguire, M.E. (1995). Magnesium transport in *Salmonella typhimurium*: *mgtA* encodes a P-type ATPase and is regulated by Mg^{2+} in a manner similar to that of the *mgtB* P-type ATPase. Journal of Bacteriology *177*, 2654-2662.

Thompson, J.A., Liu, M., Helaine, S., and Holden, D.W. (2011). Contribution of the PhoP/Q regulon to survival and replication of *Salmonella enterica* serovar Typhimurium in macrophages. Microbiology *157*, 2084-2093.

Trobro, S., and Åqvist, J. (2008). Role of Ribosomal Protein L27 in Peptidyl Transfer†. Biochemistry *47*, 4898-4906.

Tu, X., Latifi, T., Bougdour, A., Gottesman, S., and Groisman, E.A. (2006). The PhoP/PhoQ two-component system stabilizes the alternative sigma factor RpoS in *Salmonella enterica*. Proceedings of the National Academy of Sciences of the United States of America *103*, 13503-13508.

Ude, S., Lassak, J., Starosta, A.L., Kraxenberger, T., Wilson, D.N., and Jung, K. (2013). Translation Elongation Factor EF-P Alleviates Ribosome Stalling at Polyproline Stretches. Science *339*, 82-85.

Unden, G., and Bongaerts, J. (1997). Alternative respiratory pathways of *Escherichia coli*: energetics and transcriptional regulation in response to electron acceptors. Biochimica et Biophysica Acta (BBA) - Bioenergetics *1320*, 217-234.

Véscovi, E.G., Soncini, F.C., and Groisman, E.A. (1996). Mg^{2+} as an Extracellular Signal: Environmental Regulation of *Salmonella* Virulence. Cell *84*, 165-174.

Walsh, K., and Koshland, D.E. (1984). Determination of flux through the branch point of two metabolic cycles. The tricarboxylic acid cycle and the glyoxylate shunt. Journal of Biological Chemistry *259*, 9646-9654.

Walsh, K., and Koshland, D.E. (1985). Branch point control by the phosphorylation state of isocitrate dehydrogenase. A quantitative examination of fluxes during a regulatory transition. Journal of Biological Chemistry *260*, 8430-8437.

Wang, J., Zhang, B., Zhang, J., Wang, H., Zhao, M., Wang, N., Dong, L., Zhou, X., and Wang, D. (2014). Enhanced succinic acid production and magnesium utilization by overexpression of magnesium transporter *mgtA* in *Escherichia coli* mutant. Bioresource Technology *170*, 125-131.

Wang, Y., and Xiao, M. (2012). Role of the ribosomal protein L27 revealed by single-molecule FRET study. Protein Science *21*, 1696-1704.

Washburn, R.S., and Gottesman, M.E. (2015). Regulation of Transcription Elongation and Termination. Biomolecules *5*, 1063-1078.

Wower, I.K., Wower, J., and Zimmermann, R.A. (1998). Ribosomal Protein L27 Participates in both 50 S Subunit Assembly and the Peptidyl Transferase Reaction. Journal of Biological Chemistry *273*, 19847-19852.

Yamamoto, H., Qin, Y., Achenbach, J., Li, C., Kijek, J., Spahn, C.M.T., and Nierhaus, K.H. (2014). EF-G and EF4: translocation and back-translocation on the bacterial ribosome. Nat Rev Micro *12*, 89-100.

Yan, D. (2007). Protection of the glutamate pool concentration in enteric bacteria. Proceedings of the National Academy of Sciences of the United States of America *104*, 9475-9480.

Yang, C., Huang, T.-W., Wen, S.-Y., Chang, C.-Y., Tsai, S.-F., Wu, W.-F., and Chang, C.-H. (2012). Genome-Wide PhoB Binding and Gene Expression Profiles Reveal the Hierarchical Gene Regulatory Network of Phosphate Starvation in *Escherichia coli*. PLoS ONE *7*, e47314.

Yanofsky, C. (1981). Attenuation in the control of expression of bacterial operons. Nature *289*, 751-758.

Zhao, G., Kong, W., Weatherspoon-Griffin, N., Clark-Curtiss, J., and Shi, Y. (2011). Mg^{2+} facilitates leader peptide translation to induce riboswitch-mediated transcription termination. EMBO J *30*, 1485-1496.

Zientz, E., Janausch, I.G., Six, S., and Unden, G. (1999). Functioning of DcuC as the C(4)-Dicarboxylate Carrier during Glucose Fermentation by *Escherichia coli*. Journal of Bacteriology *181*, 3716-3720.

Zientz, E., Six, S., and Unden, G. (1996). Identification of a third secondary carrier (DcuC) for anaerobic C4-dicarboxylate transport in *Escherichia coli*: roles of the three Dcu carriers in uptake and exchange. Journal of Bacteriology *178*, 7241-7247.

Zuker, M. (2003). Mfold web server for nucleic acid folding and hybridization prediction. Nucleic Acids Research *31*, 3406-3415.

Zwir, I., Latifi, T., Perez, J.C., Huang, H., and Groisman, E.A. (2012). The promoter architectural landscape of the *Salmonella* PhoP regulon. Molecular Microbiology *84*, 463-485.

PUBLICATIONS

PUBLICATIONS

Gall, A. R., Figueroa-Bossi N., Bossi L., Masuda I., Hou Y-M. and Csonka L. N. *Magnesium regulates transcription of* mgtA *in* Salmonella enterica *serovar Typhimurium via prolyl-bond formation during translation of the leader peptide MgtL*. (To be submitted)

Siriwardana, L.S., et al., *Factors affecting accumulation and degradation of curdlan, trehalose and glycogen in cultures of* Cellulomonas flavigena *strain KU (ATCC 53703).* Antonie van Leeuwenhoek, 2010. **99**(3): p. 681-695.

VITA

VITA

Aaron Robert Gall was born in Miami, Florida on April 6, 1988. When he was 10 years old, his parents, three brothers and he moved to Newnan, Georgia, so that his father could find better work. They used to go to church regularly back in Florida, and they continued going together for some time after they moved. Slowly, they stopped going as a family, but his older brother kept going for some reason.

He graduated from Northgate High School in 2006 and went to the University of West Georgia. During his first year in college, he was confronted with whether he believed the claims of the Bible, that Jesus Christ died on a cross to forgive sins, because God loves us. He grew up believing in God's existence, but what he was challenged with was God's character, whether Jesus Christ is who He says He is, and whether he could trust Him. When he was honest with himself, he knew that he was trying to fill a void in his heart the size of the Grand Canyon with pebbles. It was not working.

The Gospel (which, in Greek, means "Good News") is based on the fact that Jesus Christ died on a cross and rose from the dead to make propitiation (e.g. atonement, forgiveness) for sins. As a freshman in college, he made the greatest and most important decision of his life, a willful decision to acknowledge that he had sinned against the Living God and to place his trust (faith) in Christ alone for forgiveness of his sins.

Eventually, he graduated summa cum laude with a B.S. in Pre-Med Biology in 2009. He came into the Department of Biological Sciences at Purdue University as an M.S. student in 2010. Only after applying to several medical schools in 2011, did he consider God's will for his life, and after praying, he decided to stay in West Lafayette to grow in his faith in Christ and pursue a Ph.D. instead. Since then, he has been unashamed to share the Gospel with family, friends, faculty/staff, colleagues and students. Following his Ph.D. degree, he desires to seek first the Kingdom of God and His righteousness, no matter how that looks.